

**EVIDENCE FOR EFFECTS OF NESFATIN-1, α -MELANOCYTE STIMULATING
HORMONE, AND GLUCOSE ON THE EXCITABILITY OF INDIVIDUAL NEURONS
IN THE NUCLEUS OF THE SOLITARY TRACT**

by

Andrea Mimee

A thesis submitted to the Graduate Program in Physiology
in conformity with the requirements for the
degree of Doctor of Philosophy

Queen's University

Kingston, Ontario, Canada

October, 2014

Copyright © Andrea Mimee, 2014

Abstract

The nucleus of the solitary tract (NTS) is a medullary autonomic center with essential roles in the regulation of energy homeostasis. Understanding how the NTS contributes to the coordination of ingestive behaviors and autonomic processes is therefore critical to provide insight into the control of feeding in physiological and pathological states. Thus, here we have investigated the integration of metabolically relevant factors in individual NTS neurons.

We uncovered direct depolarizing (42% of responses, mean 7.83 ± 0.84 mV, $n=39$) and hyperpolarizing (21% of responses, mean -8.23 ± 1.00 mV, $n=20$) effects of the anorexigenic peptide nesfatin-1 on NTS neurons. Our reverse transcription PCR studies demonstrated exclusively depolarizing effects of nesfatin-1 on neurons expressing NUCB2, the gene which encodes nesfatin-1, and the orexigenic neuropeptide Y. Furthermore, *in vivo* microinjections of nesfatin-1 into the NTS elicited tachycardic and pressor effects.

We also delineated an NTS circuit engaged by the anorexigenic peptide α -melanocyte stimulating hormone (α -MSH). We established the depolarizing effects (39% of responses, mean 6.14 ± 0.54 mV, $n=16$) of α -MSH are due to postsynaptic actions on the membrane potential of NTS cells, while hyperpolarizations (22% of responses, mean -6.79 ± 1.02 mV, $n=9$) are indirect and caused by enhancement of GABAergic neurotransmission. Indeed, 50% of NTS neurons showed an increase in inhibitory postsynaptic current (IPSC) frequency in response to α -MSH. Another subset of NTS neurons was non-responsive to α -MSH due to simultaneous direct depolarizing and indirect hyperpolarizing effects of the peptide.

Finally, we established 57% of NTS neurons exhibit physiologically relevant glucose sensing properties ($n=81$, 35% glucose excited, 22% glucose inhibited). Moreover, the effects of nesfatin-1 on the excitability of NTS neurons were consistent across glycemic conditions and

categories of glucose sensing cells. α -MSH, however showed preferential effects on glucose responsive NTS neurons, and depolarized all NTS cells in hypoglycemic conditions, in contrast to the heterogeneous effects elicited in normo- and hyperglycemic states.

Taken together, our studies highlight the integration of metabolic signals in individual NTS neurons. We have also revealed critical effects of glucose concentrations on brain slice studies, findings which have important implications for electrophysiological investigations in the NTS and in other neuronal centers.

Co-Authorship

Chapter 2: RT-PCR experiments were performed with assistance from Christie Hopf. The microinjection studies were performed and analyzed by, and methods for these studies written by, Dr. Pauline Smith. All other experiments were designed, performed, and analyzed by Andrea Mimee. The manuscript was written by Andrea Mimee with the assistance of Dr. Alastair V. Ferguson.

Chapter 3: Electrophysiological recordings of dissociated neurons were performed by Markus Kuksis. All other experiments were designed, performed, and analyzed by Andrea Mimee. The manuscript was written by Andrea Mimee with the assistance of Dr. Alastair V. Ferguson.

Chapter 4: All experiments were designed, performed, and analyzed by Andrea Mimee. The manuscript was written by Andrea Mimee with the assistance of Dr. Alastair V. Ferguson.

Acknowledgements

First and foremost, I cannot properly express my enormous thanks to my mentor, Al Ferguson. Your excitement for science is infectious, your no nonsense attitude incredibly helpful and refreshing, and your genuine care for your students so deeply appreciated. Thank you for giving me the freedom to learn, to mature at my own pace, and to discover both science and myself. Your constant support and unwavering belief in my skills and abilities over the past 5 years have been essential in the success of my time at Queen's. Thank you for your guidance, patience, and for always encouraging me and believing in me, even when I doubted myself.

To my lab mates, past and present, you made the lab not only a fantastic place of learning and discussion, but also one of fun and games. To the current team, Emily Black, Nikki Cancelliere, Markus Kuksis, Rishi Malik, Will McIsaac, and Pauline Smith: thank you for all the laughs and science scheming, and for your help in getting me out of my literal and metaphorical windows.

Finally, Mark, Mommy and Daddy, thank you for always, always being there for me when I need you, whether it be the first or sixth phone call or email of the day. Mark, I will never forget when you told me I inspired you to go into science. Now it's you who motivates me to do better and aim higher every day, and I hope to be half the genius you are one day. Mommy and Daddy, I am so lucky to be your daughter. Thank you for doing absolutely everything in your power to make life as happy, full, comfortable, and loving as you have for me. You are the most wonderful family anyone could ask for, and I would be lost without you.

TABLE OF CONTENTS

Abstract	ii
Co-Authorship	iv
Acknowledgements	v
Table of contents	vi
List of Figures	viii
List of Tables	ix
List of Abbreviations	x
CHAPTER 1: General Introduction	1
The Nucleus of the Solitary Tract	3
Anatomical divisions of the NTS	3
Functions of subpopulations of NTS neurons.....	4
Regulation of cardiovascular function in the NTS.....	4
Regulation of gastrointestinal function and food intake in the NTS.....	8
Electrophysiological phenotypes of NTS neurons.....	13
Nesfatin-1	14
Anatomy of the central nefatin-1 system.....	14
Roles of centrally acting nesfatin-1 in the regulation of energy homeostasis.....	15
Roles of centrally acting nesfatin-1 in the control of glucose homeostasis.....	19
Roles of centrally acting nesfatin-1 in the control of cardiovascular function.....	20
Nesfatin-1 signaling.....	20
The central melanocortin system	21
Anatomy of the central melanocortin system.....	21
Roles of the central melanocortin system in the regulation of energy homeostasis.....	22
Genetic evidence.....	22
Pharmacological, molecular, and cellular evidence.....	23
Roles of the central melanocortin system in the control of glucose homeostasis.....	28
Roles of the central melanocortin system in the control of cardiovascular function.....	28
Central glucose sensing neurons	29
Location of central glucose sensing neurons.....	29
Functions of central glucose sensing neurons.....	30
Mechanism of glucose detection.....	31
Statement of the problem	33

CHAPTER 2: Nesfatin-1 influences the excitability of neurons in the nucleus of the solitary tract and regulates cardiovascular function	35
Abstract.....	36
Introduction.....	37
Experimental Procedures.....	38
Results.....	43
Discussion.....	50
Acknowledgements.....	56
CHAPTER 3: α-MSH exerts direct postsynaptic excitatory effects on NTS neurons and enhances GABAergic signaling in the NTS	57
Abstract.....	58
Introduction.....	59
Experimental Procedures.....	61
Results.....	64
Discussion.....	77
Acknowledgements.....	84
CHAPTER 4: The NTS contains physiologically relevant glucose sensing neurons and exhibits plasticity to the effects of α-MSH, but not nesfatin-1, as glycemc state is altered..	85
Abstract.....	86
Introduction.....	88
Experimental Procedures.....	90
Results.....	93
Discussion.....	103
Acknowledgements.....	109
CHAPTER 5: General Discussion	110
REFERENCES	125

List of Figures

- Figure 2-1 Nesfatin-1 influences the excitability of mNTS neurons
- Figure 2-2 Nesfatin-1 mediated effects on mNTS neurons are maintained in the presence of TTX
- Figure 2-3 Nesfatin-1 affects all mNTS cell types
- Figure 2-4 Nesfatin-1 depolarizes NPY and NUCB2 mNTS neurons
- Figure 2-5 Nesfatin-1 microinjection into the mNTS increases blood pressure and heart rate
- Figure 3-1 α -MSH influences the membrane potential of NTS neurons
- Figure 3-2 α -MSH exerts direct depolarizing and indirect hyperpolarizing effects on NTS neurons
- Figure 3-3 α -MSH increases the frequency of IPSCs in the NTS
- Figure 3-4 α -MSH does not influence the frequency or amplitude of miniature IPSCs in the NTS
- Figure 3-5 GABA receptor antagonism eliminates the hyperpolarizing effects of α -MSH and increases the proportion of neurons which depolarize to α -MSH
- Figure 3-6 Dissociated NTS neurons show no hyperpolarizing responses to α -MSH
- Figure 3-7 Proposed model: α -MSH exerts direct excitatory effects and indirect inhibitory effects on NTS neurons
- Figure 4-1 The NTS contains physiologically relevant glucose sensing neurons
- Figure 4-2 Nesfatin-1 exerts heterogeneous effects on both glucose responsive and glucose non-responsive NTS neurons
- Figure 4-3 The effects of nesfatin-1 on NTS neurons are consistent across glucose concentrations
- Figure 4-4 GE NTS neurons are more responsive to α -MSH than NR cells, and are selectively depolarized by α -MSH
- Figure 4-5 NTS neurons show increased responsiveness to α -MSH as extracellular glucose concentrations decrease

List of Tables

Table 2-1 Primers used in single cell RT-PCR experiments

List of Abbreviations

2DG – 2-deoxy-D-glucose

3V – third ventricle

4V – fourth ventricle

5TG – 5-thio-D-glucose

α -MSH – alpha melanocyte stimulating hormone

aCSF – artificial cerebrospinal fluid

AgRP – agouti gene-related protein

ANOVA – analysis of variance

AP – area postrema

ARC – arcuate nucleus of the hypothalamus

ATP – adenosine triphosphate

AUC – area under the curve

BAT – brown adipose tissue

BP – blood pressure

cAMP – cyclic adenosine monophosphate

CART – cocaine and amphetamine related transcript

CCK – cholecystokinin

CNS – central nervous system

CREB – cAMP response element binding protein

CRH – corticotropin releasing hormone

CVLM – caudal ventrolateral medulla

DE – delayed excitation

DMH – dorsomedial nucleus of the hypothalamus

DMV – dorsal motor nucleus of the vagus

DVC – dorsal vagal complex

EPSC – excitatory postsynaptic current

mEPSC – miniature EPSC

GABA – γ -aminobutyric acid

GAD67 – glutamate decarboxylase 67

GAPDH – glyceraldehyde 3-phosphate dehydrogenase

GE – glucose excited neuron

GI – glucose inhibited neuron

GLP-1 – glucagon-like peptide 1

GPCR – G-protein coupled receptor

HR – heart rate

icv - intracerebroventricular

IPSC – inhibitory postsynaptic current

mIPSC – miniature IPSC

KA – kynurenic acid

K_{ATP} channels – ATP sensitive K⁺ channels

LHA – lateral hypothalamic area

LV – lateral ventricle

MAP – mean arterial pressure

MAPK – mitogen activated protein kinase

MC3R – melanocortin 3 receptor

MC4R – melanocortin 4 receptor

MTII – melanotan II

mTOR – mammalian target of rapamycin

NPY – neuropeptide Y

NR – glucose nonresponsive neuron

NTS – nucleus of the solitary tract

cNTS – commissural NTS

mNTS – medial NTS

NUCB2 – nucleobindin2

PIR – post-inhibitory rebound

PKA – protein kinase A

POMC – pro-opiomelanocortin

PVN – paraventricular nucleus of the hypothalamus

RT-PCR – reverse transcription polymerase chain reaction

RVLM – rostral ventrolateral medulla

ST – solitary tract

TRH – thyrotropin releasing hormone

TTX - tetrodotoxin

VMH – ventromedial nucleus of the hypothalamus

CHAPTER 1 – General Introduction

Obesity has been identified as a global epidemic, and its worldwide prevalence is ever increasing. Somber statistics of the prevalence of overweight and obesity (defined as a body mass index of greater than 25 and 30 kg/m², respectively) report a staggering 60 and 70% of adult women and men in North America, respectively, fall into these two weight categories as of 2013. Perhaps even more alarming is the fact that nearly 30% of children in North America are now overweight or obese. Considering the global prevalence of overweight and obesity in 2013 represents a rise of 27.5% for adults and 47.1% for children from levels in 1980, and obesity was estimated to have caused 3.4 million deaths in 2010 (Ng *et al.*, 2014), it is evident there is an urgent need to understand the mechanisms underlying the disordered feeding and energy expenditure which characterize these disease states and their associated comorbidities, including cardiovascular complications and diabetes. Yet while the concept that an organism must consume appropriate amounts of food to maintain necessary energy stores is an exceedingly basic one, the processes that govern ingestive behaviour are anything but simple. The regulation of energy homeostasis involves the concerted action of various organs and a remarkable number of circulating factors which act to signal when there is a need to feed. The brain, in particular, coordinates multiple aspects of feeding, from initiation and termination of eating to the rewarding aspects of the consumption of palatable food. Despite the vast current knowledge on the molecules and regions implicated in the central regulation of ingestive behavior, new factors are continually emerging as players in the complex network of energy homeostasis, making it more and more challenging to comprehend how the multitude of metabolically relevant signals are integrated in the brain. One prime central integrative center is the medullary nucleus of the solitary tract (NTS). Understanding how the NTS contributes to the mediation of ingestive behaviors and autonomic processes is therefore necessary to provide key insight into the

coordinated regulation of feeding in physiological states. The experiments completed for this thesis have thus addressed the cellular effects of feeding related peptides and metabolic signals on the activity of neurons in this medullary center.

THE NUCLEUS OF THE SOLITARY TRACT

Anatomical divisions of the NTS

The NTS is a critical autonomic center responsible for the regulation of numerous essential reflex functions, and is the principle medullary structure which integrates visceral sensory inputs. Located in the dorsomedial medulla, the NTS is a V shaped structure which extends rostrocaudally from the facial motor nucleus to the caudal level of the pyramidal decussation and surrounds the solitary tract (ST) along its entire length. The ST itself is comprised of the afferent fibres of the facial (VII), glossopharyngeal (IX), and vagus (X) cranial nerves, which innervate second order NTS neurons in a viscerotopic pattern. Indeed, while the IX and X cranial nerves terminate in caudal portions of the NTS and relay sensory inputs, the VII nerve terminates more rostrally and transmits mainly gustatory information (Kalia & Mesulam, 1980a). Numerous subpopulations within the NTS have been defined based on differences in location, cell size, and cell density. An early, simple classification system was proposed by Torvik in the 1950s, in which the NTS was divided into medial and lateral components. In this study, the medial NTS was described as densely packed with smaller round, pear shaped, or triangular neurons in a fine network of fibres, while the lateral NTS contained more diffuse, larger multipolar cells with a richer fibre plexus (Torvik, 1956). Rostral, intermediate, and caudal subnuclei are also described in relation to the area postrema (AP), with the intermediate NTS located at the level of AP (Jean, 1991). Studies using horseradish peroxidase staining have defined further medial-lateral and dorsal-ventral subnuclei within the rostral, intermediate, and

caudal portions of NTS, providing a more precise analysis of the cytoarchitecture of these neurons. In addition to the medial and lateral nuclei already mentioned, commissural, dorsal, dorsolateral, ventral, ventrolateral, interstitial, intermediate, and gelatinous nuclei have also been described based on cell size and density (Kalia & Mesulam, 1980a; Jean, 1991). Further anatomical analyses have concluded that the NTS is generally composed of small neurons with an average diameter of 15-20 μm , with the exception of the ventrolateral nucleus whose neurons are a larger 30-40 μm (Chiba & Kato, 1978; Berger *et al.*, 1984; Jean, 1991). Interestingly, despite their small size, the dendritic trees of some NTS neurons are quite large, spanning up to 600 μm (Rogers & McCann, 1993). Thus, while considerable effort has been devoted to categorizing the cell bodies of NTS neurons into discrete anatomical boundaries, in reality the dendrites of these cells can span multiple subregions, potentially blurring the dividing lines between these defined areas.

Functions of subpopulations of NTS neurons

The NTS is a critical integrator of numerous autonomic functions, and its essential role in these processes is evident by the lethal outcome of complete lesions of the NTS (Doba & Reis, 1973). The most common functional types of NTS neurons are cardiovascular, gastrointestinal, gustatory, and respiratory cells. Of particular relevance to the studies completed for this thesis are the neurons regulating cardiovascular responses, gastrointestinal functions, and ingestive behaviors, and thus only these functions of NTS neurons will be discussed.

Regulation of cardiovascular function in the NTS

Classically, the “cardiovascular NTS” has been loosely localized in the dorsomedial caudal NTS and commissural NTS, with anatomical studies demonstrating labeling of neurons in these NTS regions following horseradish peroxidase or fluorescent dye injection into

baroreceptor areas of the aortic arch and carotid sinus, and chemoreceptor regions of the carotid body (Czachurski *et al.*, 1982;Claps & Torrealba, 1988;Torrealba & Claps, 1988;Mendelowitz *et al.*, 1992). In accordance with the anatomical distribution of baroreceptive afferents in the NTS, bilateral lesion studies in the rat demonstrate that ablation of the NTS at the level of the obex leads to a complete elimination of baroreflex responses. These rats also show severe arterial hypertension within minutes of anesthesia removal after lesioning, drastically increased peripheral resistance and left ventricular end diastolic pressure, and reduced cardiac output. These animals invariably die within 8 hours (Doba & Reis, 1973). Furthermore, stimulation of the aortic depressor nerve of the vagus or the carotid sinus nerve of the glossopharyngeal nerve, which transmit baroreceptor information from the periphery to the brain, result in activation of the NTS as detected electrophysiologically or by c-Fos expression (Deuchars *et al.*, 2000;Kumada & Nakajima, 1972;Dean & Seagard, 1995). Thus, these rather crude manipulations established the NTS as a key center in the mediation of baroreflexes.

The cellular effectors involved in the integration of cardiovascular information in the NTS have been extensively studied. It is well accepted that vagal baroreceptor inputs to NTS neurons are excitatory and that glutamate is a critical transmitter released from these fibres. Seminal studies providing evidence for glutamate as a baroreceptor transmitter were conducted by Reis and colleagues in the 1980s. These studies showed microinjection of glutamate into the medial NTS results in a potent depressor and bradycardic response, thus mimicking the baroreflex. These effects were selective to the NTS, as microinjection into neighboring regions elicited no effect. Conversely, microinjection of glutamate receptor antagonists into the NTS was shown to eliminate baroreflex responses and induce tachycardia and elevations in arterial pressure. Importantly, stimulation of vagal afferents results in increased levels of glutamate in

the NTS. Lesions of the nodose ganglia, where the cell bodies of arterial baroreceptors are located, result in a 50% decrease in glutamate uptake in the NTS (Reis *et al.*, 1981), as does sectioning of the vagus and glossopharyngeal nerves (Dietrich *et al.*, 1982), suggesting baroreceptor fibres projecting to NTS synthesize and release glutamate. Indeed, expression of the vesicular glutamate transporter 1 has been detected on axon terminals of cardiac vagal afferent fibres terminating in the NTS (Corbett *et al.*, 2005).

Following these whole animal studies strongly implicating glutamate in baroreceptor transmission, the ionotropic glutamate NMDA (Watanabe *et al.*, 1994) and non-NMDA receptors (Sato *et al.*, 1993) were localized in NTS neurons. Studies of glutamatergic signaling in the NTS then moved from the whole animal to *in vitro* preparations, where stimulation of the ST was used as a model of baroreceptor input to second order medial NTS neurons, presumed to be involved in cardiovascular processes due to their anatomical location. In all likelihood, these studies can be considered relevant to all types of ST tract input, not just baroreceptor input. Cellular studies by Andresen's group have shown that stimulation of the ST most frequently results in large excitatory postsynaptic currents (EPSCs) in the second order NTS neuron, reflecting monosynaptic inputs due to their short latency and low variability, with fewer neurons showing longer latency combinations of EPSCs and inhibitory postsynaptic currents (IPSCs) and, still fewer, only IPSCs (Andresen & Yang, 1995; Doyle & Andresen, 2001). Pharmacological studies have highlighted that antagonism of non-NMDA glutamate receptors leads to a complete block of EPSCs, while blockade of only NMDA receptors has a very minimal effect on synaptic transmission (Andresen & Yang, 1990). These *in vitro* studies highlighted the role of non-NMDA receptors as the main cellular conveyers of monosynaptic baroreceptive inputs to second order NTS neurons. Further experiments also revealed the

contribution of both non-NMDA and GABA_A receptors in mediating the unreliable IPSCs that are occasionally encountered, suggesting a polysynaptic pathway underlies these inhibitory events (Doyle & Andresen, 2001). Later experiments by the same group used a more direct approach to identify NTS neurons specifically receiving baroreceptor input. In these studies, rats were injected with an anterograde fluorescent dye in the aortic depressor nerve, which contains only baroreceptor afferents of the aortic arch. Thus any labelled neurons in the NTS could be reliably identified as baroreceptive. These experiments revealed labelled neurons were invariably excited by single stimulus shocks of the ST, and only EPSCs were observed in these cells, suggesting glutamatergic innervation of medial NTS neurons is strong, reliable and uniform (Andresen & Peters, 2008).

Briefly, numerous neuropeptides have also been shown to exert important cardiovascular effects via actions on NTS neurons. For example, microinjections of neuropeptide Y (NPY), neurotensin, and angiotensin II into the NTS induce bradycardia and depressor responses, while vasopressin and substance P cause tachycardia and pressor effects (Kubo & Kihara, 1990; Abdala *et al.*, 2003). Thus these *in vivo* studies highlight the remarkable integrative function of the NTS in mediating cardiovascular behaviors through the processing of multiple peptidergic influences.

Finally, after integrating baroreceptor afferent inputs, the NTS must relay this information to other structures which mediate behavioral responses. For example, the NTS communicates with the caudal ventrolateral medulla (CVLM) via glutamatergic projections. Activated CVLM neurons then send inhibitory GABAergic projections to neurons in the rostral ventrolateral medulla (RVLM). RVLM neurons are tonically active and excite sympathetic preganglionic motor neurons to regulate sympathetic outflow, thus their inhibition by CVLM neurons results in baroreflex behaviors (Schreihofer & Guyenet, 2002).

Regulation of gastrointestinal function and food intake in the NTS

In addition to receiving cardiovascular afferents, the NTS also receives visceral inputs pertaining to the metabolic status of the organism. More specifically, branches of the vagus nerve originating in the esophagus terminate in the central subregion of the NTS, those from the stomach in the medial, commissural and gelatinous NTS, and those from the small intestine in the medial and commissural NTS (Kalia & Mesulam, 1980b; Travagli *et al.*, 2006). The NTS is thus the gateway for the central processing of gut-derived signals, which are ultimately integrated to modulate feeding responses. The critical contribution of the NTS (and other hindbrain structures) to the regulation of gastrointestinal functions and ingestive behaviors is particularly evident in decerebrate rat models. These studies, in which all connections between the forebrain and the hindbrain at the level of the superior colliculus are severed, show that animals with only intact medullary connections are fully capable of processing signals regarding taste stimuli and gastric distension, can respond to the humoral signal cholecystokinin (CCK) which is released from the gut during a meal, and are also able to terminate a meal as assessed by measures of rejection to intraoral sucrose infusion (Grill & Norgren, 1978; Grill & Kaplan, 1992; Grill & Smith, 1988). These studies thus highlight that the hindbrain is sufficient to mediate satiation. It is important to emphasize, however, that while decerebrate rat models have shown the sufficiency of the hindbrain in mediating certain aspects of ingestive function, the NTS also has important ascending and descending connections with numerous extra-medullary regions which allow for a finer regulation of feeding behaviors. Indeed, the hypothalamus is also classically viewed as a core region governing the central control of food intake. In particular, the arcuate nucleus (ARC), which lies adjacent to the third ventricle (3V), contains two populations of neurons which exert opposing effects on ingestive behavior. These two populations of neurons

express NPY and agouti gene-related protein (AgRP), both of which stimulate feeding, or pro-opiomelanocortin (POMC) and cocaine and amphetamine related transcript (CART), which act to inhibit feeding. Additionally, the paraventricular nucleus (PVN), which also borders the 3V, receives extensive projections from the ARC, and thus serves as an integrator of numerous homeostatic systems (reviewed in (Smith & Ferguson, 2008) and see the section, “The Central Melanocortin System” in this general introduction). Importantly, the NTS has reciprocal connections with both the PVN and the ARC (Ricardo & Koh, 1978), and it is critical to recognize that ingestive behaviors ultimately result from coordinated cellular actions in multiple neuronal centers.

Signaling from gut to brain is evident as ingested food enters the stomach and causes gastric distension. Both gastric and duodenal nutrient loads are detected and integrated by the NTS, as evident by c-Fos expression (Emond *et al.*, 2001b) and altered excitability of neurons in the NTS (Barber & Burks, 1983; Ewart & Wingate, 1984). The gastric and intestinal responses to nutrient infusions are conveyed to the NTS via vagal transmission, as vagotomy attenuates the inhibitory effect of both of these processes on food intake (Barber & Burks, 1983; Yox *et al.*, 1991). In line with these findings, it is interesting to note differential effects of vagotomy on the ability of individual nutrients to suppress food intake. More specifically, vagotomy eliminates the feeding inhibitory effects of intestinally delivered maltose and oleic acid, while only attenuating the hypophagia induced by L-phenylalanine (Yox *et al.*, 1991).

The entry of food into the stomach and the small intestine also triggers the release of numerous humoral factors which contribute to the termination of the meal. These include duodenally released CCK (Lewis & Williams, 1990), glucagon-like peptide 1 (GLP-1) released by L endocrine cells of the small intestine (Kieffer & Habener, 1999), and leptin released by

gastric mucosa cells (Bado *et al.*, 1998). Indeed CCK, GLP-1, and leptin all cause increases in vagal afferent activity (Kakei *et al.*, 2002; Wang *et al.*, 1997). As is expected from these findings, intact vagal transmission is essential for the inhibitory effect of CCK and GLP-1 on food intake (Yox *et al.*, 1991; Abbott *et al.*, 2005), and for short term effects of leptin on feeding (Peters *et al.*, 2005). Importantly, the vagal activation induced by CCK, GLP-1 and leptin translates to increased expression of c-Fos by NTS neurons following peripheral injection of these peptides (Wang *et al.*, 1998; Parker *et al.*, 2013).

Much like cardiovascular inputs, vagal transmission of gut derived signals to the NTS is mediated by glutamatergic signaling. Blockade of NMDA receptors via intraperitoneal (Burns & Ritter, 1997) or fourth ventricle (4V) injection (Zheng *et al.*, 1999) has been shown to increase consumption of a sucrose solution. At the cellular level, NMDA receptor antagonism results in a decrease in the expression of c-Fos by dorsomedial, commissural, and gelatinous NTS neurons after gastric distension, highlighting the essential nature of vagal glutamatergic transmission from the gut to the NTS (Zheng *et al.*, 1999). The intake inhibitory effects of CCK are also abolished by 4V and direct NTS microinjections of NMDA receptor antagonists, and this again is reflected in attenuated c-Fos expression in the NTS after CCK treatment (Wright *et al.*, 2011). Finally, accumulation of glutamate in the NTS has been detected after consumption of a sucrose solution, reflecting a physiological context of glutamate-mediated anorexigenic effects (Bednar *et al.*, 1994).

In addition to receiving vagal inputs from the gastrointestinal tract, neurons in the NTS have also been shown to be sensitive to changes in levels of circulating glucose (Mizuno & Oomura, 1984; Dallaporta *et al.*, 1999; Balfour *et al.*, 2006; Wan & Browning, 2008a; Lamy *et al.*, 2014) and to centrally acting anorexigenic neuropeptides. For example, Grill and colleagues have

shown important effects of leptin acting in the NTS. Firstly, the leptin receptor is expressed by 30% of NTS neurons, and injections of leptin into the 4V or directly into the dorsal vagal complex (DVC, including NTS and dorsal motor nucleus of the vagus (DMV)) result in an inhibition of food intake and longer term reductions in body weight (Grill *et al.*, 2002). A direct contribution of the NTS to these anorexigenic effects is underscored by genetically modified rats which exhibit excessive food intake and weight gain, as well as increased white adipose tissue mass after knockdown of the signaling form of the leptin receptor specifically in the NTS (Hayes *et al.*, 2010). Furthermore, these behavioral effects are reflected at the single cell level, where patch clamp experiments have revealed excitatory effects of leptin on individual NTS neurons (Hisadome *et al.*, 2010). In addition to leptin, receptors for melanocortins (Kishi *et al.*, 2003), oxytocin (Baskin *et al.*, 2010), GLP-1 (Goke *et al.*, 1995), and NPY (Mahaut *et al.*, 2010) have also been localized on NTS neurons. Fourth ventricle administration of the anorexigenic peptide nesfatin-1 has been shown to decrease food intake by up to 41% in rats (Stengel *et al.*, 2009a), and melanocortin administration to the brainstem also decreases food intake and body mass (Grill *et al.*, 1998). Thus it is quite evident that a rather extensive list of feeding-related peptides exerts critical effects via the NTS.

Rather than a simple relay center for volumetric, nutritive, and humoral signals from the gut and neuropeptides of the brain, the NTS is capable of integrating these feeding-related inputs to shape ingestive behaviors. Several of these integrative functions have been reviewed by Schwartz in (Schwartz, 2006) and are described here with original references. Firstly, integration of multiple peripherally derived signals is evident in the NTS. For example, simultaneous induction of gastric distension and duodenal nutrient infusion elicits greater c-Fos expression in the NTS than either stimulation alone (Emond *et al.*, 2001b). Similarly, combined application of

CCK and induction of gastric distension also leads to enhanced c-Fos in the NTS compared to either stimulus alone (van de Wall *et al.*, 2005), thus suggesting an additive effect of gut derived signals on activation of NTS neurons. Adachi and colleagues have also demonstrated that NTS neurons responsive to gastric distension are sensitive to circulating glucose as well (Adachi *et al.*, 1995). Furthermore, the NTS integrates both peripheral and central signals to affect regulation of ingestive behaviors. It has been shown that central administration of leptin enhances the CCK or gastric load induced expression of c-Fos in the NTS (Emond *et al.*, 1999; Emond *et al.*, 2001a), and also the effects of gastric distension on NTS neuron firing frequency (Schwartz & Moran, 2002), highlighting a critical convergence of multiple inputs on these neurons. Interestingly, in contrast to the excitatory effects of leptin, the orexigenic peptide NPY decreases the responsiveness of NTS neurons to gastric distension, revealing the dynamic integrative capacity of these neurons to factors with opposing effects on feeding (Schwartz & Moran, 2002). Studies using rats with a knockdown of leptin receptor expression in the NTS have also demonstrated that intact leptin signaling in these neurons is actually required for the inhibitory effects of CCK on feeding (Hayes *et al.*, 2010), suggesting that the integration of metabolic signals in NTS neurons is essential for normal feeding responses. Similar synergistic signaling in the NTS is seen with the melanocortin-3/4 receptor agonist melanotan II (MTII) and CCK, since co-application of MTII (4V) and CCK (intraperitoneal) leads to enhanced intracellular signaling in NTS neurons compared to administration of either peptide alone. In addition, antagonism or genetic deletion of the melanocortin 4 receptor (MC4R) eliminates CCK induced intracellular signaling in NTS neurons as well as the inhibitory effect of CCK on food intake (Sutton *et al.*, 2005; Fan *et al.*, 2004), further emphasizing the necessity for the convergence of feeding related pathways onto NTS neurons.

Electrophysiological phenotypes of NTS neurons

NTS neurons express a typical array of neuronal voltage gated ion channels. These channels include L-type Ca^{2+} channels, which have a high threshold and are slowly inactivating, and T-type Ca^{2+} channels, which are activated at more hyperpolarized membrane potentials and rapidly inactivate (Kunze, 1987). Several potassium channels have been identified, including the transient A-type channel (I_A), the non-inactivating, slowly-developing potassium current I_K , and a calcium dependent potassium current. A tetrodotoxin sensitive voltage gated sodium channel has also been identified (Champagnat *et al.*, 1986; Moak & Kunze, 1993).

The expression of these conductances accounts for the electrophysiological phenotypes of NTS neurons. These include neurons with a prominent I_A current which display a delayed return to baseline membrane potential after a hyperpolarizing pulse (DE cells), and neurons with prominent T-type Ca^{2+} current which show a post-inhibitory rebound after the same hyperpolarizing pulse (PIR cells). Neurons which display neither of these characteristics have been termed NON cells (Dekin & Getting, 1984; Tell & Bradley, 1994; Vincent & Tell, 1997). Physiologically, these firing properties allow for intrinsic modulation of inputs from the ST. For example, prominent DE properties in second order NTS neurons will slow the processing of EPSPs into action potentials, thus dampening the excitability of these cells and, in turn, regulating the timing of the propagation of ST inputs (Bailey *et al.*, 2002). Furthermore, spontaneously hypertensive rats have been shown to have a shorter duration DE phase following hyperpolarizing pulses in medial NTS neurons, suggesting altered timing of transmission in these cells may contribute to the development of cardiovascular abnormalities (Sundaram *et al.*, 1997). In addition, the proportion of medial NTS neurons which display DE characteristics is decreased

with age, leading to speculation that this change in intrinsic membrane properties may contribute to the altered cardiovascular function associated with aging (Johnson & Felder, 1993).

In summary, the NTS is a complex structure, both in terms of its basic anatomy and the behaviors it integrates and mediates. While this discussion has provided a brief overview of the functions of this medullary structure, a more detailed examination of the expression and actions of two particular neuropeptides, nesfatin-1 and the melanocortins, as well as the function of medullary glucose sensing neurons, is especially relevant to the experiments performed toward the completion of this thesis.

NESFATIN-1 (Modified from (Mimee & Ferguson, 2013))

Nesfatin-1, an acronym for NEFA/nucleobindin2 encoded satiety and fat influencing protein, was discovered in 2006 by Oh-I and colleagues as they attempted to identify a novel peptide involved in the control of energy homeostasis (Oh-I *et al.*, 2006). This peptide is encoded by the nucleobindin2 (NUCB2) gene and is cleaved from a prohormone processed into three products, named nesfatin-1 (amino acids 1-82), nesfatin-2 (85-163) and nesfatin-3 (166-396). To date, only nesfatin-1 has been assigned a physiological role. While both central and peripheral expression patterns and effects of nesfatin-1 have been well described since its discovery, only CNS actions will be discussed here in light of the focus of this thesis on neuronal networks involved in the control of autonomic functions (for peripheral effects, see (Shimizu *et al.*, 2009; Zhang *et al.*, 2010; Gonzalez *et al.*, 2011; Li *et al.*, 2012; Angelone *et al.*, 2012; Li *et al.*, 2013a; Cao *et al.*, 2013)).

Anatomy of the central nesfatin-1 system

In their seminal study, Oh-I et al reported expression of NUCB2 in the ARC and PVN, as well as the lateral hypothalamic area (LHA) and supraoptic nucleus, effectively localizing

nesfatin-1 in classic feeding centers (Oh-I *et al.*, 2006). Within these nuclei, nesfatin-1 co-localizes with numerous neuropeptides involved in the coordination of feeding and drinking, as well as cardiovascular and stress responses, namely NPY, POMC, CART, as well as oxytocin, vasopressin, thyrotropin releasing hormone (TRH), and corticotropin releasing hormone (CRH) (Foo *et al.*, 2008; Brailoiu *et al.*, 2007). Outside of the hypothalamus, the medullary NTS shows dense expression of NUCB2/nesfatin-1 mRNA and protein, as do the nearby DMV, locus coeruleus, and Edinger Westphal nucleus, among others (Oh-I *et al.*, 2006; Brailoiu *et al.*, 2007; Foo *et al.*, 2008). Immunohistochemical studies in the NTS have revealed co-localization of NUCB2 with CART, POMC and tyrosine hydroxylase, while other brainstem nuclei have shown co-localization with choline acetyltransferase and serotonin in addition to these three peptides (Brailoiu *et al.*, 2007; Fort *et al.*, 2008). Thus the broad expression of nesfatin-1 throughout the brain, as well as its co-localization with numerous peptides involved in the control of several autonomic behaviors, support the emerging consensus discussed below that nesfatin-1 is implicated in the control of multiple physiological processes, such as cardiovascular regulation and the regulation of glycemia, in addition to its originally described role in the regulation of food intake.

Roles of centrally acting nesfatin-1 in the regulation of energy homeostasis

Oh-I *et al.* (2006) were the first to study the effects of nesfatin-1 when injected into the 3V. Using a modest, single dose of 5 pmol nesfatin-1, these authors reported a 50% decrease in dark cycle food intake over 6 hours in *ad libitum* fed rats, findings which have since been replicated, albeit at a higher dose (Maejima *et al.*, 2009). Chronic infusion of the same 5 pmol dose into the 3V over 10 days also caused potent anorexigenic effects which resulted in a 60% decrease in body weight gain and reductions in fat pad mass. Importantly, 3V administration of

antisense morpholino oligonucleotides designed to decrease endogenous levels of NUCB2 mRNA resulted in increases in food intake and body weight, thus establishing the critical physiological role of nesfatin-1 in the regulation of feeding (Oh-I *et al.*, 2006). Mechanistically, more recent analyses of the feeding microstructure of animals receiving intracerebroventricular (icv) nesfatin-1 have revealed the anorexigenic effects this peptide are the result of decreases in meal frequency and meal size (Goebel *et al.*, 2011).

Since the original findings of Oh-I *et al.*, injections of nesfatin-1 into the lateral ventricle (LV) have also been shown to dose dependently decrease food and water intake, as well as gastric emptying, and to lead to increases in energy expenditure (Yosten & Samson, 2009; Stengel *et al.*, 2009a; Goebel *et al.*, 2011; Konczol *et al.*, 2012; Stengel *et al.*, 2012; Yosten *et al.*, 2012; Konczol *et al.*, 2012; Wernecke *et al.*, 2014). Furthermore, localized microinjection studies have identified the PVN as the primary hypothalamic site mediating the anorexigenic effects of nesfatin-1 (Maejima *et al.*, 2009; Chen *et al.*, 2012), and neutralization of endogenous nesfatin-1 specifically in the PVN leads to increases in food intake (Sedbazar *et al.*, 2013). The pivotal role of the PVN in mediating at least a portion of the anorexigenic effects of nesfatin-1 is further emphasized by the dynamic expression pattern of NUCB2 in this nucleus during fasting and refeeding cycles, with circadian decreases in expression during hunger and increases in expression with feeding suppression (Oh-I *et al.*, 2006; Sedbazar *et al.*, 2013). Outside of the PVN, other microinjection studies have revealed less pronounced effects on food intake occurring via the LHA and the ventromedial hypothalamus (VMH) (Chen *et al.*, 2012). In addition, microinjections of nesfatin-1 into the ARC result in profound decreases in gastric motility (Li *et al.*, 2013b), thus revealing a rather broad hypothalamic circuitry engaged by this anorexigenic peptide.

While the hypothalamic sites of nesfatin-1 action have been relatively well studied, far less is known about the medullary effects of nesfatin-1. Injections of nesfatin-1 into the 4V and cisterna magna have been shown to result in a maximum 41% and 60%, respectively, dose dependent decrease in dark phase food intake, (Stengel *et al.*, 2009a; Xia *et al.*, 2012). More targeted studies have identified the DMV and NTS as nuclei activated by nesfatin-1. For example, a 4V injection of nesfatin-1 which decreases food intake and vagally mediated gastric acid secretion results in activation of the DMV, as measured by increased c-Fos expression (Xia *et al.*, 2012). More targeted microinjections of nesfatin-1 into the DVC (including the NTS, DMV, and AP) also induce acute anorexigenic effects over a 6 hour period (maximum 69% decrease in food intake), and chronic decreases in body weight gain (maximum 59% decrease) over a 10 day period with daily peptide injections. It should be noted that doses used in these studies (minimum 15 pmol) were indeed larger than those used for injections into the 3V or LV (Dong *et al.*, 2014). In addition to activating discrete brain nuclei, nesfatin-1 has also been shown to induce increases in cytosolic Ca²⁺ in nodose ganglia of the vagal afferent nerve (Iwasaki *et al.*, 2009).

Indirect activation of medullary nuclei also occurs after peripheral and hypothalamic injections of nesfatin-1. For example, intraperitoneal injections of nesfatin-1 which suppress food intake by 50% cause selective increases in c-Fos expression in the NTS and the adjacent AP, and also increase POMC and CART expression in the NTS (Shimizu *et al.*, 2009). Similarly, LV injections of nesfatin-1 have also been shown to upregulate POMC expression in the NTS (Wernecke *et al.*, 2014). Thus an attractive hypothesis is nesfatin-1 acts to reduce food intake, in part, by selectively activating POMC and/or CART expressing neurons in the NTS. Furthermore, a current model explaining the anorexigenic effects of hypothalamic nesfatin-1 involves

activation of the NTS to ultimately produce reductions in food intake. Maejima et al (2009) demonstrated that 3V administration of nesfatin-1, and microinjection of the peptide into PVN, both result in c-Fos expression in the NTS, thus establishing a nesfatin-1 induced serial activation pattern from hypothalamus to brainstem. Specifically, the authors proposed that nesfatin-1 activates PVN oxytocin neurons, which project to and activate POMC neurons in the NTS, effectively suggesting the brainstem POMC circuitry as the ultimate effector of hypothalamic nesfatin-1 anorexigenic effects (Maejima *et al.*, 2009). Indeed, both intact melanocortin and oxytocin signaling are required for nesfatin-1 to exert its effects on food intake, as antagonism of the receptors of either of these peptides abolishes the anorexigenic effects of nesfatin-1 (Oh-I *et al.*, 2006; Maejima *et al.*, 2009; Yosten & Samson, 2010). Other groups have also highlighted the necessity of CRH signaling at the level of the hypothalamus, but not brainstem, in mediating the effects of nesfatin-1 on food intake, thereby suggesting potentially separate mechanisms underlying the effects of nesfatin-1 on feeding between these two central regions (Stengel *et al.*, 2009a).

At the single cell level, studies from our laboratory have focused on the hypothalamus and have shown that nesfatin-1 exerts both direct depolarizing and hyperpolarizing effects on the membrane potential of neurons in slices obtained from the PVN (Price *et al.*, 2008a) and ARC (Price *et al.*, 2008b). Using our *post-hoc* single cell reverse transcription PCR (RT-PCR) technology, we demonstrated an inhibitory effect of nesfatin-1 on ARC NPY expressing neurons, thus identifying another component of the complex circuitry mediating the anorexigenic effects of nesfatin-1 (Price *et al.*, 2008b). We observed more heterogeneous effects of nesfatin-1 on PVN neurons, noting both depolarizing and hyperpolarizing actions of nesfatin-1 on oxytocin, vasopressin, CRH and TRH neurons in this nucleus (Price *et al.*, 2008a).

Taken together, these studies highlight the broad range of central regions and cell types influenced by nesfatin-1 to ultimately regulate energy homeostasis.

Roles of centrally acting nesfatin-1 in the control of glucose homeostasis

In addition to its direct effects on food intake, nesfatin-1 also regulates the global energy status of the organism through central effects on glucose homeostasis. For example, 3V injection of nesfatin-1 has been shown to increase insulin sensitivity and glucose uptake in muscle, while also decreasing circulating triacylglycerol levels and hepatic glucose production in rats (Yang *et al.*, 2012). These effects are abolished by short hairpin RNA mediated knockdown of hypothalamic NUCB2 (Wu *et al.*, 2014), although the effectiveness of this knockdown approach on NUCB2 expression is suboptimal.

At the cellular level, nesfatin-1 influences the firing rate of glucose sensing neurons in several hypothalamic nuclei as assessed by extracellular recording techniques. More specifically, glucose inhibited neurons of the PVN increase, while those of the LHA decrease, their firing rate in response to nesfatin-1. Furthermore, the firing rate of glucose excited neurons of the VMH is augmented by the peptide (Chen *et al.*, 2012). One study by Dong *et al.* (2014) also suggests preferential excitatory effects of nesfatin-1 on glucose excited neurons and inhibitory effects on glucose inhibited neurons in the DVC. In addition, insulin-induced hypoglycemia has been shown to activate nesfatin-1 expressing neurons in the ARC, PVN, LHA, NTS and DMV, as assessed by c-Fos expression (Bonnet *et al.*, 2013). The precise physiological consequences of these central findings relating nesfatin-1 and glucose handling, however, remain to be fully elucidated.

Roles of centrally acting nesfatin-1 in the control of cardiovascular function

Several *in vivo* studies have established a definitive role for nesfatin-1 in the central control of cardiovascular function. Indeed, injections of this peptide into the LV elicit dose dependent increases in mean arterial pressure (MAP) via a melanocortin, oxytocin, and CRH dependent pathway engaging the sympathetic autonomic nervous system (Yosten & Samson, 2009; Yosten & Samson, 2010; Yosten & Samson, 2014). Furthermore, bradycardic effects of the peptide are elicited after microinjections into the nucleus ambiguus (Brailoiu *et al.*, 2013). Collectively, these findings emphasize the roles of both the hypothalamus and brainstem as critical effectors of the cardiovascular effects of the peptide.

Nesfatin-1 signaling

At the present time, the nesfatin-1 receptor remains unknown, representing a significant hurdle in the progression of the delineation of its central mechanism of action. A limited number of studies have, however, attempted to uncover the intracellular signaling cascades engaged by this peptide. For example, using both cultured hypothalamic cells and preganglionic cardiac vagal neurons from the nucleus ambiguus, Brailoiu *et al.* (2007, 2013) have demonstrated that pre-treatment with pertussis toxin, a blocker of $G_{i/o}$ G protein coupled receptors (GPCRs), inhibits nesfatin-1 induced increases in intracellular Ca^{2+} . Additional treatment with an inhibitor of protein kinase A (PKA) also blunts nesfatin-1 activation of hypothalamic cells, thereby implicating intracellular cyclic adenosine monophosphate (cAMP) as an effector of nesfatin-1 actions (Brailoiu *et al.*, 2007). However, other groups using a neuroblastoma cell line found no evidence suggesting nesfatin-1 mediated increases in PKA activity or cAMP levels, but rather the involvement of both cAMP response element binding protein (CREB) and mitogen activated protein kinase (MAPK) kinase (Ishida *et al.*, 2012). Others still have suggested the necessity of

the serine-threonine kinase intracellular fuel sensor mammalian target of rapamycin (mTOR) in mediating the anorexigenic effects of nesfatin-1 (Zhang *et al.*, 2013). Thus at the present time there is evidently no clear consensus on the intracellular mechanism of central nesfatin-1 actions.

THE CENTRAL MELANOCORTIN SYSTEM

Anatomy of the central melanocortin system

Perhaps one of the most well studied central anorexigenic circuitries is that of the melanocortin system, comprised of the melanocortin receptors, the precursor peptide POMC and its cleavage products (including α -MSH), and the endogenous melanocortin-3 and -4 receptor antagonist, AgRP (Cone, 2005;Raffin-Sanson *et al.*, 2003;Bicknell, 2008). Descriptions of POMC cleavage products date back to as early as the 1950s (Lee & Lerner, 1956;Harris & Lerner, 1957), and of POMC itself to the late 1970s (Nakanishi *et al.*, 1979). The expression of POMC neurons in the CNS is limited to only two regions: the ARC and the commissural NTS, which contains a much smaller population of only ~200-300 POMC neurons as compared to the ~3000 in the ARC (Jacobowitz & O'Donohue, 1978;Joseph *et al.*, 1983;Cowley *et al.*, 2001;Cone, 2005;Huo *et al.*, 2006). Indeed, α -MSH levels are 11 fold higher in the ARC than the NTS (Li *et al.*, 2007). POMC neurons of the ARC send extensive projections throughout both the forebrain and hindbrain, including fibres to the PVN, and medial and commissural NTS (Jacobowitz & O'Donohue, 1978;Palkovits *et al.*, 1987). NTS POMC neurons, however, have a more limited fibre distribution within the medulla (Pilcher & Joseph, 1986). With particular reference to the NTS, studies using decerebrate rats have revealed 70% of α -MSH immunoreactive fibres in this medullary nucleus arise from ARC POMC neurons, with only 30% of NTS origin (Palkovits *et al.*, 1987;Zheng *et al.*, 2010). In the line with the expansive reach of α -MSH fibres within the brain is the broad expression of the α -MSH receptor, the MC4R,

discovered in 1993 (Gantz *et al.*, 1993). In situ hybridization studies have localized the MC4R in many central structures involved in the control of ingestive behaviors, including the PVN, dorsal and ventral hypothalamic areas, LHA, NTS and DMV (Kishi *et al.*, 2003), while immunohistochemical studies using mice expressing green fluorescent protein under the control of the MC4R have shown analogous patterns of expression (Liu *et al.*, 2003). It should be noted that while this discussion is focused on the role of the MC4R, there are a total of five melanocortin receptors with differential agonist affinities and expression patterns throughout the body. In particular, α -MSH is also an agonist of the centrally expressed melanocortin 3 receptor (MC3R) (reviewed in (Abdel-Malek, 2001)). All melanocortin receptors, however, are G_s coupled seven transmembrane GPCRs. When bound to their melanocortin agonist, these receptors activate adenylyl cyclase, leading to increases in intracellular levels of cAMP (Gantz *et al.*, 1993; Abdel-Malek, 2001). Alternative signaling pathways have also been described for the MC4R (Breit *et al.*, 2011). Finally, another component of the melanocortin circuitry, AgRP is selectively expressed by ARC neurons in the CNS, where it is co-localized with the orexigenic peptide NPY. These neurons show a dense fibre network within the ARC, and send more distant projections to the PVN, LHA, DMH and NTS, to name a few. It is interesting to note the hypothalamic innervation pattern of AgRP neurons largely mirrors the projections ARC POMC neurons (Broberger *et al.*, 1998; Bagnol *et al.*, 1999).

Roles of the central melanocortin system in the regulation of energy homeostasis

Genetic evidence

The prominent role of the melanocortin system in the control of energy homeostasis is evident upon examination of animals, and humans, with mutations in components of this circuitry. For example, mutant POMC-null mice show not only increased food intake, but also an

inability to regulate food intake in accordance with the caloric density of foods to maintain energy homeostasis, thus leading to the development of severe early-onset obesity (Yaswen *et al.*, 1999). Similarly, mutations in humans leading to a lack of POMC or of some of its cleavage products, including α -MSH, result in early onset overeating and childhood obesity (Krude *et al.*, 1998). Overexpression of the MC3/4R antagonist AgRP also leads to hyperphagia and obesity in mice (Ollmann *et al.*, 1997). Strikingly, the orexigenic effects of AgRP are essential for feeding, as ablation of ARC AgRP neurons in adulthood leads to starvation (Luquet *et al.*, 2005;Gropp *et al.*, 2005). Furthermore, the essential function of the MC4R in mediating the anorexigenic effects of α -MSH is underscored by the pronounced obesity and hyperphagia of MC4R-null mice (Huszar *et al.*, 1997;Balthasar *et al.*, 2005), with similar phenotypes observed in humans with mutations in this gene. Indeed, MC4R mutations are encountered in 3-4% of morbidly obesity individuals, and therefore represent the most common monogenic cause of obesity in humans (Farooqi *et al.*, 2000;Vaisse *et al.*, 2000). In addition to hyperphagia, MC4R knockout animals also show disrupted metabolism, evident when they are pair fed with control animals, yet gain more weight and display increased adiposity as compared to controls (Ste *et al.*, 2000). These mutant animals also do not show the increase in energy expenditure induced by injection of MTII in wild type animals (Balthasar *et al.*, 2005). Taken together, these findings highlight the necessity of the MC4R in mediating the central effects of melanocortins on metabolism.

Pharmacological, molecular and cellular evidence

In addition to genetic studies identifying the critical contribution of the melanocortin system to the regulation of energy homeostasis, numerous *in vivo* studies have clearly revealed the anorexigenic effects of centrally acting α -MSH. For example, injections of α -MSH or MTII into the 3V at concentrations as low as 100 pmol lead to dose dependent decreases in food intake

of up to 45% over 6 hours (Tsujii & Bray, 1989; Thiele *et al.*, 1998). These anorexigenic effects are the result of decreases in meal size and duration, but not meal frequency (Azzara *et al.*, 2002). Similar anorexigenic effects of both α -MSH (1.2 mmol) (Ludwig *et al.*, 1998) and MTII (3 nmol) (Fan *et al.*, 1997) are evident upon LV administration of these peptides, resulting in 50% decreases in food consumption over the same 6 hour time frame. Conversely, 3V and LV injections of the MC3/4R antagonist SHU9119 elicit increases in food intake of approximately 40% which persist for 12-24 hours (Fan *et al.*, 1997; Rossi *et al.*, 1998), while AgRP administered to the 3V elicits more potent hyperphagia (84%) over 24 hours (Rossi *et al.*, 1998). Elegant recent optogenetic experiments which selectively activated AgRP neurons also demonstrated the intense feeding response initiated within minutes of excitation of these cells (Aponte *et al.*, 2011). Furthermore, targeted microinjections of lower doses of MTII (10, 50, 600 pmol), α -MSH (600 pmol) and SHU9119 directly into the PVN have induced comparable results as ventricular injections (Giraudo *et al.*, 1998; Cowley *et al.*, 1999; Wirth *et al.*, 2001), and result in c-Fos expression in this nucleus (Singru *et al.*, 2012), thus highlighting the importance of endogenous actions of α -MSH in the PVN in controlling feeding behavior. These findings naturally narrowed attention to the hypothalamus as a primary site of action for melanocortins, and indeed a distinctive hypothalamic circuitry engaged by melanocortins to affect ingestive behavior has been delineated. As mentioned above, two separate populations of neurons are present in the ARC: anorexigenic POMC neurons, and orexigenic AgRP/NPY neurons (Cone, 2005). Electrophysiological evidence has demonstrated AgRP/NPY neurons in the ARC exert a GABAergic inhibitory influence on POMC neurons, and NPY has been shown to hyperpolarize POMC neurons as well. Together, these inhibitory inputs presumably lead to a decrease in melanocortin signaling and, thus, an increased drive to feed. Anatomically, NPY

immunoreactive axon terminals do indeed make close appositions with ARC POMC cells, and these terminals co-express GABA. This circuit can also be modified by other peptides involved in the control of food intake. For example, the anorexigenic adipokine leptin has been shown to exert direct depolarizing effects on ARC POMC neurons, and to disinhibit these cells by hyperpolarizing NPY neurons, thus decreasing GABAergic tone from NPY cells (Cowley *et al.*, 2001). Similar reciprocal actions of serotonin, which decreases food intake (Heisler *et al.*, 2002; Heisler *et al.*, 2006), and ghrelin, which stimulates food intake (Cowley *et al.*, 2003), on the melanocortin circuitry of the ARC have also been described. Projections from both ARC POMC and AgRP/NPY neurons are processed at the level of the PVN. This integration is evident from both the microinjection studies described above, and electrophysiological studies showing single neurons respond to both MTII and NPY, with opposing actions of these two peptides on evoked IPSCs in neurons recorded from PVN slices (Cowley *et al.*, 1999). Loose patch recordings have also revealed α -MSH induced increases, and AgRP induced decreases, in the firing frequency of MC4R expressing PVN neurons, while whole cell recordings show depolarizing effects of α -MSH on 96% of these MC4R expressing cells (Ghamari-Langroudi *et al.*, 2011). Collectively, these findings have established a distinct hypothalamic circuitry that is finely regulated by opposing actions of anorexigenic and orexigenic components of the central melanocortin circuitry.

In addition to hypothalamic sites of action for melanocortins, these peptides also act in the brainstem to influence energy homeostasis. Anorexigenic effects mediated by medullary MC3/4Rs are evident upon 4V injection of 0.1 nmol MTII, which elicits decreases in food intake of approximately 50% persisting for up to 24 hours, while SHU9119 induces increases in food intake of 60% over the same period. Notably, these hindbrain effects are essentially identical to

those induced by the same injections into the LV (Grill *et al.*, 1998), and again are the result of decreases in meal size but not meal frequency (Zheng *et al.*, 2005). Furthermore, tenfold lower doses of MTII and SHU9119 injected directly into the DVC produce similar effects on feeding as injections into the 4V, highlighting the role of these particular neuronal structures in mediating the medullary anorexigenic effects of melanocortins (Williams *et al.*, 2000). Indeed, the NTS may be the ultimate effector of the actions of melanocortins on food intake, as microinjection of SHU9119 directly to the NTS abolishes the hypophagia elicited by leptin induced activation of hypothalamic POMC neurons (Zheng *et al.*, 2010), and direct administration of α -MSH to the PVN leads to c-Fos expression in the NTS (Singru *et al.*, 2012). Furthermore, α -MSH and MTII injections into the NTS result in decreases in gastric motility and tone, while these compounds produce differential effects on gastric contractions after DMV microinjection (Richardson *et al.*, 2013). At the cellular level, electrophysiological studies have shown NTS POMC neurons respond to metabolically relevant signals, such as anorexigenic CCK and orexigenic opioids (Appleyard *et al.*, 2005). Moreover, α -MSH enhances glutamatergic vagal inputs onto NTS neurons via presynaptic mechanisms (Wan *et al.*, 2008), and depolarizes, and increases the frequency of IPSCs of, antrum projecting DMV neurons (Richardson *et al.*, 2013).

Melanocortin circuits are not only influenced by peptides implicated in the control of ingestive behaviors, but are also dynamically regulated by the energy status of the organism. For example, 48 hour fasting increases mRNA levels of AgRP by thirteen to twentyfold (Mizuno & Mobbs, 1999), decreases POMC mRNA in the ARC by 60-80% (Mizuno *et al.*, 1998) and in the NTS by 50% (Perello *et al.*, 2007), and increases the number of available binding sites on MC4Rs in the hypothalamus (Harrold *et al.*, 1999). Conversely, feeding increases ARC POMC

mRNA by 180% (Hagan *et al.*, 1999). Functionally, the elevations in AgRP expression during fasting correlate with an increase in the firing frequency of AgRP neurons (Takahashi & Cone, 2005), while feeding has been shown to activate 21% and 13% of ARC and NTS POMC neurons, respectively, as assessed by c-Fos expression (Fan *et al.*, 2004). Furthermore, in line with the evidence of projections from ARC cells to the PVN, fasting also results in an increase in firing frequency of MC4R expressing PVN neurons (Ghamari-Langroudi *et al.*, 2011). Interestingly, while the fasting induced decreases in POMC mRNA in the ARC correlate with decreased levels of α -MSH in the region, levels of α -MSH in the NTS actually increase after fasting despite decreases in POMC expression in this nucleus (Perello *et al.*, 2007). Thus it is evident there is complex, multipronged, and differential regulation of hypothalamic and brainstem melanocortin systems in line with changing energy stores.

In addition to the hypophagia elicited by α -MSH, this peptide also influences energy homeostasis by increasing energy expenditure, partly by enhancing thermogenesis in brown adipose tissue (BAT). Anatomically, numerous MC4R expressing central nuclei, including the PVN and NTS for example, send projections to BAT (Zheng *et al.*, 2005; Voss-Andreae *et al.*, 2007). Indeed, 4V administration of MTII leads to sympathetically mediated increases in both core and BAT temperatures for 6 hours, as well as elevated mRNA expression of the thermogenic effector, uncoupling protein-1. These effects on energy expenditure persist in decerebrate rats, highlighting the sufficiency of brainstem melanocortineric signaling in eliciting them (Williams *et al.*, 2003; Skibicka & Grill, 2008). Furthermore, the effects of melanocortins on energy expenditure appear to be mediated by MC4R expression in sympathetic, but not parasympathetic, pathways whose activity is enhanced by MC4R agonists (Rossi *et al.*, 2011; Sohn *et al.*, 2013; Berglund *et al.*, 2014).

Roles of the central melanocortin system in the control of glucose homeostasis

Central actions of melanocortins have also been shown to elicit potent effects on both glycemia and insulin secretion. For example, global MC4R knockout mice are both hyperglycemic and hyperinsulinemic, an effect recapitulated by selective knockout of this receptor in choline acetyltransferase expressing sympathetic and parasympathetic preganglionic neurons (Huszar *et al.*, 1997; Berglund *et al.*, 2014). Mice overexpressing AgRP also show hyperglycemia and hyperinsulinemia (Graham *et al.*, 1997). Pharmacological studies support these genetic findings, with LV administration of MTII and 3V injections of α -MSH producing decreases in plasma insulin levels, while improving tissue glucose uptake and inhibiting glucose production (Fan *et al.*, 2000; Obici *et al.*, 2001). Conversely, 3V administration of SHU9119 elicits increases in both serum insulin and glucagon (Adage *et al.*, 2001), highlighting the range of central melanocortin effects on the secretion of glucose regulating pancreatic peptides, and consequent handling of circulating glucose.

Roles of the central melanocortin system in the control of cardiovascular function

The central actions of melanocortins extend beyond the regulation of energy homeostasis and glucose handling to include effects on the cardiovascular system. Indeed, acute LV injections of α -MSH to conscious rats result in sympathetically mediated increases in MAP and heart rate (HR) (Dunbar & Lu, 2000; Hill & Dunbar, 2002), while 4V administration of MTII elicits increases in HR in both neurologically intact and decerebrate animals (Skibicka & Grill, 2008). While the consequences of ventricular injections of melanocortins on cardiovascular parameters are clear, the results of targeted microinjections of MTII or α -MSH into the NTS are not consistent. Some authors have reported bradycardic and hypotensive effects in anesthetized animals (Li *et al.*, 1996; Pavia *et al.*, 2003; Tai *et al.*, 2007), while others have documented

tachycardic effects in conscious animals (Skibicka & Grill, 2009). Indeed, collectively, while the hypothalamic melanocortinergic circuitries appear relatively well understood, much work remains to be done to elucidate the full contribution of medullary melanocortin signaling in the regulation of homeostasis in the whole animal.

CENTRAL GLUCOSE SENSING NEURONS

Location of central glucose sensing neurons

While glucose is used by all neurons as their main source of energy, certain populations of neurons across the brain use glucose to regulate their excitability in addition to their metabolic needs. Two types of glucose sensing neurons exist: those which are excited by increases in glucose concentrations and inhibited by decreases in glucose are termed glucose excited (GE), while those which are inhibited by increases in glucose and excited by decreases in glucose are referred to as glucose inhibited (GI). Neurons which do not respond to changes in extracellular glucose concentrations are termed non-responsive (NR). The existence of such glucose sensing neurons was demonstrated in the hypothalamus as early as 1964. Indeed, bolus intravenous injections of glucose or insulin were shown to elicit reciprocal effects in the lateral hypothalamus, the “feeding” center, and the ventromedial hypothalamus, the “satiating” center, with glucose decreasing and increasing, respectively, the firing frequency of individual, extracellularly recorded neurons in each of these regions (Anand *et al.*, 1964; Oomura *et al.*, 1964). Since these early studies, many populations of glucose sensing neurons have been described throughout the brain, including in the subfornical organ (Medeiros *et al.*, 2012), PVN (Melnick *et al.*, 2011), ARC (Muroya *et al.*, 1999; Ibrahim *et al.*, 2003), NTS (Dallaporta *et al.*, 1999), DMV (Balfour & Trapp, 2007), and AP (Riediger *et al.*, 2002).

Functions of central glucose sensing neurons

While hypothalamic glucose sensing neurons have perhaps been the most thoroughly studied at the cellular level (see (Levin *et al.*, 2011;Karnani & Burdakov, 2011)), a strong argument exists that those located in the hindbrain may in fact be of greater physiological importance. For example, central glucose sensing neurons contribute to the mounting of counterregulatory responses to hypoglycemia. This response occurs when circulating glucose levels fall below 2-3 mM, and results in feeding and activation of the sympathoadrenal axis, leading to increases in epinephrine, norepinephrine, and glucagon in order to promote hepatic glycogenolysis and inhibit insulin secretion. These responses collectively increase plasma, and therefore brain, glucose concentrations (Routh, 2002). The critical, and potentially sufficient, role of medullary glucose sensing neurons in detecting the hypoglycemia which precipitates the induction of feeding and the counterregulatory response is evident from studies using decerebrate rats. In intact animals, hypoglycemia induced by intraperitoneal injection of the glucose antimetabolite 2-deoxy-D-glucose (2DG) results in subsequent activation of the sympathoadrenal axis, and therefore elevations in circulating glucose levels in order to restore euglycemia. Importantly, these responses to 2DG persist in chronic decerebrate animals, highlighting the sufficiency of caudal brainstem centers in mediating counterregulatory responses (DiRocco & Grill, 1979). Insulin induced feeding responses are also preserved in decerebrate animals (Flynn & Grill, 1983). In addition, administration of another glucose antimetabolite, 5-thio-D-glucose (5TG), into both the LV and 4V also results in increases in plasma glucose concentrations and elicits feeding responses. A critical role for the hindbrain in mediating these glycemic responses is underscored by the fact that blockade of the cerebral aqueduct (through which CSF flows from LV to 4V) eliminates the increases in circulating

glucose levels and feeding induced by LV, but not 4V, administration of 5TG (Ritter *et al.*, 1981). Indeed, microinjections of 5TG into various medullary nuclei, including the NTS, increase both plasma glucose concentrations and food intake, while microinjections into hypothalamic areas do not (Ritter *et al.*, 2000). Furthermore, c-Fos immunoreactivity has been detected in noradrenergic neurons of the NTS after subcutaneous injection of 2DG (Ritter *et al.*, 1998). It is also interesting to note that recent optogenetic experiments selectively activating GI neurons in the NTS have been shown to elicit vagal activation and increases in glucagon secretion (Lamy *et al.*, 2014). Evidence thus points to an important role of medullary, and specifically NTS, glucose sensing neurons in detecting fluctuations in cellular energy supplies and in mediating at least a portion of the reflexive responses engaged to restore ideal glycaemic conditions. Beyond these roles, glucose sensing neurons in the NTS have also been shown to regulate gastric secretion and gastric motility (Kadekaro *et al.*, 1980; Ferreira, Jr. *et al.*, 2001), processes which may also ultimately contribute to the control of food intake.

Mechanism of glucose detection

Despite the fact that the existence of central glucose sensing neurons has been appreciated for over 60 years, the understanding of the mechanisms by which these cells detect fluctuations in extracellular glucose concentrations remains incomplete. Parallels have, however, been drawn between GE neurons and pancreatic β -cells. In this model, increases in extracellular glucose levels lead to transport of glucose into neurons via high affinity glucose transporters. Subsequent phosphorylation and glycolysis by glucokinase results in increases in intracellular ATP, leading to the closure of ATP sensitive K^+ channels (K_{ATP} channels). The closure of these channels depolarizes the neuron, and in turn activates voltage sensitive Ca^{2+} channels, thus initiating influx of Ca^{2+} into the neuron. The opposite cellular response occurs upon decreases in

extracellular glucose concentration. While K_{ATP} channels do appear to be necessary mediators of GE neuronal glucose sensing, they are not sufficient for glucose sensing capabilities in these cells and, in fact, are also expressed in neurons which do not have glucose sensing properties (Levin *et al.*, 2004). Indeed, glucokinase, AMPK, and a sodium-glucose co-transporter have also been suggested to underlie glucose sensing mechanisms in GE neurons. While GI neuron glucose sensing is much less understood, glucokinase has again been identified as a potential key mediator of this process in these cells, as has a Cl^- channel, and a leak K^+ channel (Levin *et al.*, 2011). Briefly stated, however, it ultimately remains unclear how GE and GI neurons sense, and alter their excitability in response to, changes in extracellular glucose concentrations.

Statement of the problem

Despite the current knowledge of the expression of NUCB2/nesfatin-1 and the MC4R in the NTS, few investigations have been conducted to thoroughly delineate the cellular roles for both nesfatin-1 and α -MSH in this critical medullary nucleus, and how the effects of these peptides may be modulated by glycemic state. Furthermore, while glucose sensing neurons have been identified in the NTS, the studies on this topic conducted to date have made usage of only non-physiological extracellular glucose concentration. This thesis has therefore been completed to test two hypotheses:

1. That the NTS contains neurons capable of sensing, and integrating, nesfatin-1, α -MSH, and changes in extracellular glucose at the cellular level.
2. That alterations in extracellular glucose concentrations modify the responsiveness of NTS neurons to nesfatin-1 and α -MSH.

Cellular studies have been performed using *in vitro* electrophysiological techniques to record mainly from cells in brainstem slice preparations, and in one instance from dissociated neurons. Molecular biology has also been used to characterize the identity of nesfatin-1 responsive neurons in the NTS, and *in vivo* microinjection techniques have been employed to assess the cardiovascular effects of nesfatin-1 acting in the NTS. Chapter 2 (manuscript 1) delineates the effects of nesfatin-1 on the membrane potential of electrophysiologically and genetically defined NTS neurons. *Post-hoc* RT-PCR studies are performed to characterize nesfatin-1 responsive neurons, while *in vivo* microinjection experiments assess the effects of nesfatin-1 application in the medial NTS on blood pressure and heart rate. Chapter 3 (manuscript 2) examines the direct and indirect effects of α -MSH on the excitability of NTS neurons using current-clamp recordings, and reveals actions of this peptide on inhibitory GABAergic

neurotransmission in the NTS using the voltage-clamp recording configuration. Chapter 4 (manuscript 3) investigates whether the NTS contains physiologically relevant glucose sensing neurons, and how changes in extracellular glucose concentrations modulate the effects of nesfatin-1 and α -MSH on NTS neurons.

CHAPTER 2: Nesfatin-1 influences the excitability of neurons in the nucleus of the solitary tract and regulates cardiovascular function

Abstract

Nesfatin-1 has been identified as one of the most potent centrally acting anorexigenic peptides, and it has also been shown to play important roles in the control of cardiovascular function. *In situ* hybridization and immunohistochemical studies have revealed the expression of nesfatin-1 throughout the brain and, in particular, in the medullary autonomic gateway known as the nucleus of the solitary tract (NTS). The present study was thus undertaken to explore the cellular correlates and functional roles of nesfatin-1 actions in the medial NTS (mNTS). Using current-clamp electrophysiology recordings from mNTS neurons in slice preparation, we show that bath applied nesfatin-1 directly influences the excitability of the majority of mNTS neurons by eliciting either depolarizing (42%, mean 7.83 ± 0.84 mV) or hyperpolarizing (21%, mean -8.23 ± 1.00 mV) responses. These responses were observed in all electrophysiologically defined cell types in the NTS, and were site specific and concentration dependent. Furthermore, *post-hoc* single cell RT-PCR revealed a depolarizing action of nesfatin-1 on NPY and NUCB2 expressing mNTS neurons. We have also correlated these actions of nesfatin-1 on neuronal membrane potential with physiological outcomes, using *in vivo* microinjection techniques to demonstrate that nesfatin-1 microinjected into the mNTS induces significant increases in both blood pressure (mean AUC = 3354.1 ± 750.7 mmHg*sec, $n = 6$) and heart rate (mean AUC = 164.8 ± 78.5 beats, $n = 6$) in rats. Our results provide critical insight into the circuitry and physiology involved in the profound effects of nesfatin-1, and highlight the NTS as a key structure mediating these autonomic actions.

Introduction

Nesfatin-1 has been identified as one of the most potent centrally acting anorexigenic peptides (Oh-I *et al.*, 2006). An 82 amino acid cleavage product of the nucleobindin-2 (NUCB2) protein, nesfatin-1 acutely and chronically reduces feeding in rodents when injected either intracerebroventricularly or peripherally, and these effects are dependent upon melanocortin and oxytocin signaling (Oh-I *et al.*, 2006; Shimizu *et al.*, 2009; Maejima *et al.*, 2009; Yosten & Samson, 2010). Furthermore, treatment with nesfatin-1 neutralizing antibodies markedly increases food consumption and weight gain in animals, underscoring the critical physiological, tonic inhibitory control this peptide exerts over ingestive behaviours (Oh-I *et al.*, 2006). In addition to its remarkable effects on food intake, nesfatin-1 has also been shown to play important roles in the control of cardiovascular function, water intake, blood glucose regulation, stress responses, and puberty onset (Yosten & Samson, 2009; Su *et al.*, 2010; Goebel *et al.*, 2009b; Garcia-Galiano *et al.*, 2010).

In line with its numerous functions, comprehensive immunohistochemical studies have revealed a widespread distribution of nesfatin-1 throughout the brain. Notably, the nesfatin-1 peptide is strongly expressed in regions involved in the control of energy homeostasis and autonomic function in both hypothalamic and medullary centers (Foo *et al.*, 2008), including the autonomic gateway known as the nucleus of the solitary tract (NTS). Furthermore, central or peripheral injections of nesfatin-1 result in c-Fos expression in NTS neurons (Maejima *et al.*, 2009; Shimizu *et al.*, 2009). However, despite the detailed knowledge of the central expression of nesfatin-1, to date there is minimal data describing the specific functional roles of nesfatin-1 in these autonomic nuclei, and what information is available has centered only on actions in the hypothalamus (Price *et al.*, 2008a; Price *et al.*, 2008b; Yosten & Samson, 2009; Maejima *et al.*,

2009; Yosten & Samson, 2010). The present study was thus undertaken to explore the cellular correlates and functional roles of nesfatin-1 actions in the medullary NTS using current-clamp electrophysiology, *post-hoc* single cell RT-PCR and microinjection techniques.

Experimental procedures

Slice preparation

Brains were removed from decapitated male Sprague-Dawley rats (Charles River, Quebec, Canada) aged 21-28 days and briefly immersed ice cold carbogenated slicing solution made of (in mM): 87 NaCl, 2.5 KCl, 25 NaHCO₃, 0.5 CaCl₂, 7 MgCl₂, 1.25 NaH₂PO₄, 25 glucose, 75 sucrose bubbled with 95% O₂/5% CO₂. A region of brainstem containing NTS was isolated and 300 µm coronal sections were cut using a vibratome (Leica, Nussloch, Germany). Slices were then incubated for minimum 1 hour prior to recording at 32°C in artificial cerebrospinal fluid (aCSF) made of (in mM): 126 NaCl, 2.5 KCl, 26 NaHCO₃, 2 CaCl₂, 2 MgCl₂, 1.25 NaH₂PO₄, 10 glucose saturated with 95% O₂/5% CO₂. All procedures were in accordance with the ethical criteria established by the Canadian Council on Animal Care and were approved by the Queen's University Animal Care Committee.

Electrophysiology

Slices were transferred to a recording chamber continuously perfused at a flow rate of 1-2ml/min with carbogenated aCSF warmed to approximately 32°C. Neurons were visualized at 40x magnification with an upright differential interference contrast microscope (Nikon, Tokyo, Japan). Borosilicate glass electrodes (World Precision Instruments, Sarasota, Florida, USA) were pulled on a Sutter Instruments P97 flaming micropipette puller and filled with an intracellular solution made of (in mM): 125 potassium gluconate, 10 KCl, 2 MgCl₂, 0.1 CaCl₂, 5.5 EGTA, 10 HEPES, 2 NaATP (pH 7.2 with KOH). When filled with the intracellular solution, electrodes had

a resistance of 3-5 M Ω . After establishing of a high resistance seal (>1G Ω), brief suction was applied to rupture the membrane and achieve whole cell configuration. Whole cell recordings were obtained with a Multiclamp 700B amplifier (Molecular Devices, Sunnyvale, California, USA), filtered at 2.4 kHz, and sampled at 10 kHz using a Micro 1401 interface and data were collected with Spike2 software for offline analysis (Cambridge Electronic Devices, Cambridge, UK). Neurons were rejected from further experimentation if they did not have action potentials with an amplitude greater than 60mV or a stable baseline membrane potential. A liquid junction potential calculated to be approximately 15 mV has been subtracted from all membrane potentials. Prior to experimentation in current-clamp, a series of current steps from -50 to -10 pA delivered at 5 second intervals in 10 pA increments were used to define neurons as post-inhibitory rebound (PIR), delayed excitation (DE), or neither (NON) (Vincent & Tell, 1997). Nesfatin-1 and tetrodotoxin (TTX) were applied to slices via bath perfusion. Response to nesfatin-1 was determined by comparing the membrane potential of the neuron before and after application of the peptide. A response was considered significant if the change in membrane potential after nesfatin-1 application was at least twice the amplitude of the standard deviation of the baseline membrane potential obtained during a 100 second period immediately before peptide application. Post-application membrane potential was the peak membrane potential averaged over a 100 second period of the recording showing a maximal effect. This method of analysis was employed as it provides a consistent, unbiased evaluation of effects on each individual neuron based on the variability of the baseline membrane potential of the neuron. A *t*-test was used to evaluate the significance of differences in the amplitude or latency of responses between populations of neurons. Changes in the distribution of responses between populations were assessed with the χ^2 test.

Single cell RT-PCR

Following the completion of current-clamp recordings, single cell reverse transcription polymerase reaction (RT-PCR) was performed to detect the expression of genes of interest in recorded NTS neurons. Cytoplasm was aspirated from the neuron using gentle suction, and the recording pipette was slowly withdrawn from the cell to form an outside-out patch. Neurons that did not successfully form outside-out patches were excluded from further analysis. The recording pipette was subsequently broken and its contents expelled into a 0.5 mL PCR tube containing the following to reverse transcribe the mRNA collected from the neuron: dithiothreitol (26 mM), dNTPs (10 mM), random hexamer primers (5 μ M), MgCl₂ (5 mM), RNase inhibitor (20U), and Superscript II reverse transcriptase (100U) (Invitrogen, Burlington, ON, Canada). An additional reaction mixture was made up without superscript II reverse transcriptase and served as a control for genomic contamination. The reverse transcription reaction ran overnight at 37 °C, and cDNA was stored at -80 °C until the multiplex PCR reaction was performed. A multiplex PCR approach was then used to amplify the cDNA obtained from the reverse transcription. The first step was a multiplex reaction containing “outside” primers (0.2 μ M, table 1, listed 5’ to 3’) for all the genes of interest, the cDNA from the single cell and the reagents provided in the Qiagen multiplex kit (Qiagen, Mississauga, ON, Canada) to a 100 μ l volume. The reaction mixture then underwent the following temperature protocol: 15 min at 95 °C, then 30 cycles at 94 °C for 30 s, 60 °C for 90 s, and 72 °C for 90 s. The second step consisted of individual reactions for each gene of interest using “nested” primer sets (0.2 μ M, table 1) and the reagents provided in the Qiagen multiplex kit to a 50 μ l volume. This reaction mixture then underwent 30 cycles of the temperature protocol described above. PCR products generated from the nested reaction were run on a 2% agarose gel containing ethidium bromide. With each reaction a positive and negative

control was performed in which primers were run against cDNA made from whole NTS (positive control) and in a reaction which PCR grade water replaced the cDNA template (negative control). Experiments which did not pass either control were eliminated from the study.

TABLE 2-1: Primers used in single cell RT-PCR experiments

Primer name		Outside	Nested	Product size
GAPDH	Sense	Gatggtgaaggtcggtgtg	taccagggctgccttctct	360 bp
	Antisense	Gggctaagcagttggtggt	ctcgtggttcacacccatc	
POMC	Sense	cgagattctgctacagtcgctca	ccctgttgctggccctcctg	300 bp
	Antisense	tctcggcgacattgggtaca	ctcccccgccgtctcttcc	
NPY	Sense	gccagagcagagcacc	cagagaccacagcccgcc	303 bp
	Antisense	caagttcattcccatcacca	tctcaagccttgttctgggg	
GAD67	Sense	cacaaactcagcggcataga	cacaaactcagcggcataga	147 bp
	Antisense	gagatgaccatccggaagaa	ctggaagaggtagcctgcac	
NUCB2	Sense	gattggtgactctggaggaa	ggaattcttgagagccacag	158 bp
	Antisense	Gctgatactcctgcttctgg	gcagttcatctgccttcttc	
MC4R	Sense	tctgaaaagaccccgagtga	tcagccgagagtgagctttc	219 bp
	Antisense	tcctcctgaagtgtccaa	tcctcctgaagtgtccaa	

Microinjection

Urethane-anesthetized (1.4 g/kg) male Sprague Dawley rats (150–350 g) were fitted with a tracheal cannula (PE-205; Intramedic) to facilitate breathing and a femoral arterial catheter for the measurement of blood pressure (BP) and heart rate (HR). Animals were placed on a feedback-controlled heating blanket for the duration of the experiment to maintain body temperature at 37°C. The animal was then placed in a stereotaxic frame with its head positioned vertically (nose down). The dorsal surface of the medulla was exposed by a midline incision made at the level of the obex. A microinjection cannula (150 µm tip diameter; Rhodes Medical

Instruments) was then positioned into the medial NTS (mNTS) and, after a minimum 2 min stable baseline recording was obtained, 0.5 μ l of 100 nM nesfatin-1 was microinjected into the region and the effects on BP and HR assessed.

At the conclusion of the experiment, animals were overdosed with anesthetic and perfused with 0.9% saline, followed by 10% formalin, through the left ventricle of the heart. The brain was removed and placed in formalin for at least 24 h. Using a vibratome, 50 μ m coronal sections were cut through the region of NTS, mounted, and cresyl violet stained. The anatomical location of the microinjection site was verified at the light microscope level by an observer unaware of the experimental protocol or the data obtained.

Analysis of blood pressure and heart rate data

Animals were assigned to one of two groups (mNTS or non-NTS) according to the anatomical location of the microinjection sites. Animals with injection sites that were wholly confined to regions outside of the mNTS were classified as non-NTS sites. Injections which were on the border of mNTS and thus not wholly confined within mNTS were excluded from further analysis. Normalized BP and HR data (mean baseline BP and HR were calculated for 60 s before injection and subtracted from all data points before and after injection) were obtained for each animal 60 s before the time of microinjection (control period) until 500 s after microinjection. Area under the curve (AUC) (area between baseline and each blood pressure and heart rate response) was calculated for each animal for the 500 s time period immediately after the injection, and the mean AUC for BP and HR responses were then calculated. A *t*-test was used to determine whether BP and HR observed in response to nesfatin-1 were different according to anatomical location of the microinjection site (mNTS vs non-NTS). Vehicle (aCSF) control microinjections were not performed specifically for the current study as these experiments have

been done previously in our laboratory and have been shown to be without effect on BP or HR (Hoyda *et al.*, 2009).

Chemicals and drugs

All salts used to prepare slicing solution, aCSF and internal recording solution were obtained from Sigma Pharmaceuticals (Oakville, Ontario, Canada). Nesfatin-1 was obtained from Phoenix Pharmaceuticals (Belmont, California, USA). Tetrodotoxin citrate was obtained from Alomone Laboratories (Jerusalem, Israel).

Results

Nesfatin-1 influences the excitability of mNTS neurons

Nesfatin-1 (10 nM) was bath applied to a total of 93 mNTS neurons during current-clamp recordings. The majority (63%) of neurons tested were responsive to nesfatin-1, with 42% ($n = 39$) exhibiting a slowly developing, long-lasting and reversible depolarization (Figure 2-1A). Another subset of neurons (21%, $n = 20$) showed temporally similar, reversible hyperpolarizations in response to 10 nM nesfatin-1 (Figure 2-1B). The mean depolarization observed was 7.83 ± 0.84 mV, and the mean hyperpolarization was -8.23 ± 1.00 mV. The changes in membrane potential induced by nesfatin-1 corresponded with an altered firing frequency in the affected neurons. Cells which depolarized in response to nesfatin-1 showed significant increases in firing frequency from 0.12 Hz to 1.1 Hz (paired t -test, $p = 0.001$), while those with a hyperpolarizing response were essentially silenced by nesfatin-1 (decrease from 0.6 Hz to 0.002 Hz, paired t -test, $p = 0.0007$). There was no correlation between baseline membrane potential, which ranged from -44 to -78 mV (mean: -62 mV), and response to nesfatin-1. Finally, the effects of nesfatin-1 on the membrane potential of neurons were specific to the mNTS, as 10

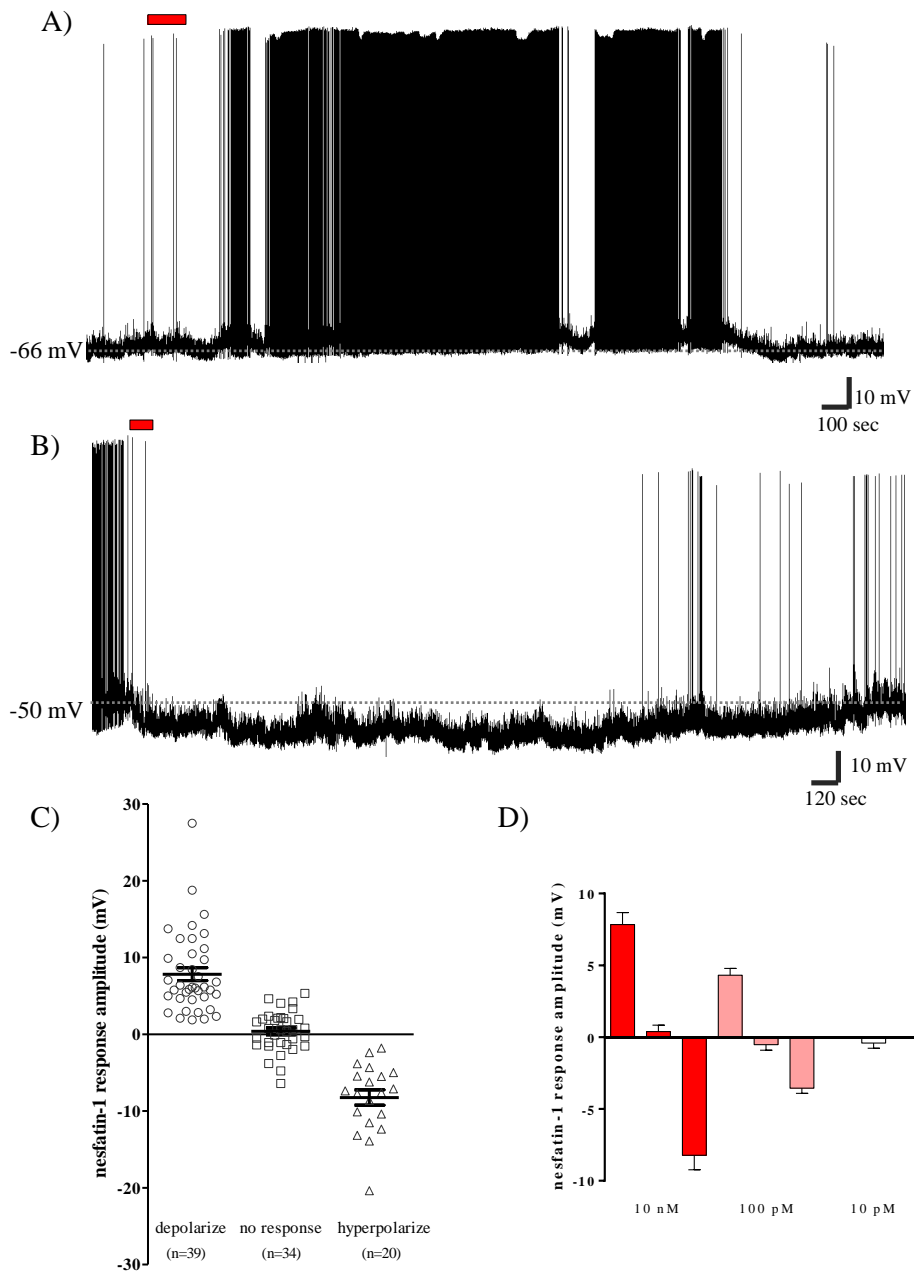


Figure 2-1 – Nesfatin-1 influences the excitability of mNTS neurons. Current-clamp recordings from two mNTS neurons in slice preparation, showing depolarizing (A) and hyperpolarizing (B) responses to 10 nM bath applied nesfatin-1 (horizontal red bar). In both neurons, a return to baseline membrane potential and firing frequency was seen after washout of nesfatin-1. (C) Scatter plot showing the range of responses elicited by bath application of 10 nM nesfatin-1. Black bars represent mean response \pm standard error while each single point represents the response of a single mNTS neuron. Mean depolarization: 7.83 ± 0.84 mV, mean hyperpolarization: -8.23 ± 1.00 mV. (D) Bar graph showing the mean responses elicited by bath application of 10 nM nesfatin-1 (red), 100 pM nesfatin-1 (pink), and 10 pM nesfatin-1 (white). Mean depolarization 10 nM: 7.83 ± 0.84 mV, $n = 39$, mean hyperpolarization 10 nM: -8.23 ± 1.00 mV, $n = 20$. Mean depolarization 100 pM: 4.31 ± 0.48 mV, $n = 17$, mean hyperpolarization 100 pM: -3.55 ± 0.37 mV, $n = 9$. 10 pM did not elicit a response in the neurons tested, $n = 11$.

nM bath applied nesfatin-1 did not have an effect on neurons in the commissural NTS ($n = 10$), a site without nesfatin-1 mRNA or protein expression (Foo *et al.*, 2008).

Nesfatin-1 effects are concentration-dependent

Nesfatin-1 was next applied at varying concentrations to determine if its effects on mNTS neurons are concentration dependent, as illustrated in Figure 2-1D. When administered at a concentration of 100 pM ($n = 43$), nesfatin-1 influenced the same proportion of neurons and the observed effects were temporally similar to those observed at a concentration of 10 nM, though the amplitude of the response was reduced. Neurons showed both reversible depolarizing ($n = 17$, mean 4.31 ± 0.48 mV) and hyperpolarizing ($n = 9$, mean -3.55 ± 0.37 mV) responses to 100 pM nesfatin-1. A concentration of 10 pM nesfatin-1 failed to elicit any response ($n = 11$).

Nesfatin-1 exerts direct effects on mNTS neurons

We next investigated whether the depolarizing and hyperpolarizing effects of nesfatin-1 could occur in the presence of the voltage-gated sodium channel blocker tetrodotoxin (TTX). A total of 12 mNTS were examined in the presence of 1 μ M TTX (Figure 2-2A, B) and, 75% were responsive to nesfatin-1 in the presence of 1 μ M TTX (Figure 2-2A, B), with 58% exhibiting a reversible depolarization ($n = 7$, mean 7.59 ± 1.37 mV) and 17% a reversible hyperpolarization ($n = 2$, mean -7.31 ± 3.37 mV). The proportion of responsive neurons in the presence of TTX was similar to that observed in its absence (Figure 2-2C, χ^2 , $p = 0.50$), and there was no significant difference between the latency of effect to nesfatin-1 between TTX treated and non TTX treated neurons (mean latency TTX treated = 139 ± 24 s, mean latency non TTX treated = 132 ± 8 s, unpaired t -test $p = 0.78$). These results thus suggest that nesfatin-1 influences the excitability of mNTS neurons via direct postsynaptic actions on these cells.

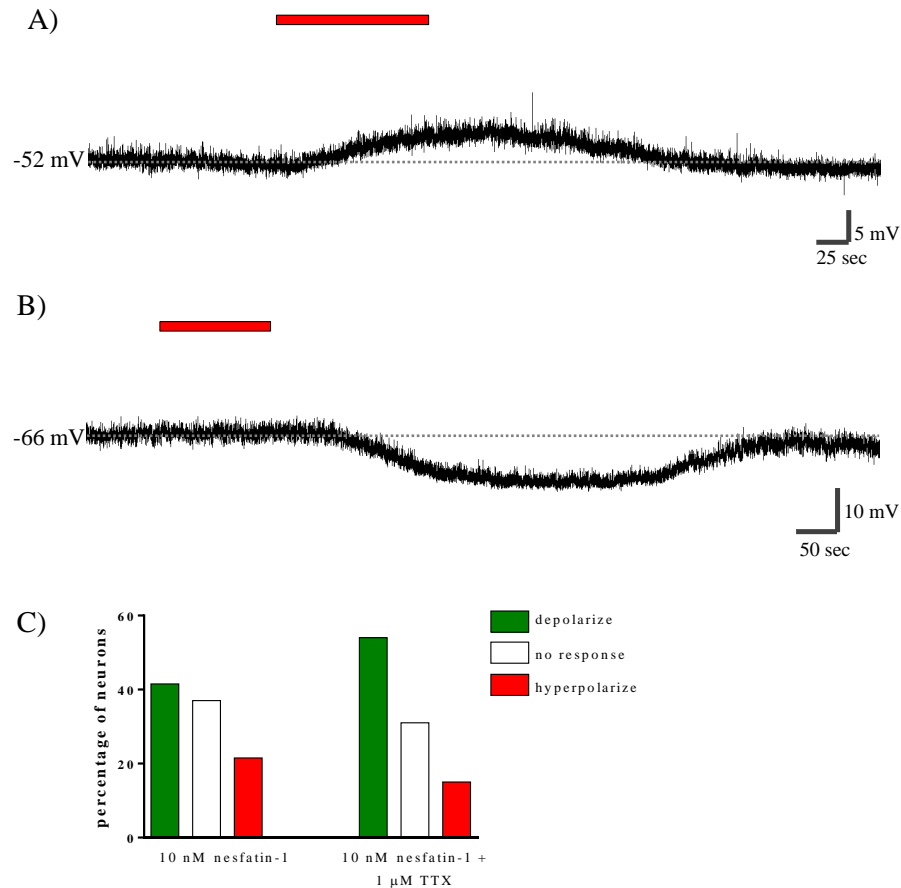


Figure 2-2 – Nesfatin-1 mediated effects on mNTS neurons are maintained in the presence of TTX. Current-clamp recordings from two mNTS neurons in slice preparation, pretreated with 1 μM TTX. Reversible depolarizing (A) and hyperpolarizing (B) responses to 10 nM bath applied nesfatin-1 (horizontal red bar) are still observed in the presence of TTX. (C) Bar graph showing the proportion of neurons that depolarize, do not respond, or hyperpolarize after bath application of 10n M nesfatin-1 with or without 1 μM TTX pretreatment.

Nesfatin-1 exerts similar effects on DE, PIR, and NON mNTS neurons

The NTS contains three electrophysiologically defined cell types categorized based on their response to a large hyperpolarizing current pulse. Neurons showing a delayed return to baseline following the pulse due to a prominent A-type K⁺ current are termed delayed excitation (DE) cells, those with a post-inhibitory rebound (PIR) action potential due to a prominent low threshold Ca²⁺ current are called PIR cells, and those with neither of these responses are NON

cells (Vincent & Tell, 1997). Since DE neurons have specifically been identified as exerting important control over autonomic processes (Johnson & Felder, 1993; Sundaram *et al.*, 1997), we investigated whether nesfatin-1 would have selective effects on this specific cell type. Nesfatin-1 influenced the membrane potential of DE (70% depolarize, 15% hyperpolarize, 15% no response $n = 13$, Figure 2-3), PIR (52% depolarize, 14% hyperpolarize, 34% no response, $n = 21$) and NON cells (43% depolarize, 33% hyperpolarize, 24% no response, $n = 21$). Nesfatin-1 thus does not preferentially affect any particular cell type in the mNTS, suggesting that these effects cannot be attributed to the unique properties of a specific electrophysiological NTS cell type (Figure 2-3).

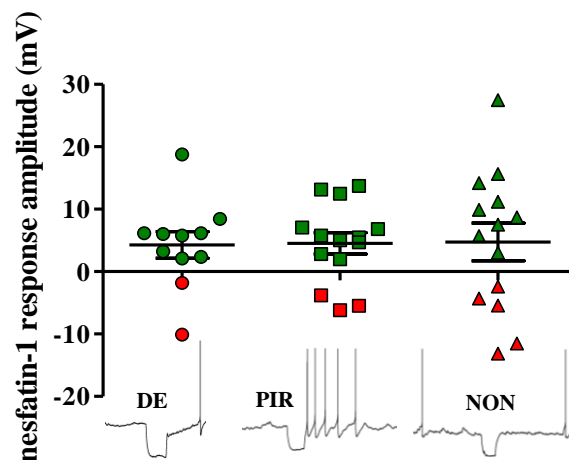


Figure 2-3 – Nesfatin-1 affects all mNTS cell types. Scatter plot grouping recorded neurons according to electrophysiological identity: either DE, PIR, or NON type cells as classified by the response of the cell to a hyperpolarizing current pulse (as shown in insets beneath scatter plot). Each grouping contains neurons which either depolarized (green), hyperpolarized (red), or did not respond (not shown in plot for clarity) to bath applied 10 nM nesfatin-1.

Nesfatin-1 depolarizes identified NPY and NUCB2 neurons, and exerts heterogeneous effects on identified GAD67 and MC4R neurons.

We next attempted to correlate electrophysiological actions of nesfatin-1 (10 nM) with the molecular phenotype of recorded neurons using *post-hoc* single cell RT-PCR of the mRNA

obtained from aspirated cytoplasm after completion of current-clamp recordings. These experiments were performed on a separate population of neurons as those used for the analyses based on electrophysiological fingerprint described above. There was no difference in the distribution of neurons which depolarized, did not respond, or hyperpolarized to 10 nM nesfatin-1 (χ^2 , $p = 0.43$) between these two sample populations, nor in the amplitude of depolarizing responses (mean depolarization, 5.61 ± 0.56 mV, unpaired t -test $p = 0.06$), however the amplitude of hyperpolarizing responses was decreased in this population of neurons (mean hyperpolarization, -4.59 ± 0.41 mV, unpaired t -test $p = 0.03$). Cytoplasm was obtained from a total of 56 neurons and was analyzed using primers directed at glyceraldehyde 3-phosphate dehydrogenase (GAPDH), pro-opiomelanocortin (POMC), neuropeptide Y (NPY), glutamate decarboxylase (GAD67, a GABAergic cell marker), NUCB2, and the melanocortin 4 receptor (MC4R). A total of 42 of the 56 recorded neurons showed expression of the housekeeping gene GAPDH, indicating successful harvesting and amplification of mRNA, and we observed that most mNTS neurons expressed multiple genes of interest. We identified 11 NPY expressing neurons, and all NPY neurons which were responsive to nesfatin-1 showed depolarizing responses ($n = 6$, Figure 2-4A, B). We found that all cells which expressed NUCB2 were depolarized by 10 nM nesfatin-1, suggesting a self-stimulatory action of this peptide on mNTS neurons ($n = 3$). Furthermore, 1 NUCB2 neuron co-expressed NPY, another NUCB2 neuron co-expressed GAD67, and a third NUCB2 neuron co-expressed both NPY and GAD67. Nesfatin-1 exerted heterogeneous effects on the 11 MC4R neurons we identified (depolarize = 6, hyperpolarize = 1) and on the 6 GAD67 neurons we identified (depolarize = 4, hyperpolarize = 2). Homogenous hyperpolarizing responses were not observed in any of the groups of identified neurons. We were unable to observe POMC expression in any of the 56 neurons examined.

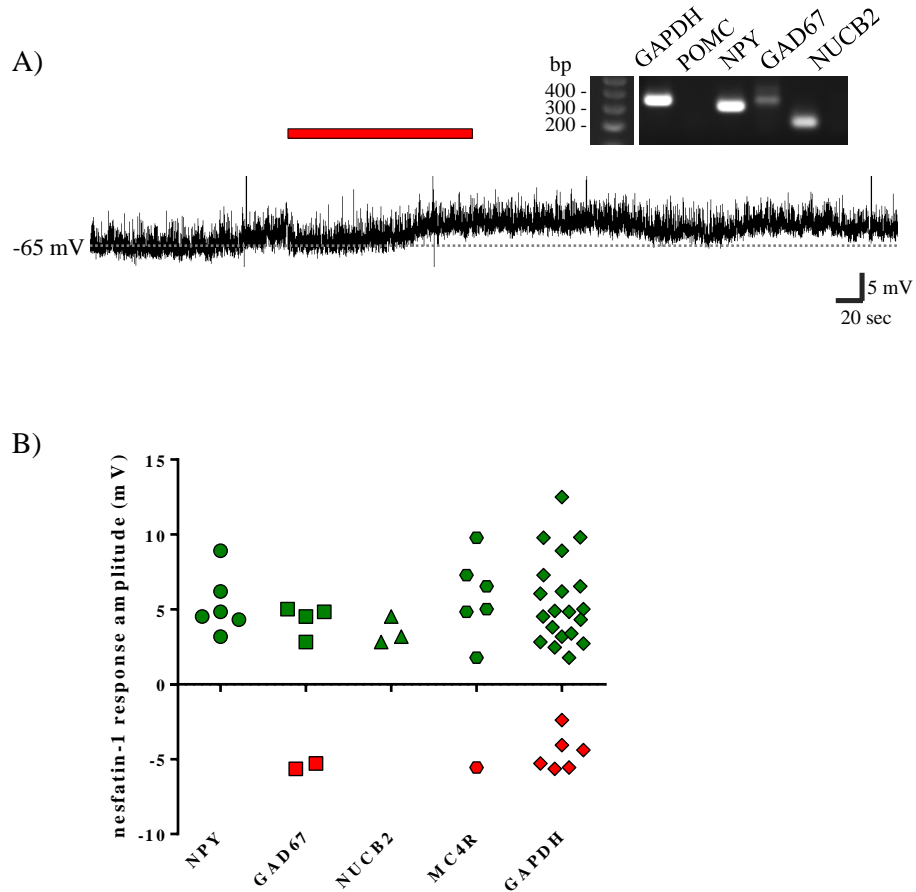


Figure 2-4 – Nesfatin-1 depolarizes NPY and NUCB2 mNTS neurons. (A) Current-clamp recording from a mNTS neuron in slice preparation, showing a depolarizing response to 10 nM bath applied nesfatin-1 (horizontal red bar). Note this neuron expresses multiple genes of interest as identified by *post-hoc* single cell RT-PCR: GAPDH, NPY, GAD67 and NUCB2 (inset). (B) Scatter plot grouping recorded neurons according to molecular phenotype as identified by RT-PCR. Neurons which responded to 10 nM bath applied nesfatin-1 and which expressed either NPY or NUCB2 exhibited only depolarizing responses. Neurons which expressed GAD67 or MC4R showed heterogeneous responses to nesfatin-1. For comparison, a scatter plot of all the nesfatin-1 responses exhibited by GAPDH positive neurons is included. (GAPDH: glyceraldehyde 3-phosphate dehydrogenase, NPY: neuropeptide Y, GAD67: glutamate decarboxylase, NUCB2: nucleobindin-2).

Cardiovascular actions of nesfatin-1 in mNTS

We next examined the cardiovascular consequences of nesfatin-1 microinjection into the mNTS in a total of 25 urethane anesthetised animals, of which 6 had microinjection sites histologically verified as within the anatomical boundaries of the mNTS, while 10 had sites outside of NTS (non-NTS). The remaining 9 animals had microinjection locations that could not

be reliably classified as either NTS or non-NTS and thus were excluded from further analysis. Microinjection of 0.5 μ l of 100 nM nesfatin-1 into the mNTS caused a rapid, long lasting increase in BP (mean AUC = 3354.1 ± 750.7 mmHg*sec, $n = 6$, $p < 0.001$ compared with non-NTS sites) which was accompanied by an increase in HR (mean AUC = 164.8 ± 78.5 beats, $n = 6$, $p < 0.05$ compared with non-NTS sites) as illustrated in Figure 2-5. These effects were shown to be site specific as microinjection into non-NTS sites was without effect on either BP (mean AUC = -638.3 ± 382.3 mmHg*sec, $n = 10$) or HR (mean AUC = 17.8 ± 6.7 beats, $n = 10$).

Discussion

The present study is the first to identify direct actions of the novel anorexigenic factor nesfatin-1 on the activity of electrophysiologically defined neuronal cell types in the NTS, and to characterize potential physiological correlates of these effects on membrane potential to influence cardiovascular function in the whole animal. Our results reveal the mNTS may be a critical site through which nesfatin-1 exerts its effects on autonomic function.

To shed light on the mechanisms that underlie the satiety-promoting actions of nesfatin-1, we conducted *in vitro* whole-cell patch clamp experiments to examine the effect of nesfatin-1 on the excitability of neurons in the NTS, one of the most prominent central sites of nesfatin-1 expression (Brailoiu *et al.*, 2007; Foo *et al.*, 2008). Similarly to our findings in previous studies we performed in the paraventricular (PVN) and arcuate (ARC) nuclei of the hypothalamus (Price *et al.*, 2008a; Price *et al.*, 2008b), nesfatin-1 exerted depolarizing or hyperpolarizing effects on different subsets of mNTS neurons tested. These opposing actions of the same peptide can potentially be attributed to the fact that nesfatin-1 may be affecting functionally separate populations of neurons which ultimately exert differential effects on cardiovascular regulation

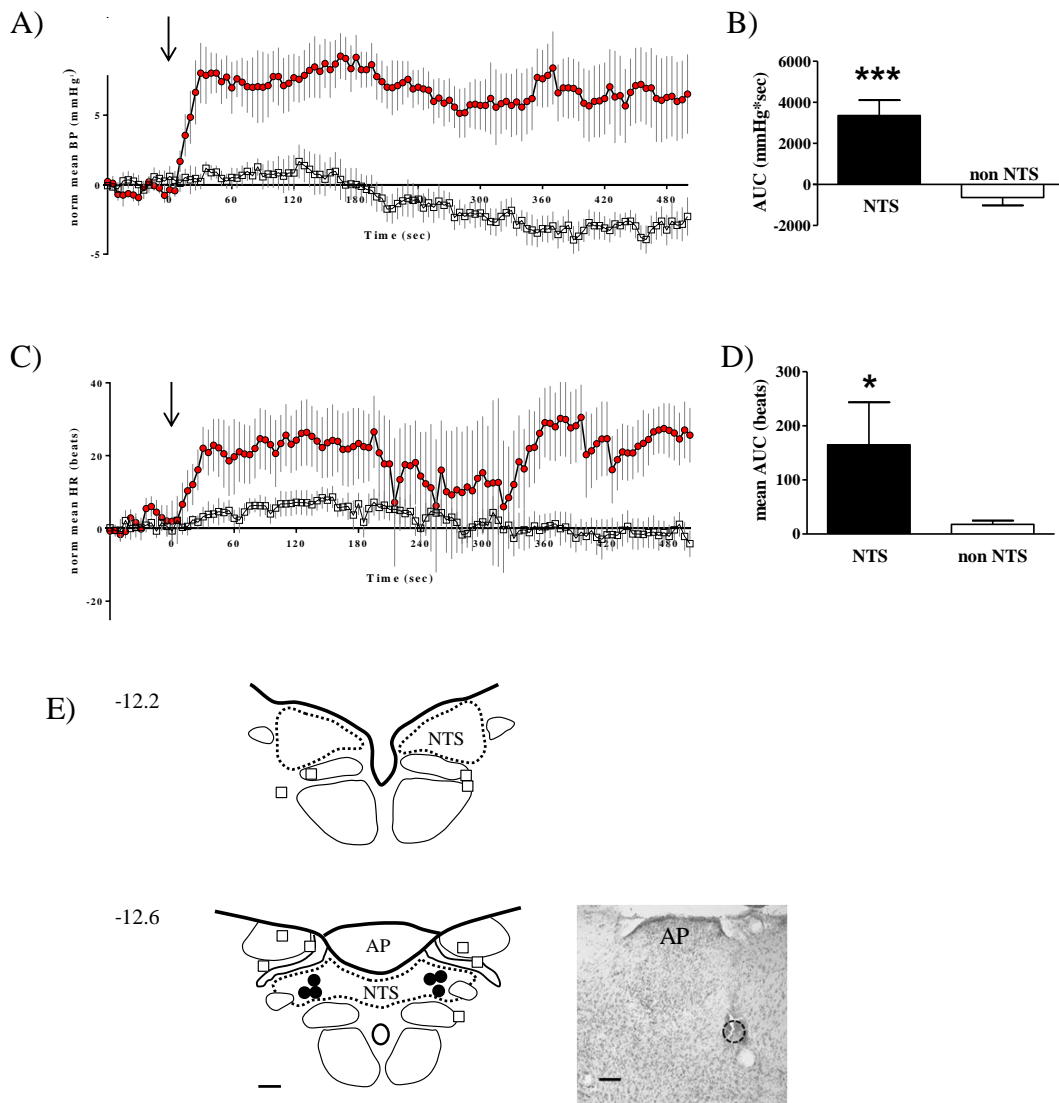


Figure 2-5 – Nesfatin-1 microinjection into the mNTS increases blood pressure and heart rate. Normalized mean BP (A) and HR (C) traces showing the response to nesfatin-1 microinjection (black arrow) into mNTS (red trace, $n = 6$) or non-NTS sites (white trace, $n = 10$). Summary bar graphs show mean area under the curve for BP (B) and HR (D) in response to nesfatin-1 microinjection in mNTS (black bar) or non-NTS sites (white bar, * indicates $p < 0.05$, *** $p < 0.001$). (E) Schematic illustrating the anatomical location of individual microinjection sites classified either as mNTS (●) or non-NTS (□). The photomicrograph on the right shows a mNTS microinjection site (dashed circle). Note the blood vessel directly underneath the microinjection site. Scale bars indicate 200 μm . Numbers in left hand corner represent coordinates relative to Bregma. (NTS: nucleus of the solitary tract; AP: area postrema).

and energy homeostasis. An examination of the effects of nesfatin-1 on the three electrophysiologically defined populations of neurons in the NTS revealed this peptide both depolarizes and hyperpolarizes DE, PIR and NON cells. Thus this categorization of neuronal populations cannot account for the differential effects of nesfatin-1. We therefore conducted studies to classify recorded neurons based on their peptide expression profile using *post-hoc* single cell RT-PCR technology. Neurons in the NTS produce numerous peptides critically involved in the regulation of cardiovascular function and energy balance in addition to nesfatin-1, including the orexigenic NPY and anorexigenic POMC-derived melanocortins (Lawrence *et al.*, 1998;Palkovits *et al.*, 1987). Indeed, our RT-PCR experiments now suggest potential co-expression of NUCB2 and NPY in NTS neurons, as has been previously reported in the ARC (Inhoff *et al.*, 2010). Furthermore, our RT-PCR studies revealed exclusively depolarizing actions of nesfatin-1 on NPY neurons in the mNTS, while our *in vivo* microinjections of nesfatin-1 into mNTS resulted in increases in BP and HR. Extensive studies conducted in the NTS have definitively established that microinjection of NPY into this medullary center causes *decreases* in BP and HR in the whole animal (Tseng *et al.*, 1989;Barraco *et al.*, 1990). Furthermore, icv NPY injections and microinjections of NPY into other autonomic centers innervated by NTS NPY neurons, namely the PVN, also elicit bradycardic and depressor responses (van *et al.*, 1994;Scott *et al.*, 1989). Thus stimulatory actions of nesfatin-1 on mNTS NPY neurons, involved either in local circuitry or projecting to higher brain centers, do not correlate with the ability of nesfatin-1 to increase HR and BP via the NTS. Our results therefore suggest that the medullary population of NPY neurons may not be responsible for the cardiovascular effects of nesfatin-1 observed in the mNTS. Future studies will thus be aimed at both identifying other neuronal populations which could mediate the nesfatin-1 induced effects on cardiovascular function (eg

catecholaminergic neurons) and at elucidating the contribution of medullary NPY neurons to the effects of nesfatin-1. Additionally, we found that nesfatin-1 exerted only depolarizing actions on NUCB2 cells. Thus, these findings raise the possibility that nesfatin-1 may exert a “self-stimulatory” effect on mNTS NUCB2 neurons, as reported by Maejima *et al* (Maejima *et al.*, 2009) in PVN neurons. Since nesfatin-1 is absent from axonal terminals, it has been proposed that this peptide could only be released dendritically or from cell bodies to act in a local, paracrine manner (Foo *et al.*, 2008;Goebel *et al.*, 2009a). While further experiments are essential to uncover the significance and mechanism of the stimulatory action of nesfatin-1 on mNTS NUCB2 neurons, our results suggest that there could be a local nesfatin-1 positive feedback loop on NUCB2 neurons in NTS which may contribute to the cardiovascular and anorexigenic effects of this neuropeptide. Ultimately, the effects of nesfatin-1 on the cardiovascular system and on food intake are likely mediated via multiple populations of neurons in the NTS with different peptidergic profiles acting as part of a neural network involving other key autonomic and energy homeostatic centers such as the PVN, ARC, and lateral nucleus of the hypothalamus, which share either direct or indirect connections with the NTS. Thus, we hypothesize that endogenous nesfatin-1 synthesized in the NTS can influence both incoming visceral signals on autonomic and energy status which are then relayed to higher brain centers, as well as inputs from hypothalamic regions, to ultimately modify cardiovascular parameters and feeding behaviour. Further studies aimed at elucidating the precise functional pathways of nesfatin-1 effects will be necessary to better understand its mechanism of action.

It is important to note that we were unable to detect the expression of POMC in any of the mNTS neurons we examined in the present study, and past experiments from our laboratory identified only 1 POMC positive neuron from a population of 37 mNTS neurons (Hoyda *et al.*,

2009). While this can partially be explained by the fact that the majority of POMC expressing cells in the NTS are located in the caudal commissural NTS (Bronstein *et al.*, 1992) and our studies were focused on the medial NTS, it is also critical to mention that the NTS population of neurons expresses only 1/10 of the POMC mRNA expressed by neurons in the ARC (Bronstein *et al.*, 1992). The lack of POMC positive NTS neurons detected in our single cell RT-PCR studies provides important emphasis on how sparse the medullary POMC neuronal population is.

We have also correlated the actions of nesfatin-1 on neuronal membrane potential with physiological outcomes, using *in vivo* microinjection techniques to demonstrate that nesfatin-1 microinjected into the NTS induces significant increases in both BP and HR in rats. These effects were site specific, as injections into sites outside of the NTS did not produce any changes in cardiovascular parameters. Our results are in accordance with previous studies demonstrating tachycardic and hypertensive effects of nesfatin-1 after icv injections into the lateral ventricle of rats (Yosten & Samson, 2009). Thus it would appear nesfatin-1 is capable of exerting important effects on the cardiovascular system at both hypothalamic and medullary levels. Furthermore, Yosten & Samson (2009) also showed the nesfatin-1 induced effects on cardiovascular parameters are sympathetically mediated, as they were blocked by a nonspecific α -adrenergic antagonist. We hypothesize the same may be true at the level of NTS, although we did not directly examine sympathetic contribution to the cardiovascular effects we observed. The NTS is a critically important site for the control of cardiovascular function, as it is the first central relay for baroreceptor afferents, and it receives projections from, and sends efferents to, multiple brain regions involved in the maintenance of cardiovascular homeostasis (Lawrence & Jarrott, 1996). Numerous peptides which exert both stimulatory and inhibitory effects on cardiovascular parameters are expressed and act at the level of the NTS to ultimately influence blood pressure

and heart rate in the whole animal. As holds true for nesfatin-1 induced effects on food intake, it has been shown that the hypothalamic nesfatin-1 mediated effects on cardiovascular function are abolished by pharmacological blockade of central melanocortin and oxytocin receptors (Yosten & Samson, 2009; Yosten & Samson, 2010). Since both melanocortin and oxytocin receptors are expressed on neurons in the NTS (Kishi *et al.*, 2003; Loup *et al.*, 1989; Baskin *et al.*, 2010), it is tempting to speculate that oxytocin and melanocortin responsive neurons, and potentially others as well, are acting together at the level of NTS to exert effects which are ultimately integrated to produce a tachycardic and vasopressor response. Future experiments will thus be aimed at evaluating the contribution of the melanocortin and oxytocin systems to nesfatin-1 induced cardiovascular effects in the medulla. Furthermore, the nesfatin-1 receptor remains unknown at the present time, and future identification of this receptor will allow us to further examine which populations of neurons are influenced by nesfatin-1 to affect cardiovascular parameters.

Perspectives and significance

Our electrophysiological, single cell RT-PCR and *in vivo* studies of the effects of nesfatin-1 on neurons in the mNTS are the first to show this peptide exerts direct actions on the excitability of this neuronal population, and these effects ultimately result in increases in BP and HR in the whole animal. Furthermore, we demonstrate that nesfatin-1 stimulates mNTS NPY and NUCB2 neurons, and provide additional evidence for a role of nesfatin-1 as a “self-stimulatory” peptide. Our results provide critical insight into the circuitry and physiology involved in the effects of nesfatin-1, and highlight the NTS as a key structure mediating these autonomic actions.

Acknowledgements

We would like to thank Ms Christie Hopf for her technical assistance. This work was supported by funding from Natural Sciences and Engineering Research Council of Canada and Le Fonds québécois de la recherche sur la nature et les technologies to AM, a Canadian Institutes of Health Research Banting and Best studentship to PMS, and Heart and Stroke Foundation of Ontario to AVF.

CHAPTER 3: α -MSH exerts direct postsynaptic excitatory effects on NTS neurons and enhances GABAergic signaling in the NTS

Abstract

The central melanocortin system plays an essential role in the regulation of energy balance. While anorexigenic effects of α -melanocyte stimulating hormone (α -MSH) acting in the nucleus of the solitary tract (NTS), a critical medullary autonomic control center, have been established, the cellular events underlying these effects are less well characterized. In this study, we used patch clamp whole cell electrophysiology to examine firstly whether α -MSH exerts direct postsynaptic effects on the membrane potential of rat NTS neurons in slice preparation, and secondly whether α -MSH influences GABAergic signaling in the NTS. In normal aCSF, perfusion of α -MSH (500 nM) resulted in a depolarization in 39% of cells ($n = 16$, mean 6.14 ± 0.54 mV), and a hyperpolarization in 22% of cells ($n = 9$, -6.79 ± 1.02 mV). Studies using tetrodotoxin to block neuronal communication revealed α -MSH exerts direct depolarizing effects on some NTS neurons, and indirect inhibitory effects on others. A third subset of neurons is simultaneously directly depolarized and indirectly hyperpolarized by α -MSH, resulting in a net lack of effect on membrane potential. The inhibitory inputs influenced by α -MSH were identified as GABAergic, as α -MSH increased the frequency, but not amplitude, of inhibitory post synaptic currents (IPSCs) in 50% of NTS neurons. α -MSH had no effect on the frequency or amplitude of miniature IPSCs. Furthermore, pharmacological blockade of GABA_A and GABA_B receptors, and physical removal of all synaptic inputs via cellular dissociation, abolished hyperpolarizations induced by α -MSH. We conclude α -MSH exerts direct, postsynaptic excitatory effects on a subset of NTS neurons. By exciting GABAergic NTS neurons and presynaptically enhancing GABAergic signaling, α -MSH also indirectly inhibits other NTS cells. These findings provide critical insight into the cellular events underlying medullary melanocortin anorexigenic effects, and expand the understanding of the circuitries involved in central melanocortin signaling.

Introduction

The medullary nucleus of the solitary tract (NTS) is a critical autonomic center which regulates numerous aspects of food intake and energy balance, ranging from the initial detection of food in the stomach to feelings of satiation, through the integration of multiple central and peripheral inputs (for reviews see (Berthoud, 2008;Grill & Hayes, 2012). Among the many peptides expressed by the NTS is pro-opiomelanocortin (POMC), the precursor for melanocortins such as α -melanocyte stimulating hormone (α -MSH) (Bronstein *et al.*, 1992;Palkovits *et al.*, 1987). The NTS is one of only two central sites in which POMC is expressed, the second, larger population of POMC neurons being located in the arcuate nucleus of the hypothalamus (Jacobowitz & O'Donohue, 1978;Cone, 2005;Huo *et al.*, 2006). Both groups of POMC cells provide α -MSH innervation to NTS neurons, where α -MSH then acts via the melanocortin-4 receptor (MC4R) to ultimately modulate autonomic processes (Zheng *et al.*, 2010;Cone, 2005). For example, injection of the long lasting melanocortin-3 and -4 receptor (MC3/4R) agonist melanotan II (MTII) into the fourth ventricle (4V) or the dorsal vagal complex (DVC, including dorsal motor nucleus of the vagus and the NTS) causes potent decreases in food intake by decreasing meal size, and also results in decreases in body weight. Conversely, 4V or DVC administration of the MC3/4R antagonist SHU9119 induces increases in food intake and body weight, underscoring the physiological significance of melanocortin effects in the brainstem (Grill *et al.*, 1998;Zheng *et al.*, 2005;Williams *et al.*, 2000). More targeted studies have revealed the medullary MC3/4Rs which mediate these anorexigenic effects may be located in the NTS, as microinjection of SHU9119 into the NTS abolishes α -MSH mediated decreases in food intake (Zheng *et al.*, 2010). In addition to direct effects of melanocortins on the regulation of energy balance, brainstem melanocortin signaling is also essential in mediating anorexigenic effects of other feeding related peptides, as 4V administration of SHU9119 attenuates the

decreases in food intake induced by leptin and cholecystokinin, for example (Zheng *et al.*, 2010; Fan *et al.*, 2004). The autonomic effects of melanocortins in the brainstem also extend beyond the control of feeding, as 4V and DVC injection of MTII has been shown influence water intake (Grill *et al.*, 1998; Williams *et al.*, 2000), and microinjection of α -MSH or MTII into the NTS alters heart rate, blood pressure (Pavia *et al.*, 2003), gastric motility, and gastric tone (Richardson *et al.*, 2013).

Although the physiological outcomes of MC3/4R activation in the brainstem and NTS are well documented, less well characterized are the cellular effectors and local circuitry through which melanocortins act in the NTS to ultimately exert effects on autonomic function. A previous study by Wan *et al.* (2008) reported presynaptic effects of α -MSH on vagal glutamatergic signaling to the NTS, as assessed by changes in the frequency of excitatory postsynaptic currents (EPSCs) and in the amplitude of EPSCs evoked by electrical stimulation of the solitary tract (Wan *et al.*, 2008). Studies from our laboratory using *post-hoc* single cell reverse transcription PCR (RT-PCR), however, have revealed the presence of postsynaptic MC4Rs in NTS neurons (Mimee *et al.*, 2012; Hoyda *et al.*, 2009). Thus in light of our previous findings, the present study was undertaken to explore a potential postsynaptic site of action for α -MSH in the NTS. To this end, we performed whole cell current-clamp recordings to examine whether α -MSH can act postsynaptically to directly influence the membrane potential of neurons in the NTS. Furthermore, while it has been established that α -MSH influences excitatory glutamatergic signaling in the NTS (Wan *et al.*, 2008), we examined whether it can also affect inhibitory γ -aminobutyric acid (GABA) transmission in the NTS using whole cell voltage-clamp recordings.

Experimental procedures

Preparation of slices for electrophysiological recording

Coronal slices containing the NTS were prepared daily from unanesthetized, 21-28 day old male Sprague-Dawley rats (Charles River, Quebec, Canada). Rats were decapitated and their brains rapidly placed in ice cold carbogenated slicing solution made of (in mM): 87 NaCl, 2.5 KCl, 25 NaHCO₃, 0.5 CaCl₂, 7 MgCl₂, 1.25 NaH₂PO₄, 25 glucose, 75 sucrose bubbled with 95% O₂/5% CO₂. A region of brainstem containing the NTS was isolated and 300 µm coronal sections were cut with a vibratome (Leica, Nussloch, Germany). Slices were then incubated at 32°C in artificial cerebrospinal fluid (aCSF) made of (in mM): 124 NaCl, 2.5 KCl, 20 NaHCO₃, 2 CaCl₂, 1.3 MgSO₄, 1.24 KH₂PO₄, 10.5 glucose saturated with 95% O₂/5% CO₂ for a minimum of 1 hour prior to electrophysiological recording. All procedures were in accordance with the ethical criteria established by the Canadian Council on Animal Care and were approved by the Queen's University Animal Care Committee.

Preparation of dissociated NTS neurons

Rat coronal brain slices were obtained as described above, and the NTS was identified and microdissected from each slice using a dissection microscope. After a 30 minute incubation at 30°C in Hibernate solution (Brain Bits, Springfield, IL, USA) containing 2mg/mL papain (Worthington Biochemical, Lakewood, NJ, USA), dissected NTS fragments were washed 3 times and then gently triturated with Hibernate solution supplemented with B27 (Life Technologies, Carlsbad, CA, USA). The dissociated NTS neurons were collected in a pellet by centrifugation at 200 g for 8 minutes at 4°C. Neurons were then resuspended in Neurobasal A medium supplemented with B27, 0.5 mM L-glutamine, and 100 U/ml penicillin-streptomycin (all Life Technologies), aliquoted to 35 mm glass-bottomed culture dishes (MatTek, Ashland,

MA, USA), and left to adhere to the dishes for approximately 3 hours in a 5% CO₂, 37°C incubator. Following adhesion, approximately 2 mL of supplemented Neurobasal A medium was added to the dishes, which were then maintained for up to 4 days in the incubator.

Electrophysiology

Brain slices were transferred to a recording chamber continuously perfused at a flow rate of 1.5-2ml/min with carbogenated aCSF warmed to approximately 32°C. Neurons were visualized at 40x magnification with an upright differential interference contrast microscope (Scientifica, East Sussex, United Kingdom). Borosilicate glass electrodes (World Precision Instruments, Sarasota, Florida, USA) were pulled on a Sutter Instruments P97 flaming micropipette puller and filled with an intracellular solution made of (in mM): 125 potassium gluconate, 10 KCl, 2 MgCl₂, 0.1 CaCl₂, 5.5 EGTA, 10 HEPES, 2 NaATP (pH 7.2 with KOH) for current-clamp recordings. A high chloride intracellular recording solution was used for voltage-clamp recordings examining inhibitory post synaptic currents (IPSCs), made of (in mM): 140 KCl, 2 MgCl₂, 0.1 CaCl₂, 5.5 EGTA, 10 HEPES, 2 NaATP (pH 7.2 with KOH). Electrodes had a resistance of 3-5.5 MΩ when filled with the intracellular solution. After obtaining a high resistance seal (minimum 1GΩ), brief suction was used to rupture the membrane and obtain whole cell access. Whole cell recordings were made with a Multiclamp 700B amplifier (Molecular Devices, Sunnyvale, California, USA), filtered at 2.4 kHz, and sampled at 10 kHz using a Micro 1401 interface and data were collected with Spike 2 software for current-clamp recordings and Signal 4 software for voltage-clamp recordings for offline analysis (Cambridge Electronic Devices, Cambridge, UK). Neurons selected for experimentation had action potentials with an amplitude of at least 60 mV and a stable baseline membrane potential. All solutions were applied to slices via bath perfusion. Response to α-MSH in current-clamp configuration was

determined by comparing the membrane potential of the neuron before and after peptide application. A response was considered significant if the change in membrane potential after α -MSH application was at least twice the standard deviation of the baseline membrane potential obtained during a 100 second period immediately before peptide application. Post-application membrane potential was the peak membrane potential averaged over 100 seconds of the recording showing a maximal effect. A calculated liquid junction potential of 15 mV for regular intracellular solution has been subtracted from all membrane potentials. A *t*-test or one-way ANOVA was used to evaluate the significance of differences in the amplitude of responses between populations of neurons. Changes in the distribution of responses between populations were assessed with the χ^2 test. For all tests, significance was defined as $p < 0.05$.

Current-clamp recordings from dissociated NTS neurons were performed 1-4 days after the dissociation process. Methods were the same as for slice recordings described above with the following exceptions: neurons were visualized and recorded from on an inverted microscope at 40x magnification (Nikon Instruments, Tokyo, Japan), and aCSF for dissociated recordings contained (in mM): 140 NaCl, 5 KCl, 1 MgCl₂, 2 CaCl₂, 10 HEPES, 5 mannitol, and 5 glucose (pH 7.2 with NaOH).

Analysis of inhibitory post synaptic currents (IPSCs) and miniature IPSCs (mIPSCs)

IPSCs and mIPSCs were recorded in voltage-clamp configuration (holding potential -61 mV with liquid junction potential for high chloride intracellular solution) in the presence of the broad spectrum glutamate receptor antagonist kynurenic acid (KA, 1 mM). Co-application of KA and bicuculline methiodide successfully inhibited all post synaptic currents (data not shown). IPSCs and mIPSCs were analysed using Mini Analysis software 6.0.7 (Synaptosoft, Decatur, GA, USA). Events were identified based on shape (rapid rise followed by slow exponential

decay) and amplitude (threshold defined in each recording as four times the baseline electrical noise of the recording). Each event identified in this manner was individually examined to exclude false (m)IPSCs. Events were grouped into 100 second bins for frequency and amplitude analysis. The baseline period was defined as the 100 seconds immediately prior to α -MSH application, and peak peptide effect as 100 seconds of the recording showing a maximal effect. The significance of an effect of α -MSH on the frequency or amplitude of (m)IPSCs in an individual neuron was established using the Kolmogorov-Smirnov test, with significance defined as $p < 0.05$. The Wilcoxon matched pairs signed rank test was used to establish group significance, with significance defined as $p < 0.05$.

Chemicals and drugs

Kynurenic acid, bicuculline methiodide, and all salts used to prepare slicing solution, aCSF and intracellular recording solution were obtained from Sigma Pharmaceuticals (Oakville, Ontario, Canada). α -MSH was obtained from Phoenix Pharmaceuticals (Belmont, California, USA), tetrodotoxin citrate from Alomone Laboratories (Jerusalem, Israel), and CGP 52432 from Tocris Biosciences (Minneapolis, Minnesota, USA).

Results

α -MSH influences the membrane potential of NTS neurons

We first sought to establish whether α -MSH influences the membrane potential of neurons in the NTS. To this end, α -MSH (500 nM, as in (Wan *et al.*, 2008)) was bath applied to a total of 41 NTS neurons during current-clamp recordings. Neurons were selected mainly from the medial, but also commissural, subregions of the NTS, in line with the expression of the MC4R in the rat NTS (Kishi *et al.*, 2003). The baseline membrane potential of the recorded neurons ranged from -54 to -79 mV (mean -66.84 ± 0.94 mV, $n = 41$), and the majority (61%) of

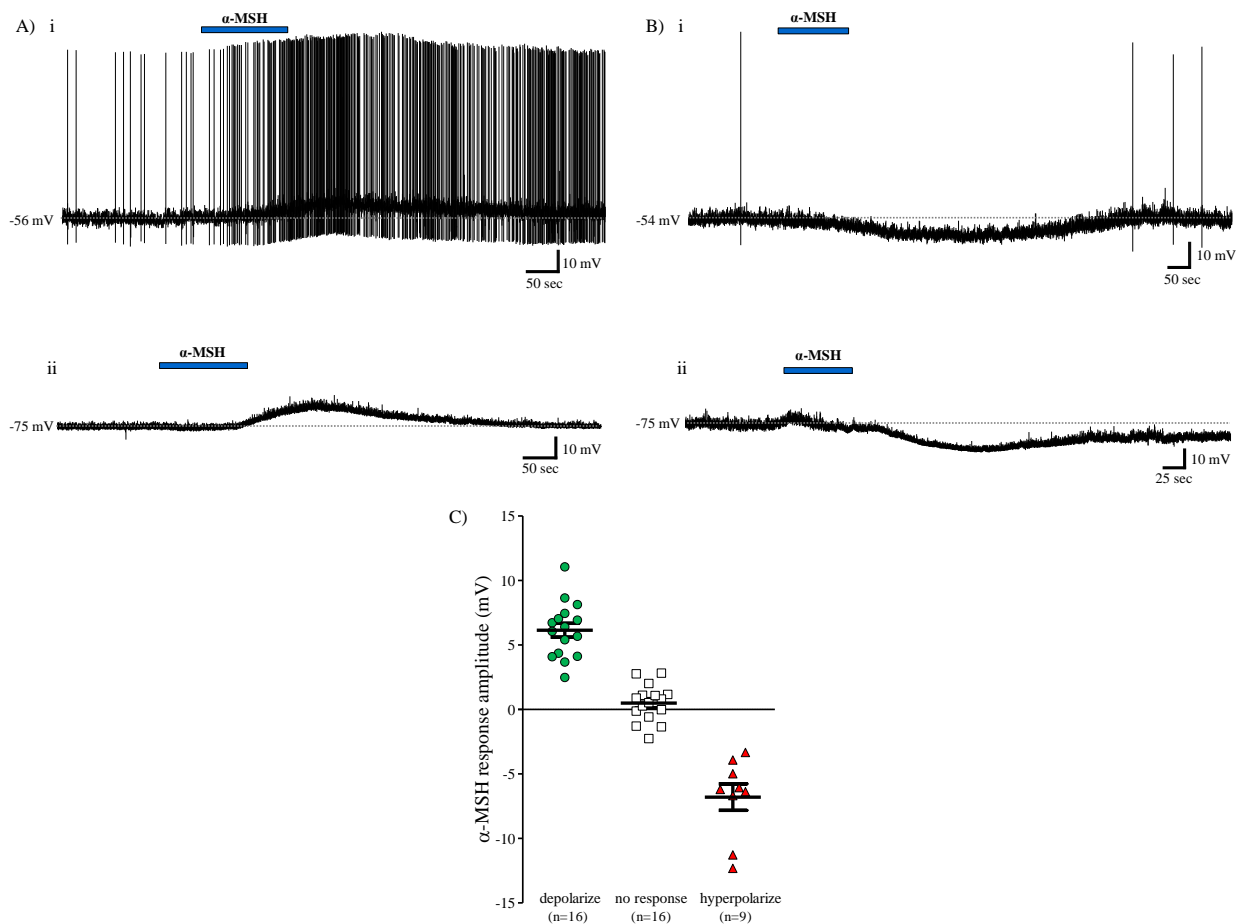


Figure 3-1 – α -MSH influences the membrane potential of NTS neurons. Current-clamp recordings from four NTS neurons in slice preparation, showing depolarizing (A) and hyperpolarizing (B) responses to 500 nM bath applied α -MSH (horizontal blue bar) at different resting membrane potentials (i vs ii). In all neurons, a recovery toward baseline membrane potential was seen after washout of α -MSH. (C) Scatter plot showing the range of responses induced by bath applied 500 nM α -MSH. Black bars represent mean response \pm standard error while each single point represents the response of a single NTS neuron. Mean depolarization: 6.14 ± 0.54 mV, mean hyperpolarization: -6.79 ± 1.02 mV.

neurons tested were responsive to α -MSH. Slowly developing depolarizing responses were observed in 39% of neurons ($n = 16$, mean depolarization: 6.14 ± 0.54 mV, Figure 3-1A, i and ii, 3-1C), 10 of which showed a complete recovery to baseline membrane potential, while the remaining 6 showed a partial recovery at the completion of the recording. A smaller subset of neurons (22%, $n = 9$) showed temporally similar hyperpolarizing responses to 500 nM α -MSH (mean hyperpolarization: -6.79 ± 1.02 mV, Figure 3-1B i and ii, 3-1C), 5 of which showed a complete recovery to baseline membrane potential, while the remaining 4 partially recovered. There was no correlation between baseline membrane potential and response to α -MSH, as the mean baseline membrane potential for both populations of responding neurons was equal (mean baseline membrane potential of depolarizing cells: -67.24 ± 1.50 mV, mean baseline membrane potential of hyperpolarizing cells: -66.83 ± 2.76 mV).while the remaining 4 partially recovered. There was no correlation between baseline membrane potential and response to α -MSH, as the mean baseline membrane potential for both populations of responding neurons was equal (mean baseline membrane potential of depolarizing cells: -67.24 ± 1.50 mV, mean baseline membrane potential of hyperpolarizing cells: -66.83 ± 2.76 mV).

α -MSH exerts direct depolarizing and indirect hyperpolarizing effects on NTS neurons

We next investigated whether the depolarizing and hyperpolarizing effects of α -MSH on NTS neurons are due to direct postsynaptic effects on these cells, or rather are dependent on action potential-mediated neuronal communication. We thus examined whether responses to 500 nM α -MSH persisted when slices were treated with the voltage-gated sodium channel blocker tetrodotoxin (TTX, $n = 12$). A total of 83% of NTS neurons were responsive to α -MSH in the presence of 1 μ M TTX (Figure 3-2A, 3-2C), with 75% exhibiting a reversible depolarization ($n = 9$, mean 7.88 ± 1.16 mV) and 8% a reversible hyperpolarization ($n = 1$, -15.06 mV). There was

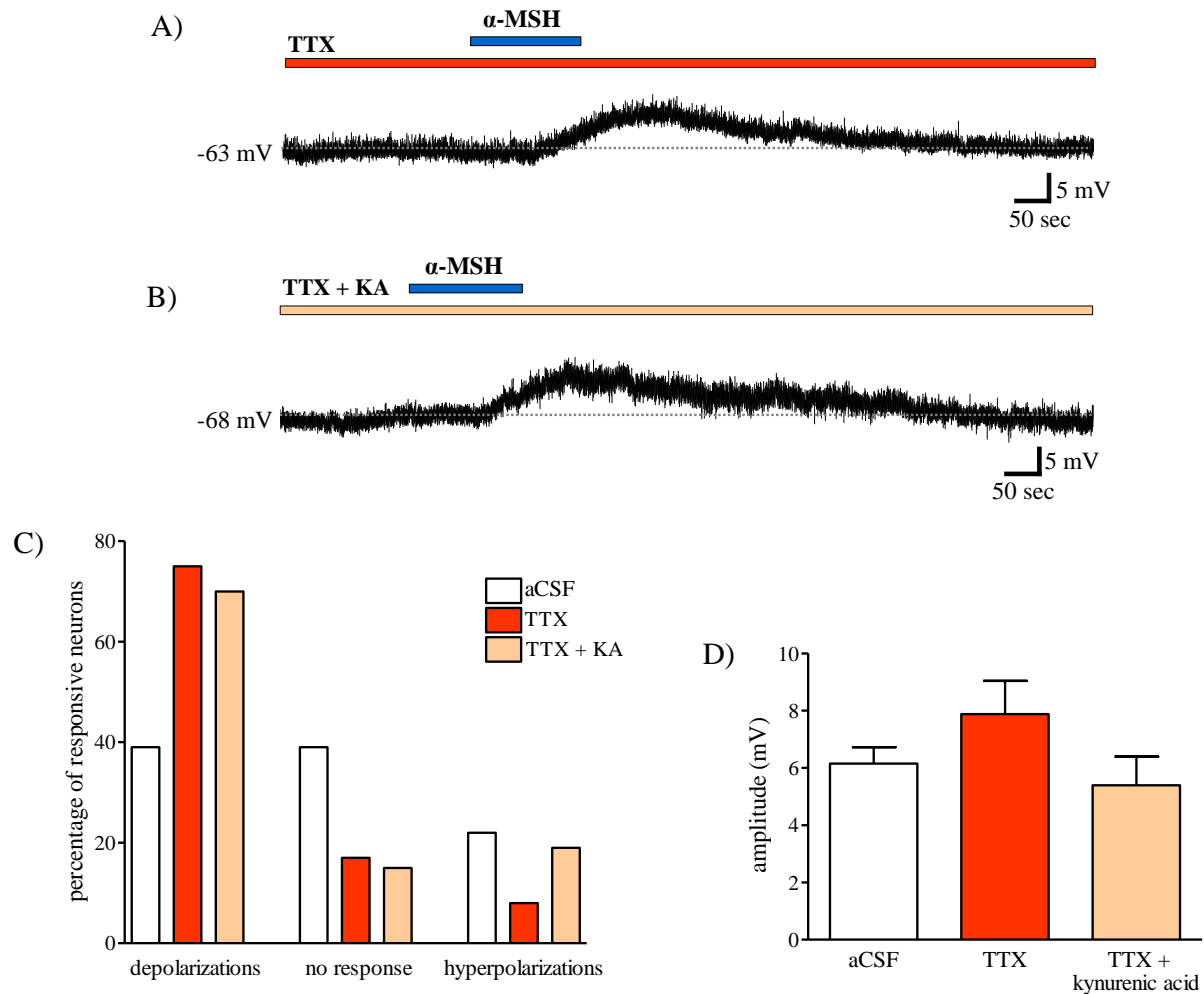


Figure 3-2 – α -MSH exerts direct depolarizing and indirect hyperpolarizing effects on NTS neurons. Current-clamp recordings from two NTS neurons in slice preparation. Reversible depolarizing responses to 500 nM bath applied α -MSH (horizontal blue bar) are maintained after treatment with both 1 μ M TTX (A) and with 1 μ M TTX and 1 mM of the broad spectrum glutamate receptor antagonist kynurenic acid (KA, B). C) Bar graph showing the percentage of NTS neurons in slice preparation which respond to 500 nM α -MSH with a depolarization, with no response, or with a hyperpolarization when slices are bathed in control aCSF (white bars), in 1 μ M TTX (dark orange bars), and in 1 μ M TTX and 1 mM KA (peach bars). D) Bar graph showing the mean depolarization \pm standard error elicited by 500 nM α -MSH in control aCSF (6.14 ± 0.54 mV), in 1 μ M TTX (7.88 ± 1.16 mV), and in 1 μ M TTX and 1 mM KA (5.39 ± 1 mV). Mean depolarizations do not significantly differ from one another across treatment groups (one-way ANOVA, $p = 0.17$).

no difference in the amplitude of the depolarization observed in neurons perfused with aCSF and neurons perfused with aCSF containing TTX (unpaired t -test, $p = 0.15$, Figure 3-2D). However, the proportion of neurons responsive to α -MSH was significantly altered in the presence of TTX (χ^2 , $p = 0.038$, Figure 3-2C), with hyperpolarizing responses nearly eliminated (8% in TTX vs 22% in aCSF), the proportion of depolarizations observed increased (75% in TTX vs 39% in aCSF), and the proportion of non-responsive neurons reduced (17% in TTX vs 39% in aCSF).

The depolarizing effects of α -MSH on NTS neurons are independent of glutamate

Since Wan *et al.* (2008) observed effects of α -MSH on glutamate transmission in the NTS, we next investigated whether the α -MSH induced depolarization of NTS neurons would persist when slices were treated with both TTX (1 μ M) and the broad spectrum glutamate receptor antagonist kynurenic acid (KA, 1 mM). Indeed, 85% of NTS neurons ($n = 13$, Figure 3-2B, 3-2C) were responsive to 500 nM α -MSH in the presence of TTX and KA, with 70% demonstrating at least a partially reversible depolarization ($n = 9$, mean 5.39 ± 1.00 mV) and 15% a reversible hyperpolarization ($n = 2$, -1.90 ± 0.41 mV). There was no difference in the amplitude of the depolarization between neurons perfused with aCSF, with TTX, or with TTX and KA (one-way ANOVA, $p = 0.17$, Figure 3-2D). There was, however, a significant change in the proportion of neurons which depolarized (70% in TTX + KA vs 39% in aCSF) or did not respond (15% in TTX + KA vs 39% in aCSF) to α -MSH after treatment with TTX and KA (χ^2 , $p = 0.035$, Figure 3-2C).

α -MSH increases the frequency of IPSCs in the NTS

Our findings from the TTX + KA and TTX studies, in which glutamate signaling and/or synaptic communication were blocked, suggest firstly that α -MSH exerts direct, postsynaptic excitatory effects on a subset of NTS neurons. Secondly, the observation that hyperpolarizing

responses are nearly eliminated in the presence of TTX suggests that the inhibitory effect of α -MSH on the membrane potential of other NTS neurons is indirect and therefore dependent on intact neuronal communication. Thirdly, the fact that a greater percentage of NTS neurons show depolarizing responses to α -MSH in the presence of TTX suggests that at baseline in normal aCSF, α -MSH may exert a direct excitatory effect on NTS neurons and, simultaneously, may indirectly enhance inhibitory inputs to these same neurons. Considering the amplitude of the depolarizing and hyperpolarizing effects of α -MSH are nearly equal in aCSF (6.14 ± 0.54 mV and -6.79 ± 1.02 mV, respectively), such simultaneous and opposing actions would result in a net lack of effect on membrane potential in this subset of neurons. Thus, based on these three observations, we hypothesized that in addition to direct excitatory effects on NTS neurons, α -MSH may exert indirect inhibitory effects on these cells by increasing local GABAergic transmission. In regular aCSF, such enhancement of GABAergic signaling would underlie the hyperpolarizing effects of α -MSH, and also account for the greater proportion of non-responsive neurons as compared to conditions of neuronal isolation in TTX.

To test this hypothesis, we first assessed whether α -MSH influences GABAergic neurotransmission in the NTS by evaluating the effects of α -MSH on the frequency and amplitude of IPSCs recorded in voltage-clamp configuration. Of the 12 neurons studied, 6 showed a reversible increase in the frequency of IPSCs in response to 500 nM α -MSH (baseline: 137.2 ± 44.63 events/100 sec, α -MSH: 345 ± 96.62 events/100 sec, recovery: 106.7 ± 29.74 events/100 sec, Wilcoxon paired test, $p = 0.031$, Figure 3-3A-C). Of the remaining 6 neurons assessed, 4 showed no change in frequency of IPSCs (baseline: 57.5 ± 14.75 events/100 sec, α -MSH: 63.25 ± 16.09 events/100 sec, recovery: 52.25 ± 12.28 events/100 sec), and 2 showed a decrease in the frequency of IPSCs (baseline: 236 ± 141 events/100 sec, α -MSH: 105 ± 78

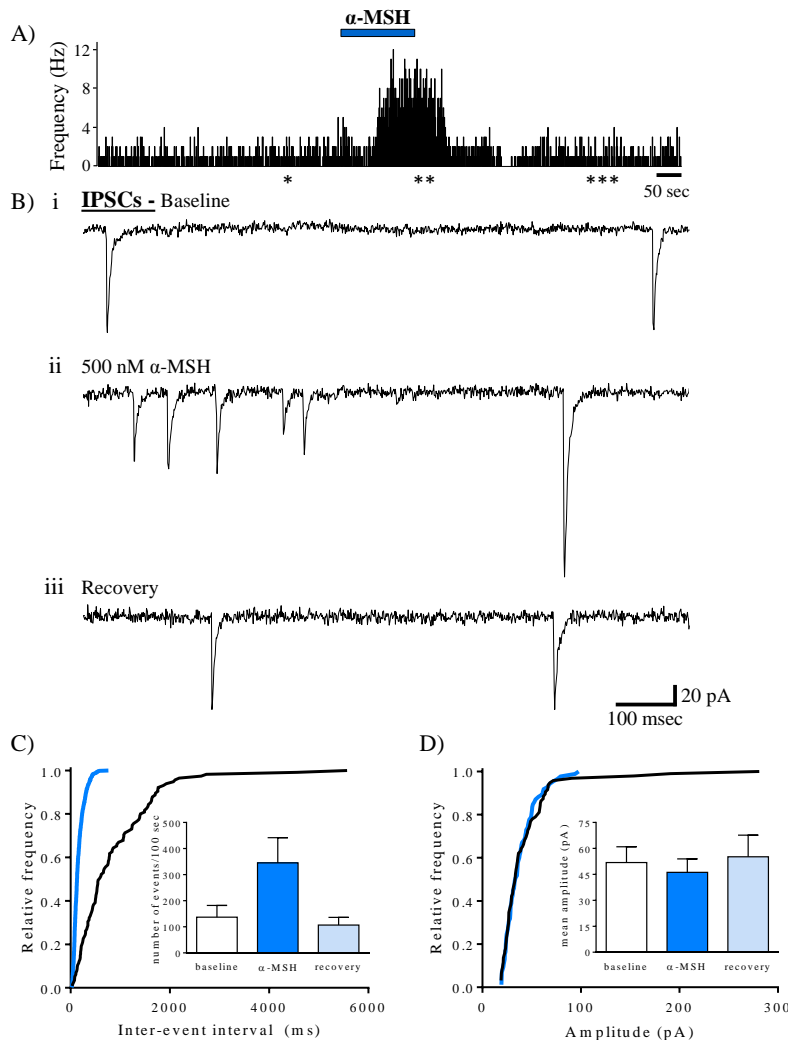


Figure 3-3 – α -MSH increases the frequency of IPSCs in the NTS. A) Frequency histogram of IPSCs in an individual NTS neuron recorded in voltage-clamp configuration. Bath application of 500 nM α -MSH (horizontal blue bar) elicited a reversible increase in the frequency of IPSCs in this neuron. B) Representative one second voltage-clamp recordings from the same neuron shown in (A) at baseline (i, time indicated by * in A), after perfusion with α -MSH (ii, time indicated by ** in A), and after recovery from the effect of α -MSH (iii, time indicated by *** in A). α -MSH induced a reversible increase in IPSC frequency but not amplitude in this neuron. C) Cumulative frequency histogram of an NTS neuron showing a decrease in the inter-event interval between IPSCs over a 100 s period after perfusion with α -MSH (blue line) as compared to 100 s of baseline (black line). The inset shows a bar graph of the number of IPSCs per 100 s time period at baseline (white bar, 137.2 \pm 44.63 events/100 s), after perfusion with α -MSH (dark blue bar, 345 \pm 96.62 events/100 s), and after recovery from the effect of α -MSH (pale blue bar, 106.7 \pm 29.74 events/100 s) in 6 neurons which showed an increase in IPSC frequency in response to α -MSH. D) Cumulative frequency histogram of an NTS neuron showing no change in the amplitude of IPSCs over a 100 s period after perfusion with α -MSH (blue line) as compared to 100 s of baseline (black line). The inset shows a bar graph of the amplitude of IPSCs at baseline (white bar, 51.85 \pm 9.11 pA), after perfusion with 500 nM α -MSH (dark blue bar, 46.2 \pm 7.74 pA), and after recovery from the effect of α -MSH (pale blue bar, 55.2 \pm 12.46 pA) in 6 neurons which showed no change in IPSC amplitude in response to α -MSH. Data in C) and D) represent mean values \pm standard error.

events/100 sec, recovery: 209.5 ± 148.5 events/100 sec, Wilcoxon paired test, $p = 0.5$), however these inhibitory effects did not reach statistical significance as a group.

In the same 12 neurons, α -MSH did not influence the amplitude of IPSCs in 6 cells evaluated (baseline: 51.85 ± 9.11 pA, α -MSH: 46.2 ± 7.74 pA, recovery: 55.2 ± 12.46 pA, Figure 3-3D). While α -MSH caused an increase in the amplitude of IPSCs in 4 cells (baseline: 46.45 ± 2.82 pA, α -MSH: 61.81 ± 6.36 pA, recovery: 55.41 ± 4.73 pA, Wilcoxon paired test, $p = 0.13$), and a decrease in the amplitude of IPSCs in 2 cells (baseline: 83.13 ± 16.17 pA, α -MSH: 52.83 ± 12.46 pA, recovery: 59.77 ± 8.9 pA, Wilcoxon paired test, $p = 0.5$), these effects did not reach statistical significance as a group. As a change in frequency of IPSCs is indicative of a presynaptic site of action, these findings suggest α -MSH enhances GABAergic neurotransmission in the NTS via a presynaptic mechanism.

α -MSH does not influence the frequency or amplitude of miniature IPSCs in the NTS

We next investigated whether α -MSH influences the frequency or amplitude of miniature IPSCs (mIPSCs) in NTS neurons ($n = 12$). α -MSH (500 nM) did not alter the frequency of mIPSCs in 7 cells examined (baseline: 78.86 ± 24.46 events/100 sec, α -MSH: 82.71 ± 28.68 events/100 sec, recovery: 75.29 ± 22.98 events/100 sec, Figure 3-4A, B). While 4 neurons showed a decrease in the frequency of mIPSCs in response to α -MSH (baseline: 317.3 ± 103.9 events/100 sec, α -MSH: 136.3 ± 59.89 events/100 sec, recovery: 184.8 ± 42.46 events/100 sec, Wilcoxon paired test, $p = 0.13$), these effects did not reach statistical significance as a group. Finally, 1 cell showed an increase in the frequency of mIPSCs in response to α -MSH (baseline: 121 events/100 sec, α -MSH: 307 events/100 sec, recovery: 108 events/100 sec).

In the same 12 neurons, α -MSH did not alter the amplitude of mIPSCs in 6 cells examined (baseline: 55.61 ± 9.11 pA, α -MSH: 59.69 ± 7.98 pA, recovery: 62.75 ± 9.05 pA,

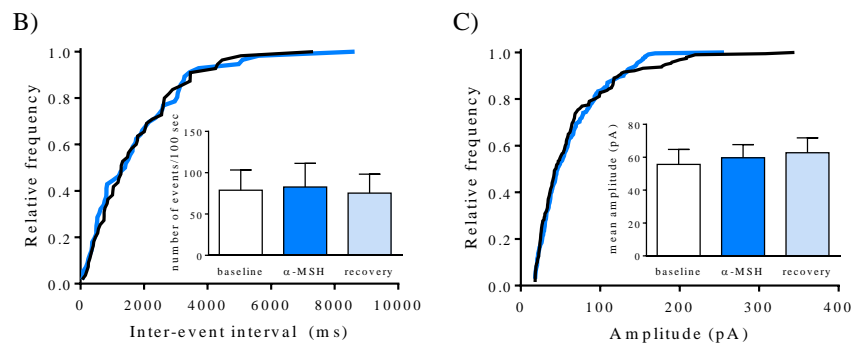
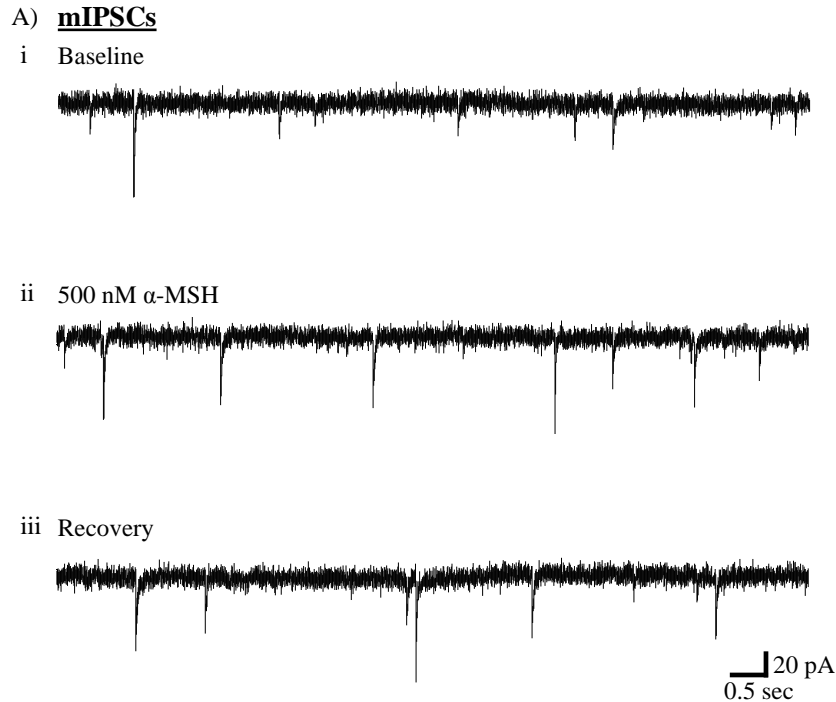


Figure 3-4 – α -MSH does not influence the frequency or amplitude of miniature IPSCs in the NTS.

A) Representative ten second voltage-clamp recordings from an individual NTS neuron showing mIPSCs at baseline (i), after perfusion with 500 nM α -MSH (ii), and after washout of α -MSH (iii). This neuron did not show a change in mIPSC frequency or amplitude in response to α -MSH. B) Cumulative frequency histogram of an NTS neuron showing no change in the inter-event interval between mIPSCs over a 100 s period after perfusion with α -MSH (blue line) as compared to 100 s of baseline (black line). The inset shows a bar graph of the number of mIPSCs per 100 s time period at baseline (white bar, 78.86 ± 24.46 events/100 s), after perfusion with α -MSH (dark blue bar, 82.71 ± 28.68 events/100 s), and after recovery from the effect of α -MSH (pale blue bar, 75.29 ± 22.98 events/100 s) in 7 neurons which showed no change in mIPSC frequency in response to α -MSH. C) Cumulative frequency histogram of an NTS neuron showing no change in the amplitude of mIPSCs over a 100 s period after perfusion with α -MSH (blue line) as compared to 100 s of baseline (black line). The inset shows a bar graph of the amplitude of mIPSCs at baseline (white bar, 55.61 ± 9.11 pA), after perfusion with α -MSH (dark blue bar, 59.69 ± 7.98 pA), and after recovery from the effect of α -MSH (pale blue bar, recovery: 62.75 ± 9.05 pA) in 6 neurons which showed no change in mIPSC amplitude in response to α -MSH. Data in B) and C) represent mean values \pm standard error.

Figure 3-4C). While α -MSH induced a decrease in the amplitude of mIPSCs in 5 cells (baseline: 68.22 ± 19.53 pA, α -MSH: 41.31 ± 7.69 pA, recovery: 57.74 ± 16.15 pA, Wilcoxon paired test, $p = 0.063$), these effects did not reach statistical significance as a group. The remaining 1 cell showed an increase in amplitude in response to α -MSH (baseline: 54.20 pA, α -MSH: 69.44 pA, recovery: 59.27 pA).

GABA receptor antagonism eliminates the hyperpolarizing effects of α -MSH and increases the proportion of neurons which depolarize to α -MSH

We next addressed whether the observed increase in GABAergic signaling caused by α -MSH underlies the hyperpolarization induced by the peptide in a subset of NTS neurons, and whether it could also account for the higher proportion of non-responsive cells observed in aCSF versus TTX-induced neuronal isolation. While fast GABAergic signaling is mediated via the GABA_A ionotropic receptor, a ligand gated Cl⁻ channel, slower GABAergic effects are mediated via the metabotropic GABA_B receptor (Chebib & Johnston, 1999). Since a portion of the hyperpolarizing responses induced by α -MSH occurred at membrane potentials more negative than the reversal potential for Cl⁻, yet we observed effects on GABA_A mediated IPSCs, we hypothesized that activation of both GABA_A and GABA_B receptors underlies the inhibitory effects of this melanocortin in the NTS. In order to determine the relative contribution of each GABA receptor subtype in mediating the inhibitory effects of α -MSH, we treated slices with either the GABA_A receptor antagonist bicuculline (10 μ M) or the GABA_B receptor antagonist CGP 52432 (5 μ M) alone, or with both antagonists simultaneously. Recordings were obtained from 12 neurons in each of the 3 treatment conditions, and the proportions of responses observed in each condition are summarized in Figure 3-5D. α -MSH depolarized 58% of cells treated with bicuculline alone ($n = 7$, mean 4.49 ± 0.46 mV, Figure 3-5A, 3-5D), 67% of cells treated with

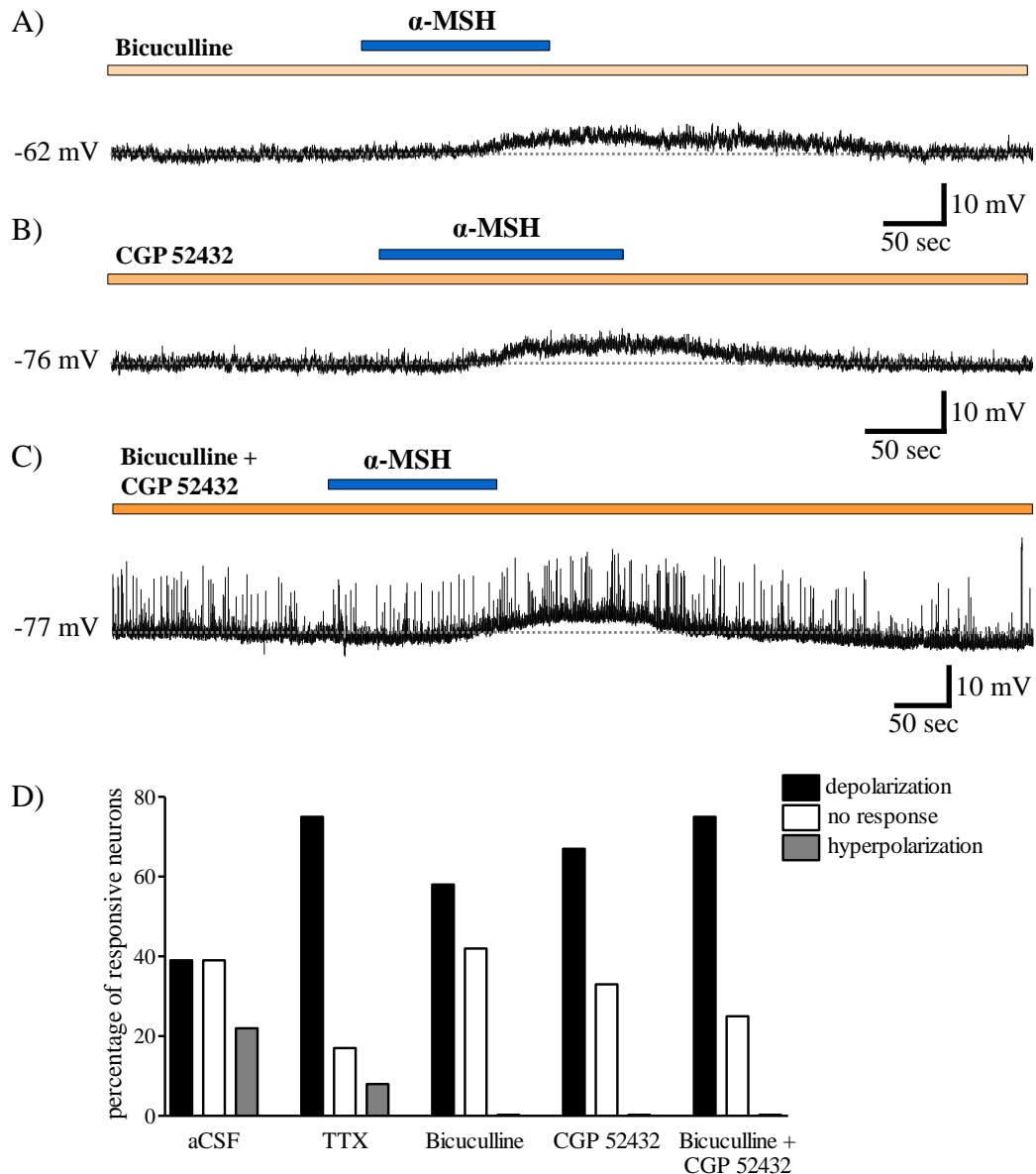


Figure 3-5 – GABA receptor antagonism eliminates the hyperpolarizing effects of α -MSH and increases the proportion of neurons which depolarize to α -MSH. Current-clamp recordings from three NTS neurons, one treated with the GABA_A receptor antagonist bicuculline (10 μ M) alone (A), another with the GABA_B receptor antagonist CGP 52432 (5 μ M) alone (B), and a third with both bicuculline and CGP 52432 simultaneously (C – note excitatory post synaptic potentials are maintained in this neuron). Reversible depolarizing responses to 500 nM bath applied α -MSH (horizontal blue bar) are maintained in each treatment condition. D) Bar graph showing the percentage of NTS neurons in slice preparation which respond to α -MSH with a depolarization (black bars), with no response (white bars), or with a hyperpolarization (grey bars) when slices are bathed in control aCSF, in TTX, in bicuculline alone, in CGP 52432 alone, and in bicuculline and CGP 52432 simultaneously. No hyperpolarizing responses are observed after antagonism of either GABA receptor subtype. When both GABA_A and GABA_B receptors are antagonized, a larger percentage of NTS neurons depolarize to α -MSH as compared to control conditions, and as compared to antagonism of each receptor subtype alone. Note the proportion of cells which depolarize to α -MSH after antagonism of both GABA_A and GABA_B receptors is equal to that observed in TTX.

CGP 52432 alone ($n = 8$, mean 7.79 ± 1.39 mV, Figure 3-5B, 3-5D), and 75% of cells treated with both antagonists simultaneously ($n = 9$, mean 7.51 ± 1.89 mV, Figure 3-5C, 3-5D). The remaining neurons in each group did not respond to α -MSH, and we therefore did not observe hyperpolarizing responses to α -MSH in any treatment condition. There was no difference in the amplitude of the depolarization between control neurons perfused with aCSF and neurons perfused with bicuculline, with CGP 52432, or with bicuculline and CGP 52432 (unpaired t -test, $p = 0.07, 0.19, 0.39$, respectively). Thus, pharmacological blockade of either GABA_A or GABA_B receptors eliminates hyperpolarizing responses to α -MSH. Furthermore, our findings suggest that activity at both GABA_A and GABA_B receptors contributes to the proportion of α -MSH non-responsive cells, since antagonism of both receptors essentially replicates the distribution of responses to α -MSH observed in TTX-induced neuronal isolation (Figure 3-5D).

Dissociated NTS neurons show no hyperpolarizing responses to α -MSH

In addition to pharmacological inhibition of GABAergic transmission in the NTS, we investigated whether physical removal of synaptic contacts between NTS neurons would abolish α -MSH induced hyperpolarizations. We thus conducted current-clamp recordings in dissociated NTS neurons, which lack GABAergic and all other forms of neuronal input due to a lack of neurites and, therefore, synaptic contacts. Hyperpolarizing responses to α -MSH were not observed in any of the 12 dissociated neurons recorded from, while 5 of these cells depolarized to α -MSH (mean: 7.37 ± 1.98 mV, Figure 3-6). There was no difference in the amplitude of the depolarization between neurons in slice preparation perfused with aCSF and in dissociated neurons (unpaired t -test, $p = 0.39$). Thus, elimination of GABAergic neurotransmission via physical dissociation abolishes hyperpolarizing responses induced by α -MSH in NTS neurons.

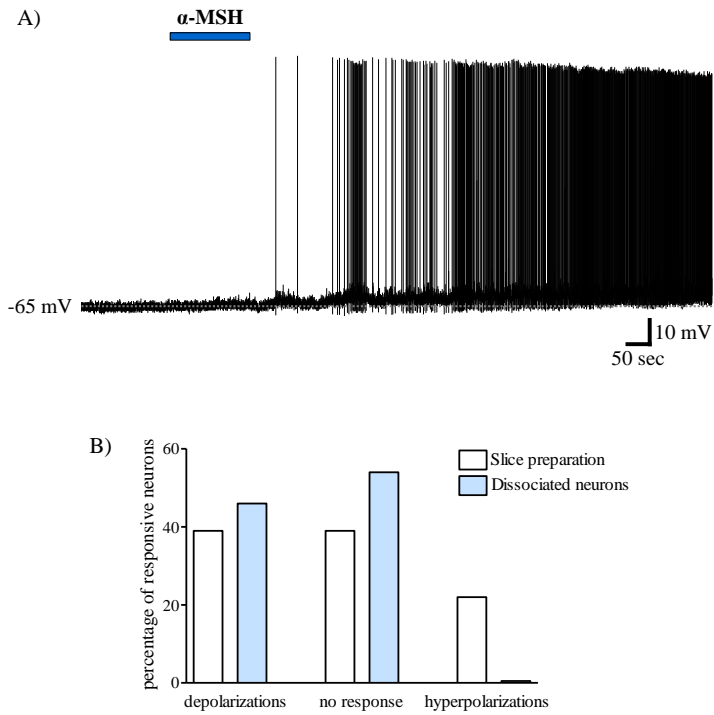


Figure 3-6 – Dissociated NTS neurons show no hyperpolarizing responses to α -MSH. A) Current-clamp recording from a dissociated NTS neuron showing a depolarizing response to bath applied 500 nM α -MSH (horizontal blue bar). B) Bar graph showing the percentage of dissociated NTS neurons which respond to α -MSH with a depolarization, with no response, or with a hyperpolarization. No hyperpolarizing responses to α -MSH are observed in dissociated neurons.

Discussion

The present study is the first to detail direct, postsynaptic excitatory actions of α -MSH on neurons in the NTS, and to characterize stimulatory effects of this melanocortin on local GABAergic signaling in the NTS. Our findings expand the understanding of the subcellular sites of action of α -MSH and the neural circuitries it influences in the NTS, from a formerly mainly presynaptic and glutamatergic centered view (Wan *et al.*, 2008). Our proposed model of action for α -MSH in the NTS is depicted in Figure 3-7 and discussed below.

To shed light on the mechanisms that underlie the medullary satiety-promoting actions of α -MSH, we conducted *in vitro* whole cell patch clamp experiments to firstly examine the effect of α -MSH on the membrane potential of neurons in the NTS, an important central site of α -MSH action and MC4R expression (Kishi *et al.*, 2003;Zheng *et al.*, 2010). While we applied exogenous α -MSH in our studies, endogenous, physiological sources of α -MSH acting in the NTS would arise from both the arcuate nucleus of the hypothalamus and from the NTS, as it has been estimated that 70% of α -MSH present in the NTS is of hypothalamic origin, and the remaining 30% is derived from the brainstem (Zheng *et al.*, 2010). Our electrophysiological results show that in normal aCSF, intended to mimic the physiological condition found in the whole animal, α -MSH exerts both excitatory (Figure 3-7A) and inhibitory effects (Figure 3-7B) on separate subpopulations of NTS neurons. The dual effects on membrane potential induced by α -MSH are typical of numerous neuropeptides (Mimee *et al.*, 2012;Hoyda *et al.*, 2009;Dai *et al.*, 2013;Fry & Ferguson, 2009;Price *et al.*, 2009;Lakhi *et al.*, 2013;Mercer *et al.*, 2013;Cowley *et al.*, 2003), and further experiments will be required to examine whether particular genetically defined populations of NTS neurons are preferentially depolarized or hyperpolarized by α -MSH. The NTS expresses numerous anorexigenic peptides, such as nesfatin-1(Oh-I *et al.*, 2006;Foo *et*

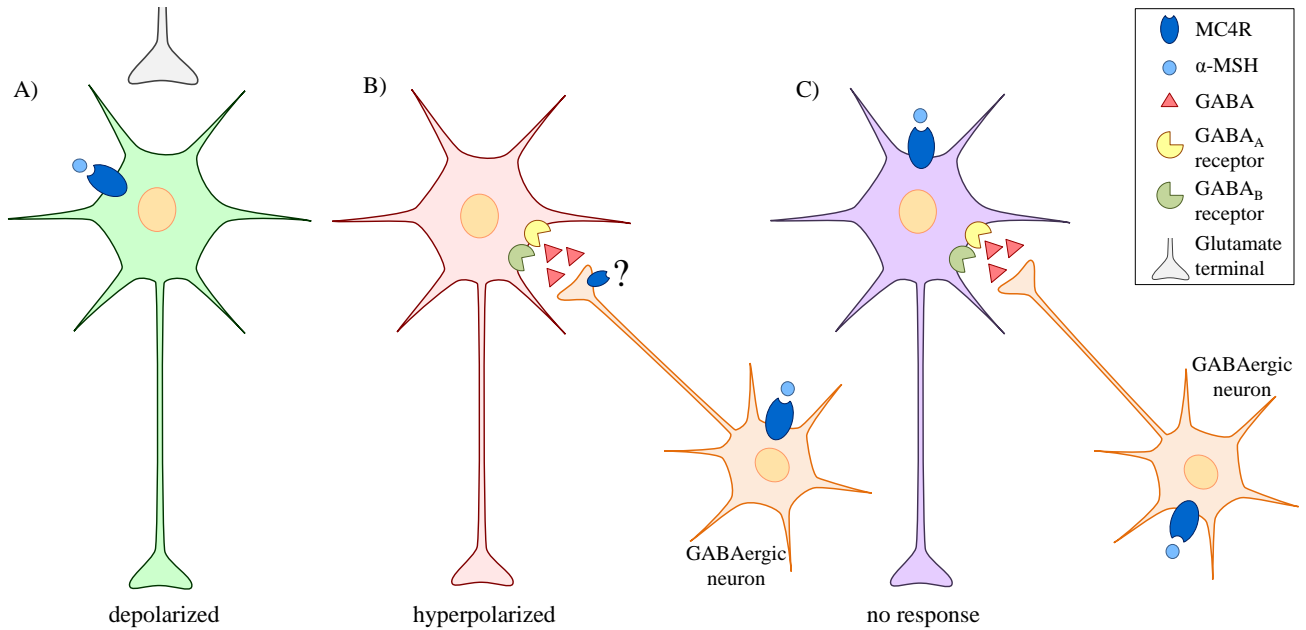


Figure 3-7 – Proposed model: α -MSH exerts direct excitatory effects and indirect inhibitory effects on NTS neurons. Schematic illustrating the proposed sites of action for α -MSH in the NTS. Most neurons in the NTS express postsynaptic MC4 receptors (blue transmembrane ovals), and α -MSH (pale blue circles) can exert direct, depolarizing effects on both undefined (A, green) and GABAergic (B, orange) NTS neurons. Release of GABA (red triangles) from these GABAergic cells indirectly inhibits other NTS cells (red neuron) which express GABA_A and GABA_B receptors, but not MC4Rs, resulting in a hyperpolarization of the membrane potential of these cells (B). MC4Rs may also be present at the presynaptic terminals of GABAergic neurons (B). A third subset of neurons (purple, C) experiences direct excitatory effects of α -MSH and simultaneous indirect, inhibitory effects of α -MSH, resulting in a net lack of effect on the membrane potential of these cells. The grey synaptic terminal represents a glutamatergic vagal afferent, where MC4Rs are expressed and α -MSH acts to presynaptically influence glutamate release (as described in Wan *et al.*, 2008).

al., 2008), glucagon-like peptide 1 (Larsen *et al.*, 1997), brain derived neurotrophic factor (Bariohay *et al.*, 2009;Conner *et al.*, 1997), and POMC (Bronstein *et al.*, 1992;Palkovits *et al.*, 1987), and it is possible, though speculative, that excitation of any of these cell types could contribute to the medullary anorexigenic effects of α -MSH. Alternatively, since α -MSH decreases food intake by decreasing meal size, α -MSH may act on NTS neurons which participate in vago-vagal reflexes controlling ingestive behaviors (Berthoud, 2008), though this is likely not the only medullary mechanism of action for α -MSH as studies have shown the anorexigenic effects of MTII persist after vagotomy (Williams *et al.*, 2000). Furthermore, medullary α -MSH may modulate food intake and energy expenditure by influencing the activity of NTS neurons which project to other brainstem or hypothalamic sites known to be involved in the control of feeding (Berthoud, 2008), or of NTS neurons which project to brown adipose tissue (Zheng *et al.*, 2005). While each of these scenarios is plausible, and likely several occur together to ultimately contribute to the anorexigenic effects of α -MSH, it is evident that further studies are warranted and necessary to fully elucidate the NTS cell types which mediate α -MSH induced satiety at the level of the brainstem.

By treating slices with TTX to block synaptic communication between neurons, we also evaluated whether the effects of α -MSH on membrane potential are direct or rather mediated via neuron to neuron signaling. Interestingly, when slices were treated with TTX we observed a clear shift in the proportion of responses elicited by α -MSH, with nearly twice as many neurons showing a depolarization to α -MSH as compared to control conditions. These observations clearly indicate α -MSH exerts direct, postsynaptic excitatory effects on NTS neurons (Figure 3-7A). Furthermore, when glutamatergic signaling in the NTS was blocked with KA, the depolarizing responses induced by α -MSH persisted, indicating that glutamate is not required for

α -MSH to exert its excitatory effects in the NTS. Thus while a previous report suggested a predominantly presynaptic site of action for α -MSH in the NTS and glutamate as a critical player in mediating medullary melanocortin effects (Wan *et al.*, 2008), our current findings provide an important expansion to these already defined actions of α -MSH in the brainstem. It should be emphasized that Wan *et al.* (2008) did not specifically examine effects of α -MSH on membrane potential of NTS neurons or directly explore potential postsynaptic actions of the peptide. Our results are therefore not in disagreement with theirs, but rather build upon a growing model of medullary sites of action for α -MSH. In addition, our findings in TTX and in TTX + KA suggest between 70-75% of NTS neurons express functional MC4Rs, providing more quantification to previous reports of relatively dense expression of the MC4R in the NTS (Kishi *et al.*, 2003).

Our studies in TTX suggest that the hyperpolarizing responses to α -MSH observed in control conditions are likely indirect and dependent on local neuronal communication in the NTS, as the inhibitory responses induced by α -MSH were nearly eliminated in TTX. In order to verify whether GABAergic neurotransmission in the NTS underlies the indirect hyperpolarizations induced by α -MSH, we first performed voltage-clamp recording to examine effects of the melanocortin on the frequency and amplitude of both IPSCs and mIPSCs. While we observed no significant effects on mIPSCs, α -MSH did induce significant increases in the frequency, but not the amplitude, of IPSCs in 50% of neurons tested, suggesting presynaptic enhancement of GABAergic signaling by α -MSH. Next, in order to demonstrate the necessity of GABA in mediating the hyperpolarizing effects of α -MSH, we pharmacologically antagonized GABA_A and/or GABA_B receptors in the NTS. When either GABA receptor subtype was blocked, α -MSH induced hyperpolarizations were entirely eliminated. These findings suggest that both GABA_A and GABA_B receptors are necessary for α -MSH to exert a hyperpolarizing

effect on NTS neurons. Finally, physical removal of all neuronal inputs to NTS neurons using dissociated cells confirmed GABAergic signaling is required for α -MSH to induce inhibitory effects on these neurons, as dissociated cells showed no hyperpolarizations in response to α -MSH. Taken together, our results indeed indicate that the inhibitory effects of α -MSH in the NTS are indirect and mediated via GABAergic neurotransmission. We thus propose that at least some GABAergic NTS neurons express MC4Rs and are excited by α -MSH, resulting in a release of GABA onto neighboring NTS neurons, which themselves are then hyperpolarized (Figure 3-7B). This model is strongly supported by anatomical evidence of α -MSH immunoreactive axonal varicosities forming frequent and close contacts with GABAergic NTS neurons in the mouse (Zheng *et al.*, 2005) and by single cell RT-PCR studies from our laboratory showing expression of both GAD67 (glutamate decarboxylase, a GABAergic cell marker) and the MC4R on a subset of NTS neurons (Mimee *et al.*, 2012). Further studies using either immunohistochemical techniques or electrophysiology and RT-PCR will, however, be required to definitely establish an excitatory effect of α -MSH on GABAergic cells in the NTS.

It should be noted that while we did observe nearly the same proportion of hyperpolarizations in KA + TTX as compared to aCSF, the amplitude of these responses was significantly blunted as compared to aCSF. Furthermore, one of twelve neurons tested in TTX also showed a hyperpolarizing response to α -MSH. Our studies with the GABA receptor antagonists and in dissociated cells do confirm α -MSH-induced inhibitory effects are exclusively indirect and the result of presynaptic enhancement of GABAergic signaling. Thus we reason that perhaps the small number of hyperpolarizations that persist after TTX treatment are indeed indirect effects, and could be mediated by MC4Rs located at the synapse between a GABAergic NTS neuron and the cell which hyperpolarizes to α -MSH. As TTX leaves intact all spontaneous

release of vesicles at the synapse, synaptically located MC4Rs, once activated, could promote the release of GABA from the presynaptic neuron, ultimately hyperpolarizing the post synaptic cell (Figure 3-7B). This hypothesis is supported by the fact that we did observe an increase in mIPSC frequency in a small percentage of neurons tested, although these effects on mIPSCs did not reach statistical significance.

Finally, by increasing the proportion of neurons which depolarized to α -MSH, TTX treatment effectively decreased the percentage of neurons which did not respond to this melanocortin. In light of our findings that α -MSH enhances GABAergic transmission, these observations imply that TTX treatment removes this α -MSH induced GABAergic inhibitory input to NTS neurons, thereby unmasking an excitatory effect of α -MSH on these cells and resulting in a greater proportion of depolarizing responses. We thus propose that in normal aCSF, a subset of NTS neurons experiences simultaneous direct excitatory effects of α -MSH and indirect, GABAergic inhibitory input induced by α -MSH, resulting in an overall lack of effect on membrane potential (Figure 3-7C). This model is firstly supported by our findings in conditions of GABA receptor blockade, where inhibition of GABAergic signaling resulted in a large proportion of depolarizations and a low proportion of non-responders, as seen in TTX. Secondly, our findings in TTX show 17% of NTS neurons do not respond to α -MSH, in other words, do not express MC4Rs. This would imply that of the 39% of neurons categorized as non-responders in control aCSF conditions, 22% may in fact be receiving the simultaneous and opposing α -MSH effects we propose. Added to the 22% of neurons which hyperpolarize to α -MSH in aCSF, we would expect α -MSH to be enhancing GABAergic signaling to approximately 45% of NTS neurons. Indeed, this is precisely what we observed in our analysis of α -MSH effects on IPSCs in the NTS, as 50% of cells showed an increase in IPSC frequency after application of α -MSH, thus

lending further support to our hypothesis that α -MSH can simultaneously excite and inhibit a portion of NTS neurons to result in a net lack of effect on membrane potential in regular aCSF.

Our present work has revealed effects of α -MSH on GABAergic signaling in the NTS, and indeed actions of GABA in the NTS have been implicated in the control of feeding related processes. For example, GABA actions in the NTS impact swallowing (Wang & Bieger, 1991) and gastric motility (Herman *et al.*, 2009). Furthermore, effects of GABA on medial NTS neurons receiving gastric vagal input have been demonstrated (Yuan *et al.*, 1998), and GABAergic NTS neurons project to and regulate the activity of neurons in the dorsal motor nucleus of the vagus, which themselves control multiple activities of the gastrointestinal tract, such as gastric acid secretion and gastric motility (reviewed in (Browning & Travagli, 2010; Travagli *et al.*, 2006). Thus by altering GABAergic signaling in the NTS, α -MSH has the potential to ultimately shape the transmission of peripheral information from the gut to the brain, and also influence motor outputs governing the activity of gastrointestinal organs. The physiological consequences of the cellular effects of α -MSH on GABAergic neurotransmission we have observed, however, remain to be examined.

We conclude that α -MSH exerts direct, depolarizing actions on a subset of NTS neurons (Figure 3-7A), and indirect hyperpolarizing effects on other NTS cells via enhancement of GABAergic neurotransmission (Figure 3-7B). A third group of neurons experiences each of these opposing effects of α -MSH simultaneously, resulting in a net lack of effect of the melanocortin on the membrane potential of these cells (Figure 3-7C), while a small percentage of NTS neurons do not express the MC4R. Taken together, our results provide important additions to the understanding of the neurocircuitries affected by α -MSH in the NTS, which now include presynaptic vagal sites of action, direct, postsynaptic effects on NTS neurons, as well as

modulation of both glutamatergic and GABAergic signaling. While further experiments are necessary to fully elucidate the physiological contribution of each of these elements on the ultimate effects of α -MSH on autonomic function, our studies highlight the NTS as an important cellular effector of the coordinated central actions of melanocortins.

Acknowledgments

This work was supported by funding from the Natural Sciences and Engineering Research Council of Canada, Le Fonds québécois de la recherche sur la nature et les technologies, and the Heart and Stroke Foundation of Ontario.

CHAPTER 4: The NTS contains physiologically relevant glucose sensing neurons and exhibits plasticity to the effects of α -MSH, but not nesfatin-1, as glyceimic state is altered

Abstract

The nucleus of the solitary tract (NTS) is a critical medullary integrative center with multiple roles in the coordinated control of energy homeostasis. Among the many metabolically relevant factors expressed in this nucleus are the anorexigenic peptides nesfatin-1 and α -melanocyte stimulating hormone (α -MSH). NTS neurons have also been described as glucose responsive, however the studies leading to these conclusions made use of non-physiological changes in glucose concentrations for the brain. In this study, we used whole cell current-clamp recordings on rat NTS neurons in slice preparation to evaluate whether the NTS contains physiologically relevant glucose responsive neurons (GR), whether nesfatin-1 and α -MSH influence the excitability of GR cells, and whether the effects of these peptides are altered in accordance with glycemic status. The majority of NTS neurons ($n = 81$) were found to be GR, with 35% exhibiting a glucose excited (GE) phenotype (mean absolute change in membrane potential in response to a change in glucose concentration: 9.48 ± 1.07 mV), and 22% a glucose inhibited (GI) response (mean: 6.27 ± 0.68 mv). Nesfatin-1 exerted heterogeneous effects on the membrane potential of GE, GI, and glucose non-responsive (NR) NTS neurons. Furthermore, the proportion and amplitude of depolarizing and hyperpolarizing responses of NTS neurons to nesfatin-1 was consistent across hypo-, normo-, and hyperglycemic conditions. In contrast, α -MSH preferentially influenced the membrane potential of GR versus NR NTS neurons, as 81% of GR cells, but only 50% of NR neurons, responded to the peptide. Furthermore, NTS neurons showed increasing responsiveness to α -MSH as extracellular glucose concentrations were decreased, and in hypoglycemic conditions all NTS neurons were depolarized by α -MSH (mean 10.57 ± 3.15 mV, $n = 8$). Finally, decreasing levels of extracellular glucose correlated with a significant hyperpolarization of the baseline membrane potential of NTS neurons, highlighting

the modulatory effect of glucose on the excitability of cells in this region. Our findings firstly reveal individual NTS cells are capable of integrating multiple sources of metabolically relevant input. Furthermore, we suggest nesfatin-1 may act as a neuromodulatory peptide at the level of the NTS, rather than a mediator of ingestive behavior. Our findings do, however, support an important and dynamic role for α -MSH in the control of energy homeostasis in this region, and highlight the rapid capacity for plasticity in medullary melanocortin circuits.

Introduction

The medullary nucleus of the solitary tract (NTS) is a complex integrative autonomic center with numerous critical roles in the coordinated control of ingestive behaviors. The NTS receives vagal inputs arising from the gastrointestinal tract which transmit information regarding the mechanical status, and presence of nutrients, in the gut, as well as descending inputs from higher brain areas involved in the control of feeding behaviors, such as the hypothalamus (for reviews see (Berthoud, 2008;Grill & Hayes, 2012)). In addition to its role as a relay center for multiple sources of inputs, the NTS also produces and senses numerous neuropeptides involved in the control of food intake and energy balance. Among these peptides are nesfatin-1 (Oh-I *et al.*, 2006;Foo *et al.*, 2008) and alpha-melanocyte stimulating hormone (α -MSH) (Bronstein *et al.*, 1992), as well as the α -MSH receptor, the melanocortin 4 receptor (MC4R) (Kishi *et al.*, 2003). Fourth ventricular injections of nesfatin-1 (Stengel *et al.*, 2009a) and the melanocortin 3 and 4 receptor (MC3/4R) agonist melanotan II (MTII) (Grill *et al.*, 1998;Zheng *et al.*, 2005) lead to profound decreases in food intake, as do more localized injections of both peptides into the dorsal vagal complex (including NTS and the dorsal motor nucleus of the vagus (DMV)) (Williams *et al.*, 2000;Dong *et al.*, 2014). Furthermore, the receptors mediating the medullary anorexigenic effects of melanocortins appear to be located in the NTS, as antagonism of MC3/4Rs specifically in the NTS abolishes α -MSH induced decreases in feeding (Zheng *et al.*, 2010).

In addition to its ability to sense peptides involved in the control of feeding, NTS neurons can also detect fluctuations in levels of extracellular glucose, leading to alterations in gastric motility (Ferreira, Jr. *et al.*, 2001), glucagon secretion (Lamy *et al.*, 2014), and to the stimulation of feeding in hypoglycemic conditions (Ritter *et al.*, 2000). Indeed, both glucose excited (GE)

and glucose inhibited (GI) neurons have been described *in vitro* in this region (Mizuno & Oomura, 1984; Dallaporta *et al.*, 1999; Balfour *et al.*, 2006; Wan & Browning, 2008a). These studies, however, have used supra-physiological concentrations of glucose, or very large changes in glucose concentrations not likely to be encountered by CNS neurons *in vivo*. Furthermore, while it is clear individual NTS neurons process multiple sources and types of converging inputs regarding the metabolic status of the organism, many *in vitro* studies in this region evaluate the effects of only one individual input at a time, rather than assessing the integrative properties of these cells. In addition, many such studies are conducted at only one extracellular glucose level (usually 10 mM, which represents hyperglycemia in the CNS), thereby mimicking only one feeding state of the whole animal. This approach evidently does not allow for a full appreciation of the range of actions of peptides across the spectrum of hunger to satiety.

The present study was thus undertaken, firstly, to provide evidence of physiologically relevant glucose sensing neurons in the NTS, and to evaluate the ability of these cells to integrate additional metabolically relevant signals. Furthermore, we assessed whether the responsiveness of NTS neurons to anorexigenic peptides is altered as extracellular glucose concentrations are modified *in vitro*. We report the presence of physiologically relevant GE and GI neurons in the NTS and their ability to respond to both nesfatin-1 and α -MSH. While we find nesfatin-1 exerts heterogeneous effects on both glucose responsive and nonresponsive cells, we demonstrate GE neurons are selectively depolarized by α -MSH. Furthermore, while we find the effects of nesfatin-1 on NTS neurons are consistent across hyper- to hypoglycemic conditions, we document an increased excitatory effect of α -MSH on NTS cells with decreasing glucose concentrations, thereby reflecting the dynamic medullary effects of this peptide with changing metabolic status.

Experimental Procedures

Preparation of NTS slices for electrophysiology

Coronal slices at the level of the NTS were prepared daily from 3-4 week old male Sprague-Dawley rats fed *ad libitum* (Charles River, Quebec, Canada). Unanesthetized rats were decapitated and their brains submerged in ice cold slicing solution made of (in mM): 87 NaCl, 2.5 KCl, 25 NaHCO₃, 0.5 CaCl₂, 7 MgCl₂, 1.25 NaH₂PO₄, 25 glucose, 75 sucrose bubbled with 95% O₂/5% CO₂. A region of the brainstem containing the NTS was isolated and 300 µm coronal sections were cut with a vibratome (Leica, Nussloch, Germany). Slices were then incubated at 32°C in artificial cerebrospinal fluid (aCSF) made of (in mM): 124 NaCl, 2.5 KCl, 20 NaHCO₃, 2 CaCl₂, 1.3 MgSO₄, 1.24 KH₂PO₄ bubbled with 95% O₂/5% CO₂. The glucose concentration of the aCSF varied and was either 5, 3 or 0.2 mM. At each concentration, the osmolarity of the aCSF was adjusted to that of standard aCSF containing 10 mM glucose with equimolar substitution with sucrose. Slices were incubated at 32°C for a minimum of 1 hour before electrophysiological recordings were performed. All procedures were in accordance with the ethical criteria established by the Canadian Council on Animal Care and were approved by the Queen's University Animal Care Committee.

Electrophysiology

Brain slices were moved to a recording chamber perfused with carbogenated aCSF warmed to approximately 32°C at a flow rate of 1.5-2 ml/minute. An upright differential interference contrast microscope at 40x was used to visualize neurons (Scientifica, East Sussex, United Kingdom). Borosilicate glass electrodes (World Precision Instruments, Sarasota, Florida, USA) were pulled on a Sutter Instruments P97 flaming micropipette puller and filled with an intracellular solution made of (in mM): 125 potassium gluconate, 10 KCl, 2 MgCl₂, 0.1 CaCl₂,

5.5 EGTA, 10 HEPES, 2 NaATP (pH 7.2 with KOH). Electrodes had a resistance of 3-5.5 M Ω when filled with the intracellular solution. After obtaining a high resistance seal (minimum 1G Ω), brief suction was used to rupture the membrane and obtain whole cell access. Whole cell recordings were made with a Multiclamp 700B amplifier (Molecular Devices, Sunnyvale, California, USA), filtered at 2.4 kHz, and sampled at 10 kHz using a Micro 1401 interface. Data were collected with Spike 2 software for offline analysis (Cambridge Electronic Devices, Cambridge, UK). At all glucose concentrations used, neurons selected for experimentation had action potentials with an amplitude of at least 60 mV and a stable baseline membrane potential. Of note, while it was more challenging to obtain recordings as extracellular glucose concentrations were decreased, once cells were obtained, there was no appreciable difference in the quality or duration of recordings at low glucose concentrations.

All solutions were applied to slices via bath perfusion. Responses to changes in glucose concentration, to α -MSH, or to nesfatin-1 were assessed by comparing the membrane potential of the neuron before and after glucose or peptide application. A response was deemed significant if the change in membrane potential after glucose or peptide application was at least twice the standard deviation of the baseline membrane potential obtained during a 100 second period immediately before application of the test solution. Post-application membrane potential was the peak membrane potential averaged over 100 seconds of the recording showing a maximal effect. A calculated liquid junction potential of 15 mV has been subtracted from all membrane potentials. A *t*-test or one-way ANOVA was used to evaluate the significance of differences in the amplitude of responses between populations of neurons. Changes in the distribution of responses between populations were assessed with the χ^2 test. For all tests, significance was defined as $p < 0.05$.

Glucose concentrations and characterization of glucose responsiveness

We selected 5 mM to mimic central hyperglycemia, 3 mM glucose to mimic central normoglycemia, and 0.2 mM glucose to mimic central hypoglycemia. These concentrations were chosen based firstly on measurements obtained *in vivo* from the rat brain (Ono *et al.*, 1983;Silver & Erecinska, 1994;Hu & Wilson, 1997;Routh, 2002), and secondly on previous *in vitro* electrophysiological experiments in rat brain slices (Burdakov *et al.*, 2005;Burdakov *et al.*, 2006;Lamy *et al.*, 2014;Melnick *et al.*, 2011;Song *et al.*, 2001;Wang *et al.*, 2004;Williams *et al.*, 2008). To further mimic physiological transitions in glucose concentrations, steps were only made from normoglycemic conditions to hypo- or hyperglycemic conditions, or vice versa (ie no steps from hypo- directly to hyperglycemic conditions, or vice versa, were performed). Neurons were considered GE if they depolarized in response to an increase in glucose concentration, or hyperpolarized in response to a decrease in glucose concentration. Cells were classified as GI if they depolarized in response to a decrease in glucose concentration, or hyperpolarized in response to an increase in glucose concentration. The mean responses to alterations in glucose concentration in GE and GI neurons are reported as absolute changes in membrane potential (ie the sign removed from hyperpolarizations and pooled with depolarizations).

Chemicals and drugs

Slicing solution, aCSF and intracellular recording solution were made with salts obtained from Sigma Pharmaceuticals (Oakville, Ontario, Canada). Nesfatin-1 and α -MSH were obtained from Phoenix Pharmaceuticals (Belmont, California, USA).

Results

The NTS contains physiologically relevant glucose sensing neurons

We first assessed whether NTS neurons respond to changes in glucose concentrations which fall within the physiological range measured in the CNS. To this end, we bath perfused varying concentrations of extracellular glucose (5, 3 and 0.2 mM, see Methods for rationale) on a total of 81 medial NTS neurons during current-clamp recordings. The majority (57%) of the cells examined were found to be glucose responsive. Overall, 28 cells were GE neurons (35%, mean absolute change in membrane potential: 9.48 ± 1.07 mV, Figure 4-1A, 4-1C, 4-1D), and 18 cells were GI neurons (22%, mean absolute change in membrane potential: 6.27 ± 0.68 mV, Figure 4-1B, 4-1C, 4-1D). The remaining 35 neurons (43%) did not respond to changes in glucose concentrations. In the 23 GE cells in which the extracellular glucose concentration was returned to initial baseline levels, 17 cells showed a recovery toward baseline membrane potential. Furthermore, in the 14 GI cells in which the extracellular glucose concentration was returned to baseline levels, 9 showed a recovery toward baseline membrane potential. Finally, there was no correlation between baseline membrane potential and the cellular response to changes in glucose concentration, as the baseline membrane potential of GE, GI, and glucose non-responsive (NR) cells were not different from one another (mean baseline membrane potential GE neurons: -69.51 ± 1.39 mV, GI neurons: -71.37 ± 1.12 mV, NR neurons: -69.09 ± 0.87 mV, one-way ANOVA, $p = 0.41$).

We also examined the distribution of GE, GI, and NR phenotypes at each glucose step performed, as summarized in Figure 4-1E. When extracellular glucose levels were changed from 0.2 to 3 mM ($n = 15$), we found 73% of neurons were GE, 20% were GI, and 7% were non responsive to changes in glucose (NR). Conversely, when glucose concentrations were decreased

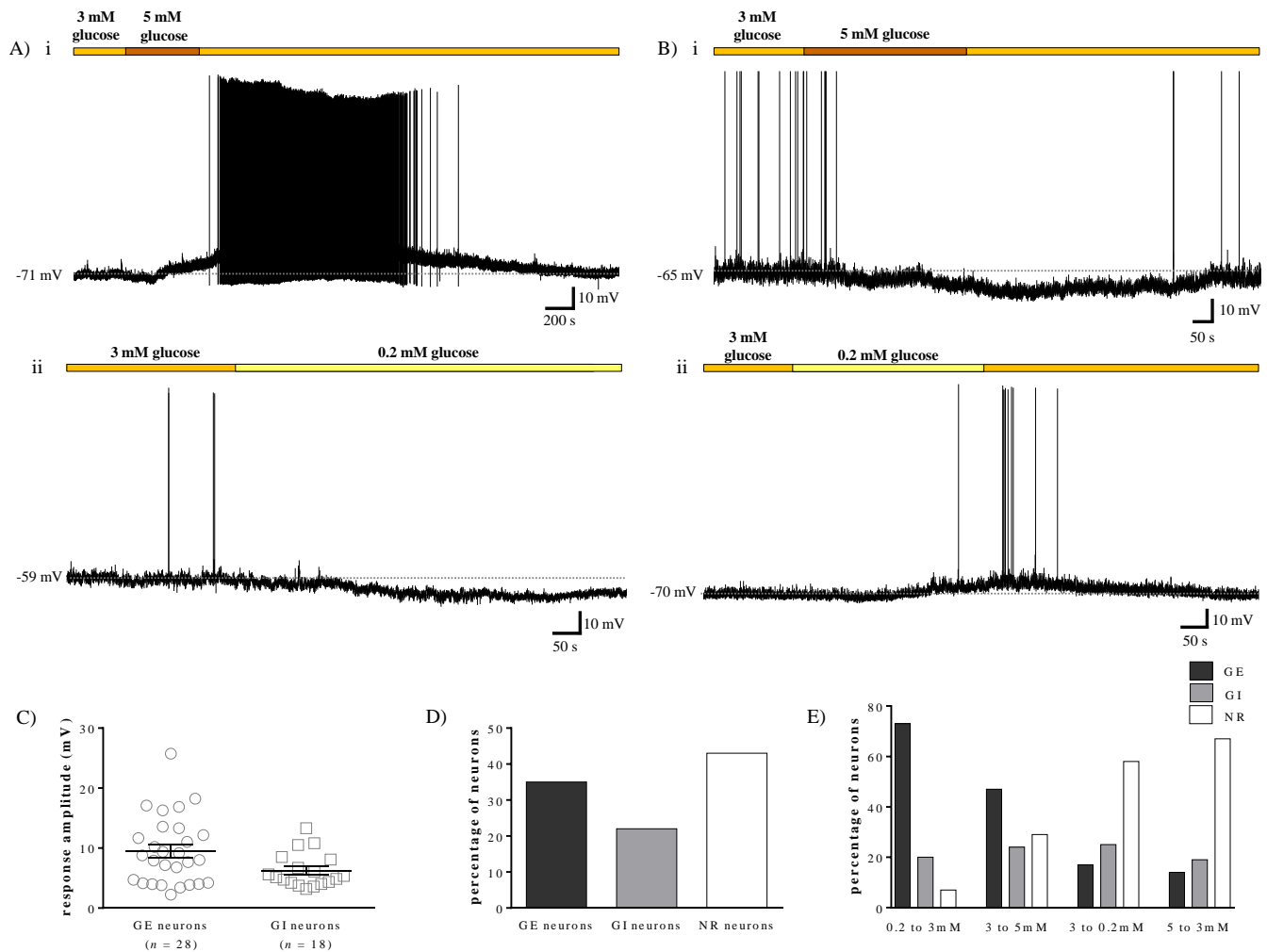


Figure 4-1 – The NTS contains physiologically relevant glucose sensing neurons. A) and B) Representative current-clamp recordings from four separate NTS neurons in slice preparation. An increase in glucose concentration from a baseline of 3 mM to 5 mM in (A, i) caused a reversible depolarization in this GE cell, while a decrease in glucose concentration from 3 to 0.2 mM elicited a hyperpolarization in the GE neuron in (A, ii). In B), an increase from 3 to 5 mM glucose caused a reversible hyperpolarization in the GI cell in (i), while a decrease from 3 to 0.2 mM glucose elicited a reversible depolarization in the GI neuron in (ii). C) Scatter plot depicting the range of responses elicited by changes in glucose concentration in NTS neurons. Black bars represent the absolute mean change \pm standard error in membrane potential induced by altered glucose concentrations in GE and GI neurons, while each single point represents the response of a single neuron. Mean GE response: 9.48 ± 1.07 mV ($n = 28$), mean GI response: 6.27 ± 0.68 mV ($n = 18$). D) Bar graph showing the percentage of NTS neurons which displayed a GE, GI, or NR phenotype in response to changes in glucose concentration. E) Bar graph illustrating the percentage of NTS neurons which exhibited a GE, GI, or NR phenotype at each step in glucose concentration employed.

from 3 to 0.2 mM ($n = 24$), 17% of cells were GE, 25% were GI, and 58% were NR. Furthermore, when stepping from 3 to 5 mM glucose ($n = 21$), 47% of neurons were GE, 24% were GI, and 29% were NR. Conversely, when glucose levels were decreased from 5 to 3 mM ($n = 21$), 14% of cells were GE, 19% were GI, and 67% were NR. These findings thus suggest NTS neurons are more responsive to increases in extracellular glucose concentrations than to decreases in glucose levels (χ^2 , $p < 0.0003$ for all comparisons of increases versus decreases in glucose concentration, $p > 0.05$ for all comparisons of changes in glucose concentration in the same direction).

Nesfatin-1 exerts heterogeneous effects on both glucose responsive and glucose non-responsive NTS neurons

Since nesfatin-1 expressing NTS neurons exhibit c-Fos immunoreactivity in response to systemic hypoglycemia in rats (Bonnet *et al.*, 2013), and since we have previously demonstrated effects of nesfatin-1 on the excitability of NTS neurons (Mimee *et al.*, 2012), we next investigated whether nesfatin-1 may exert preferential effects on a particular subtype of glucose sensing cell. To this end, 40 of the neurons tested for glucose responsiveness were also evaluated for nesfatin-1 responsiveness. Nesfatin-1 exerted heterogeneous effects on GE ($n = 13$), GI ($n = 8$), and NR ($n = 19$) cells in this region, as summarized in Figures 4-2C and 4-2D. More specifically, nesfatin-1 depolarized 38% of GE and GI neurons (mean depolarization: 6.40 ± 3.17 mV and 6.56 ± 3.03 mV, respectively) hyperpolarized 24% of GE and GI neurons (mean hyperpolarization: -6.73 ± 1.50 mV and -5.61 ± 0.96 mV, respectively, Figure 4-2A) and exerted no effect on the remaining 38% of GE and GI neurons. Furthermore, 42% of NR cells were depolarized by nesfatin-1 (mean depolarization: 5.16 ± 0.96 mV, Figure 4-2B), 11% of NR neurons hyperpolarized in response to nesfatin-1 (mean hyperpolarization: -6.29 ± 0.61 mV), and

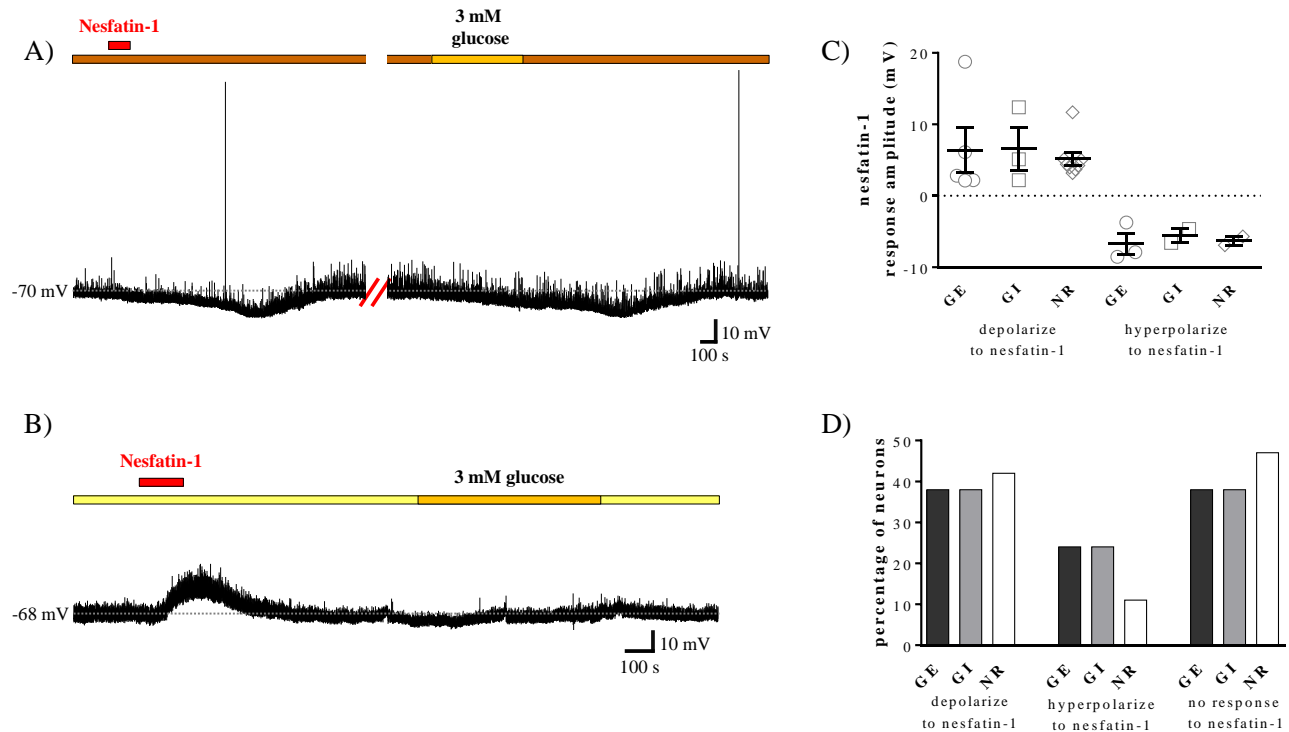


Figure 4-2 – Nesfatin-1 exerts heterogeneous effects on both glucose responsive and glucose non-responsive NTS neurons. A) and B) Representative current-clamp recordings from two separate NTS neurons. A) Nesfatin-1 (10 nM, horizontal red bar) elicited a reversible hyperpolarization in this neuron subsequently identified as GE following a decrease in glucose concentration from a baseline of 5 mM to 3 mM. B) Nesfatin-1 elicited a reversible depolarization in this NR NTS neuron. C) Scatter plot depicting the range of responses elicited by 10 nM nesfatin-1 in GE, GI, and NR NTS neurons. Mean nesfatin-1 induced depolarization GE: 6.40 ± 3.17 mV, GI: 6.56 ± 3.03 mV, NR: 5.16 ± 0.96 mV. Mean nesfatin-1 induced hyperpolarization GE: -6.73 ± 1.50 mV, GI: -5.61 ± 0.96 mV, NR: -6.29 ± 0.61 mV. D) Bar graph showing the percentage of GE ($n = 18$), GI ($n = 13$), and NR ($n = 19$) NTS neurons which also responded to nesfatin-1. There is no difference in the amplitude (ANOVA, $p > 0.8$) or distribution (χ^2 , $p > 0.3$) of nesfatin-1 responses across subtypes of glucose sensing NTS neurons.

the remaining 47% did not respond to nesfatin-1. Thus, both the amplitude (one-way ANOVA, $p > 0.8$, Figure 4-2C) and the distribution (χ^2 , $p > 0.3$, Figure 4-2D) of the effects of nesfatin-1 on the membrane potential of NTS neurons was consistent between GE, GI, and NR cells.

The effects of nesfatin-1 on NTS neurons are consistent across glucose concentrations

We next evaluated whether the effects of nesfatin-1 on the excitability of NTS neurons may be altered as extracellular glucose concentrations are modified. We therefore maintained rat brain slices containing the NTS at either 5, 3, or 0.2 mM glucose and subsequently bath perfused 10 nM nesfatin-1 to evaluate the effects of this peptide on the membrane potential of NTS cells. Our findings are summarized in Figure 4-3. Previous studies from our laboratory using slices maintained at 10 mM glucose showed effects of nesfatin-1 on 63% of NTS neurons, 42% of which depolarized ($n = 39$, mean 7.83 ± 0.84 mV), 21% of which hyperpolarized ($n = 20$, -8.23 ± 1.0 mV), and the remaining 37% of which did not respond to 10 nM nesfatin-1 ($n = 34$) (Mimee *et al.*, 2012). At 5 mM extracellular glucose, 64% of NTS neurons ($n = 14$) responded to nesfatin-1; 36% with a reversible depolarization ($n = 5$, mean 5.57 ± 0.80 mV) and 28% with a hyperpolarization ($n = 4$, mean: -6.10 ± 0.95 mV, 2 reversible). When extracellular glucose concentrations were decreased to 3 mM, 59% of NTS neurons ($n = 32$) responded to nesfatin-1; 41% with a depolarization ($n = 13$, mean 6.70 ± 1.23 mV, 11 at least partially reversible, Figure 4-3Ai) and 18% with a hyperpolarization ($n = 6$, mean: -7.53 ± 0.96 mV, 3 reversible, Figure 4-3Bi). Finally, at 0.2 mM extracellular glucose, 71% of NTS neurons ($n = 17$) responded to nesfatin-1; 47% with a depolarization ($n = 8$, mean: 5.83 ± 1.44 mV, 6 at least partially reversible, Figure 4-3Aii) and 24% with a reversible hyperpolarization ($n = 4$, mean: -6.59 ± 1.01 mV, Figure 4-3Bii). Thus, firstly, there was no difference in the amplitude of the depolarizations or hyperpolarizations observed at all extracellular glucose concentrations employed (one-way

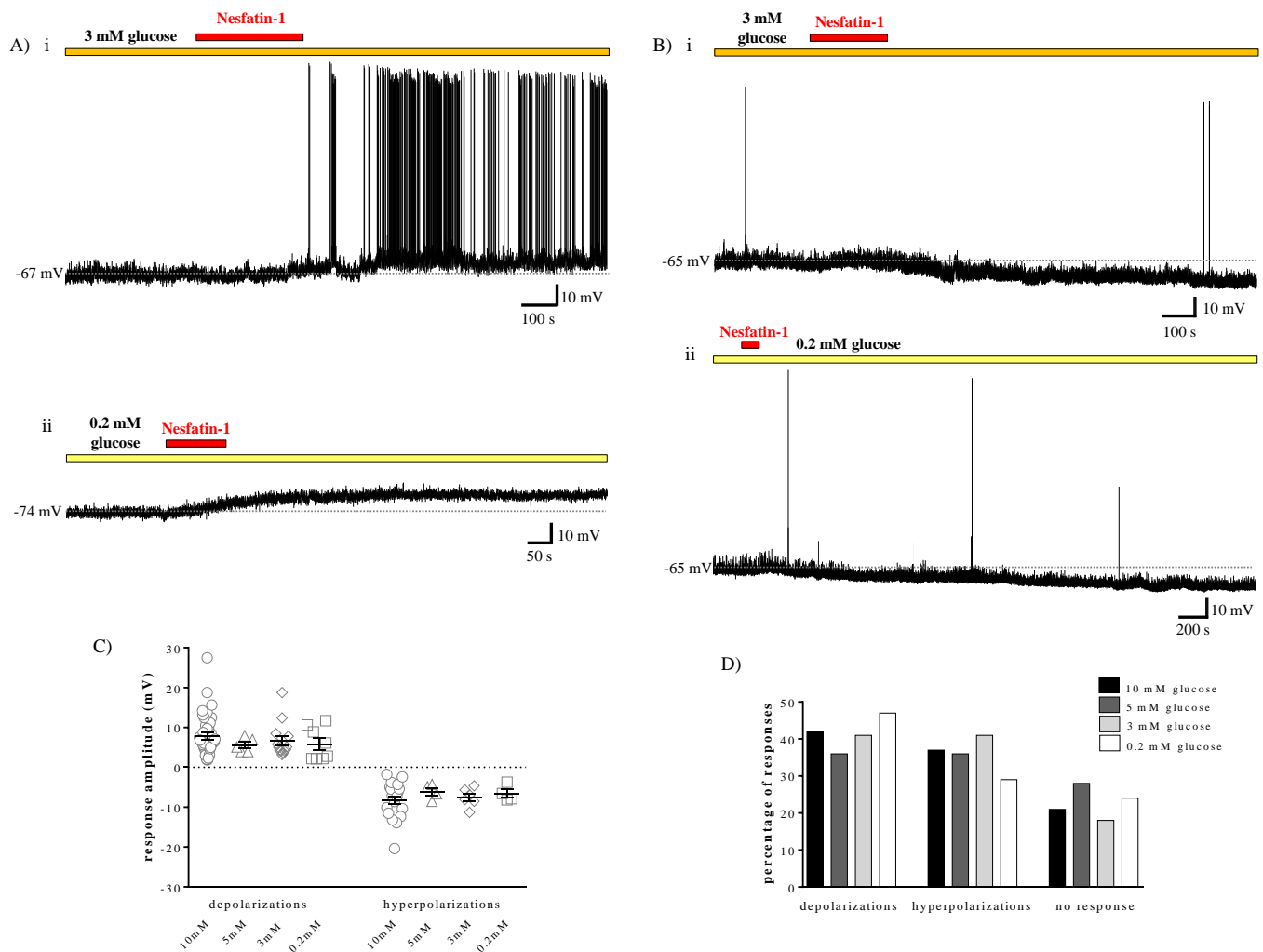


Figure 4-3 – The effects of nesfatin-1 on NTS neurons are consistent across glucose concentrations.

A) and B) Representative current-clamp recordings from four separate NTS neurons. In both A) and B), neurons in (i) are bathed in aCSF containing 3 mM glucose, while neurons in (ii) are bathed in aCSF with 0.2 mM glucose. Ai and ii) Bath applied nesfatin-1 (10 nM) caused a depolarizing effect of similar amplitude in both these cells. Bi and ii) Nesfatin-1 elicited a hyperpolarization of similar amplitude in these neurons. C) Scatter plot depicting the range of responses elicited by 10 nM nesfatin-1 at varying extracellular glucose concentrations. Mean depolarization 10 mM: 7.83 ± 0.84 mV ($n = 39$), 5 mM: 5.57 ± 0.8 mV ($n = 5$), 3 mM: 6.7 ± 1.23 mV ($n = 13$), 0.2 mM: 5.83 ± 1.44 mV ($n = 8$). Mean hyperpolarization 10 mM: -8.23 ± 1.0 mV ($n = 20$), 5 mM: -6.1 ± 0.95 mV ($n = 4$), 3 mM: -7.53 ± 0.96 mV ($n = 6$), 0.2 mM: -6.59 ± 1.01 mV ($n = 4$). D) Bar graph showing the percentage of NTS neurons which respond to nesfatin-1 with a depolarization, hyperpolarization or no response across all glucose concentrations used. There is no difference in the amplitude (ANOVA, $p > 0.5$) or distribution of nesfatin-1 responses across groups (χ^2 , $p > 0.5$). Data at 10 mM glucose obtained from Mimeo *et al.*, 2012.

ANOVA, $p = 0.58$ and 0.70 for depolarizations and hyperpolarizations, respectively, Figure 4-3C). Secondly, there was no change in the proportion of NTS neurons depolarized, hyperpolarized, or unaffected by nesfatin-1 across the range of glucose concentrations used (χ^2 , $p > 0.5$ for all possible pairs, Figure 4-3D). These findings therefore indicate the effects of nesfatin-1 on the membrane potential of NTS neurons are unchanged as extracellular glucose concentrations are altered.

GE NTS neurons are more responsive to α -MSH than NR cells, and are selectively depolarized by α -MSH

Since the anorexigenic peptide α -MSH and the MC4R have been shown to be involved in the autonomic processes regulating glucose homeostasis (Fan *et al.*, 2000; Obici *et al.*, 2001; Rossi *et al.*, 2011), and since we have previously demonstrated effects of α -MSH on the membrane potential of NTS cells (Mimee *et al.*, 2014), we conducted parallel experiments evaluating whether α -MSH exerts selective effects on the excitability of a particular subtype of glucose sensing NTS neuron. Our results are summarized in Figure 4-4. We found 75% of GE neurons were depolarized by α -MSH ($n = 6$, mean depolarization: 9.35 ± 4.15 mV, Figure 4-4A), while the remaining 25% of GE cells were unaffected by the peptide ($n = 2$). We thus did not observe hyperpolarizing effects of α -MSH on GE neurons. In addition, 63% of GI neurons depolarized ($n = 5$, mean depolarization: 9.47 ± 2.0 mV, Figure 4-4B), 17% hyperpolarized ($n = 2$, mean hyperpolarization: -8.59 ± 1.34 mV), and 12% did not respond ($n = 1$) to α -MSH. Finally, 33% of NR neurons depolarized ($n = 4$, mean depolarization: 4.51 ± 1.33), 17% hyperpolarized ($n = 2$, mean hyperpolarization: -6.90 ± 0.02), and 50% did not respond ($n = 6$) to α -MSH. While there was no difference in the amplitude of depolarizations (one-way ANOVA, $p = 0.52$) or hyperpolarizations (unpaired t -test, $p = 0.34$) between groups, our findings do indicate

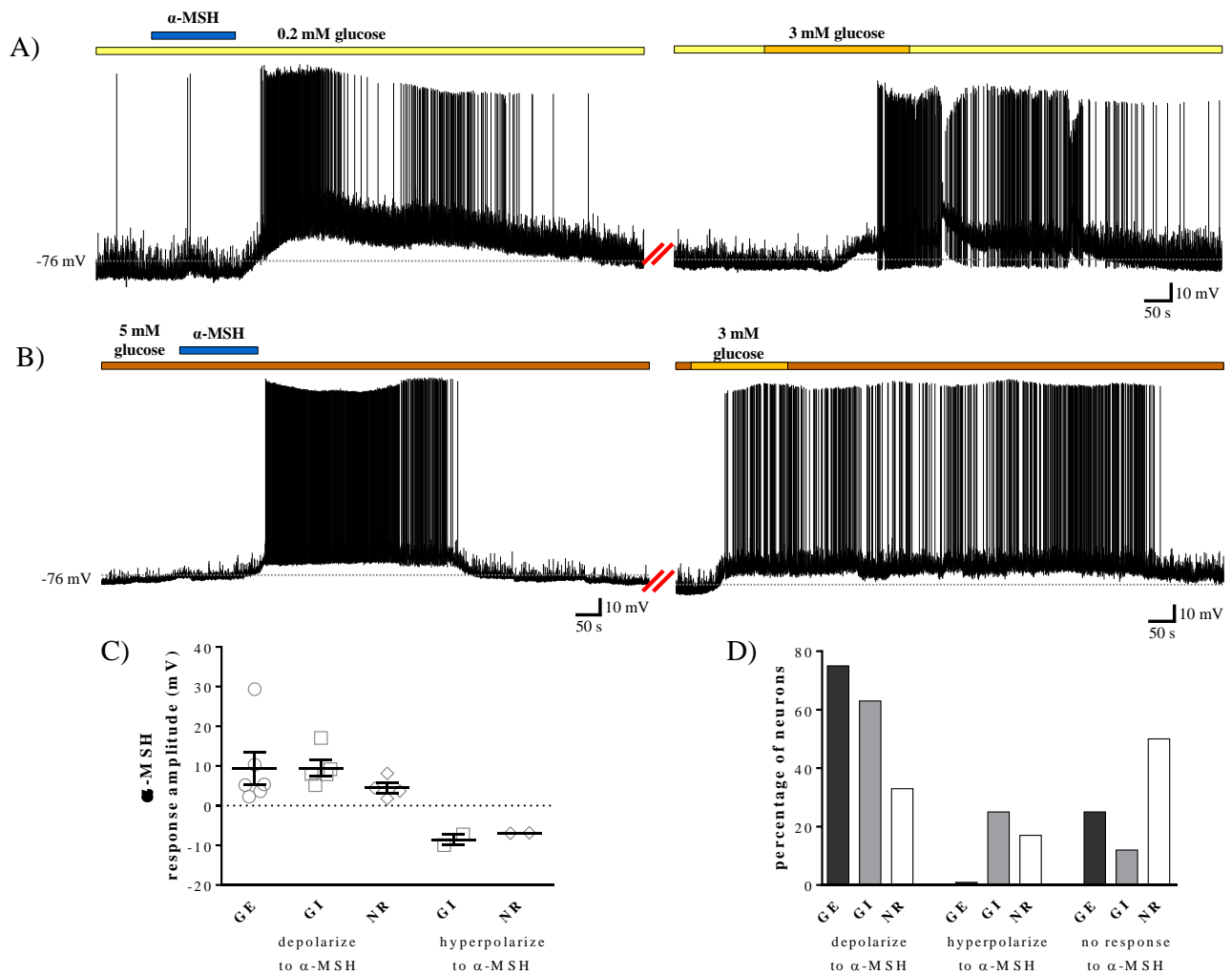


Figure 4-4 – GE NTS neurons are more responsive to α -MSH than NR cells, and are selectively depolarized by α -MSH. A) and B) Current-clamp recordings from two separate NTS neurons. A) α -MSH (500 nM, horizontal blue bar) elicited a reversible depolarization in this neuron subsequently identified as GE following an increase in glucose concentration from a baseline of 0.2 mM to 3 mM. We note the amplitudes of these effects are above average for the population sampled. B) α -MSH elicited a reversible depolarization in this cell subsequently identified as GI following a decrease in glucose concentration from a baseline of 5 mM to 3 mM. C) Scatter plot depicting the range of responses elicited by 500 nM α -MSH in GE, GI, and NR NTS neurons. Mean α -MSH induced depolarization GE: 9.35 ± 4.15 mV, GI: 9.47 ± 2.0 mV, NR: 4.51 ± 1.33 mV. Mean α -MSH induced hyperpolarization GI: -8.59 ± 1.34 mV, NR: -6.90 ± 0.02 mV. D) Bar graph showing the percentage of GE ($n = 8$), GI ($n = 8$), and NR ($n = 14$) NTS neurons which also responded to α -MSH. More GE neurons exhibit depolarizing responses to α -MSH than NR NTS neurons (χ^2 , $p = 0.04$). There was no difference in the amplitude of α -MSH induced effects across groups (ANOVA, $p = 0.52$ for depolarizations, unpaired t -test, $p = 0.34$ for hyperpolarizations).

GE NTS neurons show significantly more depolarizing responses to α -MSH than NR cells (χ^2 , $p = 0.04$). Furthermore, our results show glucose responsive cells collectively (*ie* GE and GI combined) are significantly more responsive to α -MSH than NR neurons (χ^2 , $p = 0.009$).

NTS neurons show increased responsiveness to α -MSH as extracellular glucose concentrations decrease

We next investigated whether the effects of α -MSH on the membrane potential of NTS neurons would be modified by changes in extracellular glucose concentrations. Again, we maintained rat brain slices containing the NTS at either 5, 3, or 0.2 mM glucose and subsequently bath perfused 500 nM α -MSH to evaluate the effects of this peptide on the excitability of NTS cells. Our findings are summarized in Figure 4-5. Previous studies from our laboratory using slices maintained at 10 mM glucose revealed effects of α -MSH on 61% of NTS neurons, with 39% of cells showing a depolarization ($n = 16$, mean 6.14 ± 0.54 mV), 22% of cells a hyperpolarization ($n = 9$, -6.79 ± 1.02 mV), and the remaining 39% of cells no response ($n = 16$) (Mimee *et al.*, 2014). After decreasing the extracellular glucose concentration to 5 mM, 64% of NTS neurons responded to α -MSH. More specifically, 53% of neurons showed a depolarization ($n = 10$, mean: 6.69 ± 1.43 mV), 11% a hyperpolarization ($n = 2$, -9.65 ± 0.28 mV), and 36% no response ($n = 7$) to α -MSH. All but one of the responses to α -MSH at 5 mM glucose were at least partially reversible upon washout. At 3 mM extracellular glucose, 71% of neurons responded to α -MSH, with 50% of cells showing a depolarization ($n = 12$, mean: 7.26 ± 0.84 mV, 9 at least partially reversible), 21% a reversible hyperpolarization ($n = 5$, -7.66 ± 1.83 mV), and 29% no response ($n = 7$) to α -MSH. Finally, at 0.2 mM extracellular glucose, 100% of neurons depolarized to α -MSH ($n = 8$, mean: 10.57 ± 3.15 mV, 5 at least partially reversible). The amplitudes of the depolarizations and hyperpolarizations to α -MSH across all four glucose

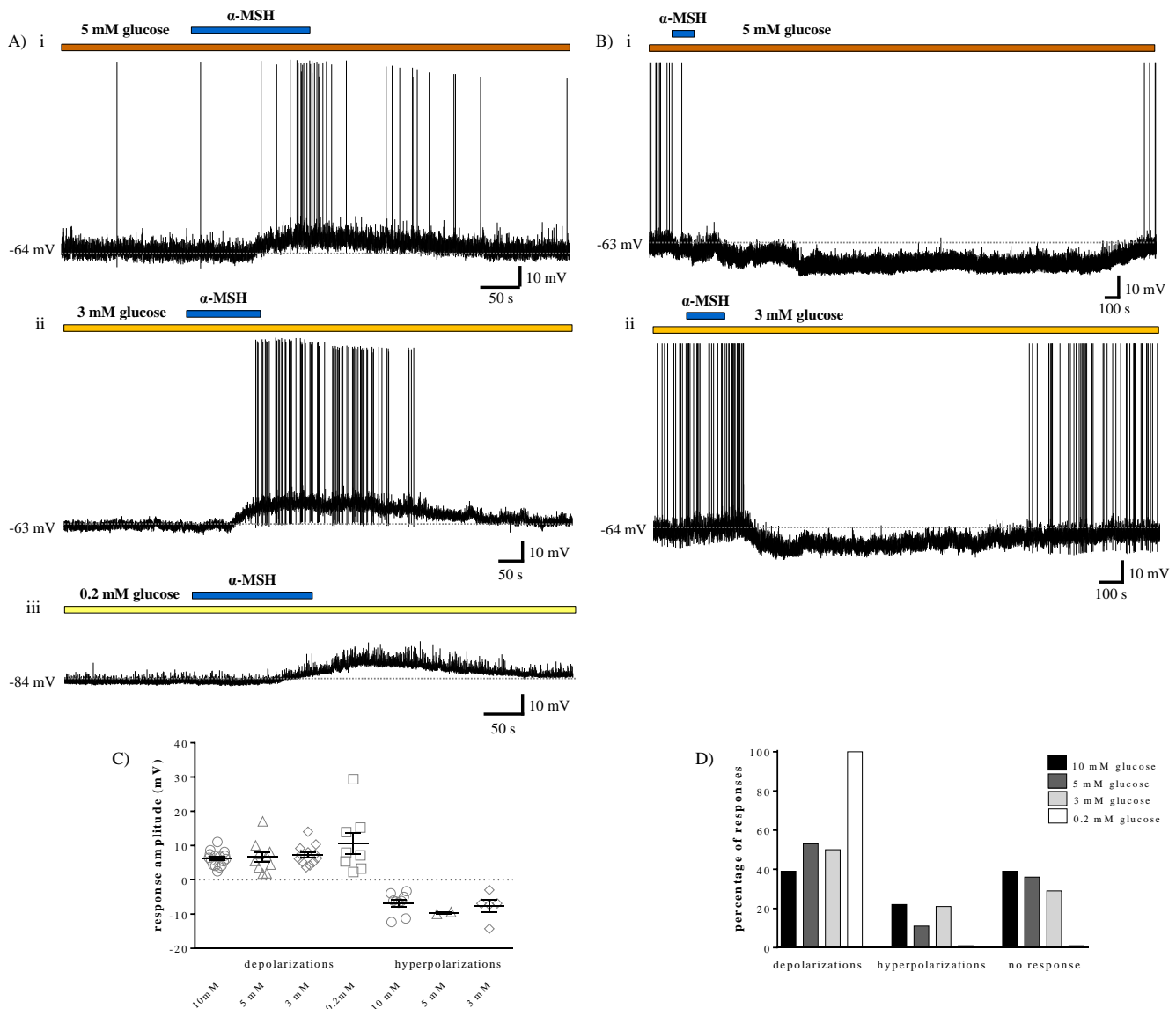


Figure 4-5 – NTS neurons show increased responsiveness to α -MSH as extracellular glucose concentrations decrease. A) and B) Representative current-clamp recordings from five separate NTS neurons. A) Bath applied α -MSH (500 nM, horizontal blue bar) induced reversible depolarizing effects on neurons bathed in aCSF containing 5 mM extracellular glucose (i), 3 mM glucose (ii) and 0.2 mM glucose (iii). B) α -MSH induced reversible hyperpolarizing effects in NTS cells at both 5 mM glucose (i) and 3 mM glucose (ii). C) Scatter plot depicting the range of responses elicited by 500 nM α -MSH at varying extracellular glucose concentrations. Mean depolarization 10 mM: 6.14 ± 0.54 mV ($n = 16$), 5 mM: 6.69 ± 1.43 mV ($n = 10$), 3 mM: 7.26 ± 0.84 mV ($n = 12$), 0.2 mM: 10.57 ± 3.15 mV ($n = 8$). Mean hyperpolarization 10 mM: -6.79 ± 1.02 mV ($n = 9$), 5 mM: -9.65 ± 0.28 mV ($n = 2$), 3 mM: -7.66 ± 1.83 mV ($n = 5$). D) Bar graph showing the percentage of NTS neurons which respond to α -MSH with a depolarization, hyperpolarization or no response across all glucose concentrations used. Neurons at 0.2 mM glucose are significantly more responsive to α -MSH than cells at 3, 5 and 10 mM glucose. There is no difference in the amplitude of α -MSH responses across groups (ANOVA, $p > 0.15$). Data at 10 mM glucose obtained from Mimee *et al.*, 2014.

concentrations were not different from one another (one-way ANOVA, $p = 0.18$ and 0.55 for depolarizations and hyperpolarizations, respectively). The distribution of responses to α -MSH was, however, significantly different between 0.2 and 10 mM, 0.2 and 5 mM, and 0.2 and 3 mM extracellular glucose (χ^2 , $p = 0.0019$, 0.03 , and 0.02 , respectively). These findings thus suggest an increased responsiveness of NTS neurons to α -MSH with decreasing extracellular glucose concentrations, specifically with reference to depolarizing effects of this peptide.

The resting membrane potential of NTS neurons is more hyperpolarized as extracellular glucose concentrations decrease

In performing the series of experiments at 5, 3 and 0.2 mM, we noted the baseline membrane potential of NTS neurons was more hyperpolarized as extracellular glucose concentrations were decreased. The mean baseline membrane potential of neurons without holding current at 10 mM was -64.21 ± 0.86 mV ($n = 82$, from (Mimee *et al.*, 2012) and (Mimee *et al.*, 2014)), at 5 mM was -69.08 ± 0.94 mV ($n = 21$), at 3 mM was -69.97 ± 0.84 mV ($n = 40$), and at 0.2 mM was -74.66 ± 1.66 mV ($n = 21$). Indeed, the baseline membrane potential of neurons at 0.2 mM extracellular glucose was significantly more hyperpolarized than that at both 5 mM and 10 mM glucose, as was the baseline membrane potential of cells at 3 and 5 mM glucose versus 10 mM (one-way ANOVA with Tukey's multiple comparisons test, $p < 0.0001$). These observations suggest that altering extracellular glucose concentrations has functionally relevant effects on the baseline excitability of NTS neurons.

Discussion

The present study provides conclusive evidence of the integrative capacity of single NTS neurons. Furthermore, we have shown the responses of these neurons to α -MSH are dynamically altered in accordance with the energy status of the region and, by extension, the feeding status of

the organism. This is, to the best of our knowledge, the first documentation of changes in the responsiveness of individual NTS neurons to peptide signals as a consequence of altered extracellular glucose concentrations.

We firstly sought to establish whether NTS neurons can respond to physiological changes in extracellular glucose concentration *in vitro*. Studies simultaneously measuring circulating blood glucose levels in relation to central extracellular glucose levels in rats have found the latter range from 0.16 ± 0.03 in hypoglycemia to 4.5 ± 0.4 in hyperglycemia (Silver & Erecinska, 1994). Our chosen concentrations of 0.2, 3 and 5 mM extracellular glucose therefore provide a closer mimic of the range of concentrations that may be encountered by NTS neurons *in vivo* than previous whole cell patch clamp studies in the region, where large decreases from 10 to 3 or 0 mM, or large increases from elevated baselines of 10 mM to 20 or 30 mM glucose have been used (Balfour *et al.*, 2006; Wan & Browning, 2008a). These previous studies, as well as others using extracellular recording techniques, have found between 20-81% of NTS neurons respond to changes in extracellular glucose concentrations, with contradicting reports of the predominance of GE versus GI phenotypes (Mizuno & Oomura, 1984; Yettefti *et al.*, 1997; Dallaporta *et al.*, 1999; Dallaporta *et al.*, 2000; Balfour *et al.*, 2006; Wan & Browning, 2008a; Wan & Browning, 2008b). Our observation that 57% of NTS neurons are glucose responsive falls in the middle of the previously documented range of responses, and is similar to those of the most physiological of previous studies, where 51-56% of NTS neurons responded to 2 mM changes in glucose concentrations. Indeed, as we have shown, these studies also found more GE versus GI neurons (Dallaporta *et al.*, 1999; Dallaporta *et al.*, 2000). Interestingly, we have documented a greater responsiveness of NTS neurons to increases in extracellular glucose concentration versus decreases. Further studies will be required to elucidate the mechanism that

may underlie these differences and their physiological relevance. It is worth noting, however, that while the responses of NTS cells to increases in glucose concentrations appear to be mediated via direct effects on the cell (*ie* they are preserved in conditions of neuronal isolation in tetrodotoxin), the responses of NTS neurons to decreases in glucose levels appear to be mediated via indirect actions at presynaptic target sites (Wan & Browning, 2008a). Whether these observations may account for our present findings remains to be examined.

We also noted a gradual hyperpolarization of the membrane potential of NTS cells with decreasing glucose concentrations. This shift away from the action potential threshold of neurons likely reflects a compensatory mechanism of these cells to preserve energy with waning sources of extracellular fuel, as the generation and processing of action potentials is very energetically costly (Attwell & Laughlin, 2001). Furthermore, as the frequency of excitatory postsynaptic potentials (EPSCs) is increased as extracellular glucose concentration rises (Wan & Browning, 2008a), it can be assumed that the opposite would be true as glucose levels decrease. This expected decline in excitatory inputs to NTS neurons at low extracellular glucose concentrations may ultimately contribute to the hyperpolarizing trend of the membrane potential we observed. In future studies, it will be interesting to note whether there is a correlation between extracellular glucose levels and inhibitory postsynaptic potentials in the NTS as well.

Unexpectedly, we found no cellular evidence to indicate nesfatin-1 preferentially affects glucose sensing neurons over glucose unresponsive cells in the NTS. Our findings contrast those of a recent study by Dong et al. (2014), who noted predominantly excitatory effects of nesfatin-1 on GE neurons, and inhibitory effects of the peptide on GI cells. These authors, however, recorded from both the NTS and neighboring DMV, and it is therefore possible that their findings are more reflective of actions of nesfatin-1 in the DMV. Furthermore, glucose sensing

neurons were characterized based on a step from 25 to 5 mM extracellular glucose, versus the more physiological changes in glucose concentration used herein. While hypoglycemia has been shown to activate nesfatin-1 expressing neurons in the NTS, this same *in vivo* manipulation also induced activation of several hypothalamic areas with projections to the NTS, thereby making it difficult to determine whether the hypoglycemia-induced medullary activation is direct or a downstream effect of excitation of hypothalamic sites. Moreover, nesfatin-1 expressing neurons undoubtedly express a variety of other neuropeptides (Brailoiu *et al.*, 2007) which may indeed be the relevant mediators of glucose regulation at the level of the NTS, rather than nesfatin-1 itself. Thus, based on these considerations and our current findings, we reason that nesfatin-1 may not in fact be involved in the coordination of physiological responses to alterations in central glucose levels via actions in the NTS. Furthermore, since we noted the effects of nesfatin-1 are entirely consistent across the range of glucose concentrations we employed, representing hunger to satiety in the animal, we conclude that nesfatin-1 may not act as a functionally relevant regulator of energy status in the NTS. While evidence does exist for a role of nesfatin-1 in modulating ingestive behaviors via actions in the dorsal vagal complex (Dong *et al.*, 2014), these effects may be due to actions of nesfatin-1 in the DMV rather than in the NTS. Alternatively, nesfatin-1 may act in the NTS to affect food intake not through its own intrinsic, direct actions on neurons in this region, but rather by modulating the effects of other feeding related neuropeptides produced either locally or released from descending hypothalamic inputs (Maejima *et al.*, 2009). Indeed, it has been shown that nesfatin-1 upregulates POMC mRNA expression in the NTS, which may lead to altered α -MSH expression and subsequent effects on glycemia or food intake (Wernecke *et al.*, 2014). Thus, while it is evident future studies will be required to more accurately assess the precise role of the NTS in mediating the anorexigenic effects of nesfatin-1, our findings

suggest this peptide may act predominantly as a local autocrine/paracrine modulator of neuronal function in the NTS rather than a metabolically relevant signaling molecule.

Our studies have revealed preferential actions of α -MSH on glucose responsive NTS neurons. Moreover, we did not observe any hyperpolarizing effects of α -MSH on GE neurons in the region. In light of our previous observations of excitatory actions of α -MSH on GABAergic NTS cells (Mimee *et al.*, 2014), it is interesting to note others have hypothesized GE NTS neurons are also GABAergic and their activation ultimately leads to decreases in gastric motility and tone via modulation of cholinergic parasympathetic signaling (Wan & Browning, 2008a). Furthermore, activation of at least a subset of GI NTS neurons results in glucagon secretion (Lamy *et al.*, 2014). As we noted both depolarizing and hyperpolarizing effects of α -MSH on GI neurons in the NTS, by extension we can speculate that cellular actions of α -MSH in this region may modulate circulating glucagon levels to contribute to the maintenance of normoglycemia in the animal.

Finally, we have shown a gradual increase in the responsiveness of NTS neurons to α -MSH with decreasing concentrations of extracellular glucose. This rapid shift in responsiveness on the order of hours complements the observations that pro-opiomelanocortin neurons in the NTS play important roles in acute, but not chronic, control of feeding (Zhan *et al.*, 2013). While we did not elucidate the mechanism underlying the shift in responsiveness to α -MSH we observed, it should be noted that fasting leads to both increased levels of α -MSH in the NTS (Perello *et al.*, 2007), and to increased availability of MC4R binding sites in several hypothalamic nuclei (Harrold *et al.*, 1999), although similar studies have not yet been conducted in the NTS. Taken together, it is tempting to speculate that these potential changes in both α -MSH expression and MC4R activity may explain a shift towards more depolarizing actions of

this peptide in hypoglycemic conditions. Furthermore, as our previous studies demonstrated the necessity for presynaptic, GABAergic signaling in mediating the hyperpolarizing actions of α -MSH (Mimee *et al.*, 2014), the elimination of these inhibitory effects in hypoglycemia may be a consequence of the hyperpolarized membrane potential of NTS neurons maintained in low glucose. At these resting membrane potentials, the passage of Cl^- through ionotropic GABA_A receptors may serve to depolarize neurons, thereby abolishing the hyperpolarizing effects of α -MSH.

In conclusion, our findings demonstrate the presence of physiologically relevant glucose sensing neurons in the NTS, and provide cellular confirmation that the actions of α -MSH in this medullary region make important contributions to the regulation of energy homeostasis in the organism. Furthermore, the progressive shift towards more depolarizing responses to α -MSH, and a complete lack of hyperpolarizing responses, with decreasing extracellular glucose concentrations provides indisputable evidence of the ability of alterations in local glucose levels to profoundly modify the responsiveness of NTS neurons to, at the very least, metabolically relevant signals. In light of the fact that many electrophysiological studies in the region are conducted at elevated levels of glucose (5 and 10 mM – see (Branchereau *et al.*, 1993;Appleyard *et al.*, 2005;Wan *et al.*, 2008;Peters *et al.*, 2008;Hisadome *et al.*, 2010;Mimee *et al.*, 2014) for example), these findings are of particular relevance and highlight a need to potentially adopt the usage of more physiological recording solutions to obtain the most relevant, accurate and translational *in vitro* results. Overall, our observations have important implications for future electrophysiological studies on the effects of feeding related peptides not only in the NTS, but in other central regions regulating the control of ingestive behaviors.

Acknowledgments

This work was supported by funding from the Natural Sciences and Engineering Research Council of Canada, Le Fonds québécois de la recherche sur la nature et les technologies, and the Heart and Stroke Foundation of Ontario.

CHAPTER 5 - General Discussion

Taken together, the findings derived from this thesis have provided further evidence to support the role of the NTS as a critical integrator of metabolically relevant signals. While we have limited our studies to the examination of effects of nesfatin-1, α -MSH, and glucose on the excitability of NTS neurons, it is important to highlight that this medullary region expresses a veritable plethora of neuropeptides and receptors implicated in the control of energy homeostasis and autonomic function (Jean, 1991; Lawrence & Jarrott, 1996; Grill & Hayes, 2012). Thus, much work evidently remains to be done to enable the construction of a complete model of neurotransmission in an individual NTS neuron.

We have demonstrated effects of nesfatin-1, α -MSH and glucose on the majority (63%, 61%, and 57%, respectively) of NTS cells, thus implying single neurons in this region can be influenced by all three of these molecules. In support of this notion, our RT-PCR studies demonstrated the expression of the MC4R on nesfatin-1 sensing neurons. Furthermore, we revealed heterogeneous effects nesfatin-1 on GE, GI, and NR NTS neurons, but preferential actions of α -MSH on glucose responsive cells in the region, thus suggesting overlap between glucose sensing and the signaling of both nesfatin-1 and α -MSH in individual NTS neurons. Moreover, these observations lend additional support to the importance of melanocortin signaling in the NTS in the control of energy homeostasis, but suggest nesfatin-1 may act as a local neuromodulator, rather than a metabolically relevant peptide at the level of the NTS. Indeed, our *in vivo* microinjection studies have established a definitive role for nesfatin-1 in the control of cardiovascular function via effects in the NTS. Beyond the actions of factors involved in energy homeostasis, we have also uncovered important effects of GABAergic neurotransmission in the NTS as a modulator of peptidergic signaling, at least in the case of α -MSH. Thus, in brief, it is evident individual NTS neurons are constantly processing multiple

sources of locally and distantly derived neural signaling factors in order to ultimately regulate numerous critical autonomic and ingestive behaviors.

Unique properties of nesfatin-1 signaling (modified from (Mimee & Ferguson, 2013))

We have demonstrated direct depolarizing and hyperpolarizing effects of nesfatin-1 on mNTS, but not cNTS neurons, reflecting selective actions of this peptide in the NTS region in which NUCB2 is expressed. Furthermore, we have documented exclusively depolarizing effects of nesfatin-1 on both NUCB2 and NPY expressing NTS neurons. Taken together, the findings that nesfatin-1 exerts cellular effects exclusively in the NTS subregion in which it is synthesized, coupled with the suggestion of self-stimulatory actions in the mNTS, lend support to the hypothesis that nesfatin-1 may act in a local autocrine and/or paracrine fashion. It is necessary to highlight, however, that our study, and virtually all other studies on nesfatin-1, have indeed used exogenous administration of nesfatin-1 to draw conclusions on the endogenous central actions of this peptide. Of critical importance is the fact that the nesfatin-1 receptor remains unknown, and the actual neuronal release sites and mechanism of action of nesfatin-1 are also unclear. Nesfatin-1 has indeed been detected in cerebral spinal fluid and is thus appropriately located to exert endogenous central effects (Oh-I *et al.*, 2006; Tan *et al.*, 2011). Furthermore, multiple groups have identified the presence of NUCB2/nesfatin-1 in key autonomic nuclei (Oh-I *et al.*, 2006; Brailoiu *et al.*, 2007; Foo *et al.*, 2008). With the exception of the original study by Oh-I *et al.*, however, the commercial antibody used in immunohistochemical experiments is not specific to the 82 amino acid nesfatin-1 fragment, but rather detects the full length NUCB2 prohormone. This technical consideration raises the possibility that NUCB2, rather than the nesfatin-1 fragment, is the biologically active portion of the peptide, and, furthermore, adds uncertainty as to whether NUCB2 is actually cleaved into nesfatin-1 and released by neurons (Goebel *et al.*,

2009a). Additionally, nesfatin-1 has only been localized in neuronal cell bodies and dendrites, and is apparently absent from axons/terminals (Foo *et al.*, 2008). In fact, icv treatment with colchicine, an experimental manipulation which causes accumulation of axonal products in the soma, actually results in a decrease in the intensity of nesfatin-1 staining in the cell body, providing additional evidence that nesfatin-1 is not present in axons or terminals (Foo *et al.*, 2008). Since nesfatin-1 has been detected in secretory granules (Maejima *et al.*, 2009), an attractive current hypothesis is that nesfatin-1 may be released from dendrites and/or the cell body of neurons to exert local paracrine effects. There is, however, currently no evidence to support or disprove this theory. Alternatively, since nesfatin-1 can cross the blood brain barrier (Price *et al.*, 2007;Pan *et al.*, 2007), and numerous reports have documented peripheral expression of NUCB2/nesfatin-1 in the pancreas (Gonzalez *et al.*, 2009;Foo *et al.*, 2010;Zhang *et al.*, 2010), in adipose tissue (Ramanjaneya *et al.*, 2010;Osaki *et al.*, 2012), and in the gastric mucosa (Stengel *et al.*, 2009b), it is possible that centrally acting nesfatin-1 may be derived from a peripheral source. In any case, the lack of definitive conclusions as to the source of centrally acting nesfatin-1 does not diminish the importance of the potent effects of this peptide in the brain, but rather adds to the unique and novel properties of this neuropeptide. Experiments showing endogenous release of nesfatin-1 from specific neuronal cell groups, as well as a clear demonstration of cellular actions following such release, will provide essential information regarding the mechanism of action and precise neuronal circuitries mediating the effects of nesfatin-1. Furthermore, identification of the nesfatin-1 receptor will be absolutely essential to both understanding exactly which neuronal cell types are directly activated by this peptide, and to designing specific antagonists which will greatly aid in the elucidation of the detailed cellular mechanisms of action of nesfatin-1.

The importance of recording conditions in whole cell patch clamp electrophysiology

Our studies assessing the effects of alterations in extracellular glucose concentrations during electrophysiological recordings have revealed several critical changes in NTS cellular excitability as a consequence of modified glucose levels. Firstly, we observed a significant hyperpolarization of the resting membrane potential of NTS neurons with decreasing extracellular glucose concentrations. While we did not delineate the cellular mechanism underlying this shift toward a more hyperpolarized membrane potential, we hypothesize a decrease in excitatory, vagal glutamatergic inputs to these NTS neurons may underlie the changes we observed (Wan & Browning, 2008a). Furthermore, we demonstrated a profound shift in the responsiveness of NTS neurons to the anorexigenic peptide α -MSH with decreasing concentrations of extracellular glucose. More specifically, as glucose levels were lowered, a greater proportion of NTS neurons showed a change in membrane potential in response to α -MSH. Most profoundly, all cells recorded from in hypoglycemic conditions showed depolarizing responses to α -MSH, in stark contrast to the heterogeneous depolarizations, hyperpolarizations, and lack of responses to the peptide in normo- and hyperglycemic conditions. It is also interesting to note these changes in the cellular response of NTS neurons to α -MSH occurred very quickly, over the course of hours, suggesting a rapid capacity for plasticity of melanocortin circuits in the NTS in accordance with energy status. Taken together, our findings have critically important implications for cellular studies in the NTS, and potentially other regions of the CNS, when one considers virtually all electrophysiological recordings in this region, and in fact throughout the brain, are performed at supra-physiologically elevated levels of extracellular glucose. While normoglycemic levels for the CNS are roughly 2.5 mM, central hypoglycemic levels are below 1 mM and hyperglycemic levels are 4.5 mM (Silver & Erecinska, 1994).

Despite the knowledge of these physiological concentrations of glucose in the brain, essentially all electrophysiological studies on brain slices are performed at concentrations of 10 mM extracellular glucose. Our findings, however, show that such elevated levels of glucose are not necessary to maintain neuronal integrity, as cells bathed at 0.2 mM glucose are fully capable of firing action potentials of high amplitude, of maintaining a stable baseline membrane potential, of being held for long duration electrophysiological recordings, and of surviving for over 6 hours *in vitro*. There is thus no valid reason to continue using supra-physiological concentrations of glucose for whole cell patch clamp recordings from cells in slice preparation, at least in the NTS. In fact, elevating extracellular glucose concentrations in the aCSF bathing NTS slices has been shown to increase the frequency of EPSCs of vagally innervated NTS neurons (Wan & Browning, 2008a). Thus if electrophysiological recordings in the region are continuously performed at supra-physiological levels of glucose, this would imply studies may uniformly overestimate and overinflate the magnitude of glutamatergic signaling in the NTS. Such errors may have significant implications for our understanding of neurotransmission in this medullary center, especially when one considers the established critical importance of glutamatergic signaling as a principal mediator of vagally transmitted information to the NTS from the cardiovascular and gastrointestinal systems, as discussed in the general introduction of this thesis. To the best of our knowledge, the effects of variations in extracellular glucose concentrations on the frequency or amplitude of spontaneous or miniature IPSCs in the NTS have not been evaluated, and present the basis for intriguing future studies. Indeed, as we found increases in GABAergic signaling are required for the indirect hyperpolarizing effects of α -MSH on NTS neurons at 10 mM glucose, and contribute to a net of lack effect of α -MSH on a separate subset of these cells as well, it would be interesting to evaluate whether the uniform depolarizing

actions of α -MSH in hypoglycemic conditions may be at least partially caused by diminished GABAergic neurotransmission in the NTS in low glucose states.

While gigaohm seal whole cell recordings from brain slice preparations began only in the late 1980s, and are thus relatively recent additions to the repertoire of electrophysiological techniques (Blanton *et al.*, 1989; Edwards *et al.*, 1989), brain slices have been used in experiments since the 1930s (Ashford & Dixon, 1935). Remarkably, and seemingly arbitrarily, glucose concentrations in the aCSF bathing slices *in vitro* have been consistently set at a minimum of 10 mM, and sometimes as high as 25 mM, from the time of these initial studies onward (as observed, for example, in studies on cortex (Hillman & McIlwain, 1961; Lipton, 1973), hippocampus (Skrede & Westgaard, 1971; Sakmann *et al.*, 1989), and cerebellum (Llinas & Sugimori, 1980)). A particular review in 1980 by Dingleline *et al.*, again stating 10 mM glucose should be used in standard bathing solution, even acknowledged the composition of the aCSF used in slice experiments may be inaccurate and cautioned that scientists should “keep in mind the use of a non-physiological perfusion fluid may lead to insidious problems, especially when more subtle aspects of synaptic function are being examined” (Dingleline *et al.*, 1980). These cautions should have been heeded when Silver and Erecinska used *in vivo* methods to determine physiological levels of glucose in the CNS in hypo-, normo-, and hyperglycemic states (Silver & Erecinska, 1994). For reference, central hyperglycemia of 4.5 mM glucose described in their study corresponded to a blood glucose level of 15 mM. While perhaps too simple a calculation, if a doubling of central glucose levels to approximately 10 mM corresponds with a parallel doubling of blood glucose levels, this would equate to a circulating concentration of 30 mM glucose. *In vivo*, such high blood levels of glucose can lead to severe diabetic ketoacidosis and hyperosmolar hyperglycemic state, corresponding with a state of stupor or coma in the

individual, and potential brain injury as well (Gouveia & Chowdhury, 2013). These are evidently not physiological conditions for the organism. It is therefore quite alarming that electrophysiological studies across the brain continue to use the vastly elevated concentration of 10 mM glucose. While this excessive level of glucose may potentially lead to false baseline measures of cellular excitability across all electrophysiological studies, one would think special attention would be paid to using correct levels of glucose, the main energy source of neurons, in studies in the field of the central control of energy homeostasis, especially when considering the existence of GE and GI neurons has been known since 1964 (Anand *et al.*, 1964).

As we observed alterations in the responsiveness of NTS neurons to α -MSH, but not nesfatin-1, with changing concentrations of glucose in the aCSF, it is important to highlight that seminal studies evaluating the signaling of melanocortins in the ARC and PVN were conducted at 10 mM glucose or higher (Cowley *et al.*, 1999; Cowley *et al.*, 2001), as were subsequent high impact electrophysiological studies evaluating effects of leptin (Spanswick *et al.*, 1997; Pinto *et al.*, 2004), serotonin (Heisler *et al.*, 2006), and NPY (Roseberry *et al.*, 2004) on ARC neurons. While plasticity in melanocortin signaling in accordance with extracellular glucose levels may indeed be restricted to the brainstem, the profound changes in the cellular effects of α -MSH we observed do lead to the question of whether similar observations may also apply to hypothalamic studies. The potential for such plasticity in the hypothalamus is substantiated by ample evidence of changes in the expression of receptor and peptide components of the melanocortin circuitry, as well as modifications in the excitability, and number of dendritic spines, of neurons comprising the hypothalamic melanocortin networks in accordance with fasting and refeeding (as reviewed in (Zeltser *et al.*, 2012)). Electrophysiological studies evaluating potential alterations in melanocortin signaling in the ARC and PVN as glucose levels are modified are thus well

warranted. If such alterations are indeed observed, this could have profoundly important implications for the field and potentially challenge the current dogmatic view of the ARC and PVN melanocortin circuitries.

Advantages and limitations of the NTS brain slice as an experimental model

The NTS slice preparation we have employed in the studies completed for this thesis has offered several experimental advantages. Firstly, in contrast to dissociated cultured neurons, brain slices preserve local neuronal connectivity, thus allowing for an electrophysiological evaluation of local synaptic activity. Indeed, the maintenance of local GABAergic circuits was essential in delineating the effects of α -MSH on spontaneous and miniature IPSCs in the NTS in the studies presented in Chapter 3. Other groups have made extensive usage of a horizontal NTS slice preparation which preserves a portion of the solitary tract in the slice, permitting a direct examination of glutamatergic vagal transmission to NTS neurons (see for example (Andresen & Yang, 1990)). In addition, studies coupling this horizontal slice preparation with retro- or anterograde labeling techniques provide a means to assess the electrophysiological properties of NTS neurons receiving inputs from, or sending projections to, specific brain regions or organs, thus allowing for a greater appreciation of the physiological relevance of these cells. If such labeling techniques are combined with *post-hoc* RT-PCR methods as well, the genetic identity, inputs, and projections of individual neurons can be correlated with their electrophysiological properties and their modulation by relevant neuropeptides and signaling molecules. This arsenal of combinatory techniques allows for a powerful evaluation of multiple aspects of the function of an individual neuron. Furthermore, simple pharmacological tools, such as TTX, are also available to artificially isolate cells in slices from neuronal inputs, a process necessary when determining whether effects of peptides on membrane potential are due to direct versus indirect

actions. This inducible cellular isolation was employed to establish the indirect, GABA mediated hyperpolarizing effects of α -MSH in Chapter 3. The slice preparation therefore enables a thorough characterization of the physiology of individual neurons, all while maintaining their local connectivity.

Brain slices do, however, present certain experimental limitations. Chiefly, as they are an *in vitro* preparation, they do not allow for a direct correlation of cellular effects with behavioral outcomes in the animal. For example, while we may observe depolarizing or hyperpolarizing effects of a peptide on a particular genetically defined cell type, or on neurons projecting to a specific brain region or organ, we cannot actually assess the true physiological impact of these selective effects on membrane potential, as such studies evidently require an intact organism. Furthermore, while brain slices do indeed maintain local neural circuits, they do not preserve more distant neuronal connections which span areas outside of the slice. Indeed, while it is well known the hypothalamus and the NTS reciprocally communicate with one another, an NTS slice evidently abolishes the projections between the medulla and the hypothalamus. Studies evaluating synaptic activity in brain slices are therefore limited to the local circuits that are preserved, and do not offer a direct method of evaluating the impact of stimulation of one brain area on activity in its distant projection sites. This is a significant shortcoming considering the integrated regulation of behaviors is mediated via coordinated activity at multiple brain sites. Furthermore, as we have discussed, artificial recording conditions in electrophysiological studies on slices may yield findings that may be quite discordant with the processes that actually occur *in vivo*. These, however, are inevitable problems encountered with any *in vitro* preparation, and efforts to make use of more physiological recording solutions may help minimize such issues. Ultimately, it is critical to recognize that no experimental preparation is flawless. Despite its

limitations, the brain slice does offer an excellent *in vitro* set-up to evaluate electrophysiological effects of signaling molecules at the single cell and local network level, while enabling a useful, albeit limited, examination of the potential physiological impacts of such cellular actions using a combination of complimentary techniques.

The challenges and shortcomings of current studies in the field of the central control of energy homeostasis

The CNS has long been recognized as a critical regulator of virtually all aspects of ingestive behavior, including the processing of tastes, the initiation and termination of meals, the assigning of rewarding versus aversive associations with particular foods, and the long term regulation of energy balance. For decades, research in the field of food intake has been largely centered on the hypothalamus, perhaps because the nuclei which comprise this neuronal area were identified as critical mediators of feeding behaviors so early in the chronology of the field. Seminal lesion studies in the early 1950s, for example, identified the ventromedial hypothalamus as the “satiety” center and lateral hypothalamic area as the “hunger” center (Anand & Brobeck, 1951), thus effectively targeting attention to these two regions, and to the hypothalamus in general. Indeed, reviews of the central control of food intake are often focused on discussions of the contributions of specific hypothalamic nuclei and cell types (see for example (Schwartz *et al.*, 2000; Woods & D'Alessio, 2008)). This hypothalamus-centered view is also evident when one considers how well delineated the cellular circuitries of the ARC and PVN, and their specific involvement in the control of ingestive behavior, are in comparison to those of the NTS, as was discussed in the introductory sections on nesfatin-1 and α -MSH. It goes without saying, however, that it is essential to recognize the critical contribution of extra-hypothalamic regions in the regulation of energy homeostasis, including, of course, the NTS, but also structures

mediating hedonic aspects of feeding, such as the ventral tegmental area. Increasing attention is being paid to these sites (see for example (Grill & Hayes, 2012) and (Berthoud, 2011;Meye & Adan, 2014)), reflecting the recognition that a comprehensive and global mapping of the neuronal circuits implicated in the many aspects of energy homeostasis is crucial to genuinely understanding how the brain controls this process. Ultimately, however, the reality is that the field, and the scientific method in general, remains focused on addressing a single question at a time, typically in a single brain region at a time. Thus, knowledge continues to be built in an incremental fashion, which is critical to gradually teasing apart the incredible complexities of the brain. This method, however, can fall short in terms of reassembling individual pieces of knowledge into a coherent and accurate working model, potentially leading to an oversimplified and overly fragmented view of neuronal systems. Indeed, in the example of the central melanocortin system, considerable effort has been made to assign specific, divergent roles to melanocortin signaling in the hypothalamus versus elsewhere in the brain. For instance, Balthasar and colleagues have shown selective re-expression of the MC4R in the PVN and/or amygdala of MC4R null mice completely reverses the severe hyperphagia observed in null mutants, but does not have any restorative effect on the decreased energy expenditure of these knockout animals (Balthasar *et al.*, 2005). These findings thus suggest signaling in the PVN and/or amygdala is entirely responsible for the anorexigenic effects of melanocortins, while having no role in energy expenditure, a potentially unexpected conclusion given the projections of MC4R expressing PVN neurons to BAT, a key adipose tissue implicated in energy expenditure (Voss-Andreae *et al.*, 2007). Despite the attractiveness of this proposed segregated, divergent system for the effects of melanocortins on energy homeostasis, studies conducted prior to those of Balthasar *et al.* demonstrated anorexigenic effects of MTII following 4V and DVC

injections (Grill *et al.*, 1998; Williams *et al.*, 2000), thus implying hindbrain MC4Rs also contribute to the hypophagia elicited by activation of these receptors. Indeed, microinjections of MTII into both the PVN and the NTS elicit increases in core temperature, a measure of energy expenditure, and decreases in food intake, highlighting the role of both hypothalamic and hindbrain sites in the effects of melanocortins on energy homeostasis (Skibicka & Grill, 2009). Thus while efforts to classify strict all-or-none divergent effects of melanocortins according to brain region may offer a useful, organized view of the signaling of this neuropeptide system, they are likely inaccurate and overly simplistic. Rather, the physiological outcomes of neuropeptide signaling at the cellular level more likely reflect graded, coordinated, and potentially redundant actions at distributed anatomical sites throughout the CNS, adding to the ultimate challenge of developing a comprehensive model of their underlying mechanism of action.

A second critical consideration for studies pertaining to the central control of food intake is the need to recognize that no peptide system acts in isolation on an individual neuron. Rather, neurons simultaneously receive and integrate multiple sources of converging inputs, a fact that is being increasingly acknowledged in local system, but not always cellular, level studies in the field. Furthermore, ample evidence has been obtained to indicate that anorexigenic peptides act in synergy with, and in fact require, intact signaling of other similar peptides in order to exert their effects on ingestive behaviors. For example, melanocortin signaling is necessary for the anorexigenic effects of leptin (Seeley *et al.*, 1997), nesfatin-1 (Oh-I *et al.*, 2006), oxytocin (Maejima *et al.*, 2009), serotonin (Heisler *et al.*, 2006), and CCK (Fan *et al.*, 2004), while oxytocin signaling is essential for nesfatin-1 to elicit decreases in food intake (Maejima *et al.*, 2009). Moreover, leptin signaling is required for CCK induced decreases in food intake (Hayes

et al., 2010). Thus it is evident there is a remarkably complex, multi-layered neural circuitry, distributed across numerous anatomical sites, which ultimately synergizes to regulate the seemingly simple task of eating. We have made attempts in the nesfatin-1 studies presented in Chapter 2 and the glucose responsiveness studies in Chapter 4 to study this integrated cellular level signaling, and contribute to the growing literature on the NTS as a hub for converging inputs regarding energy status. For example, the RT-PCR studies conducted in Chapter 2 revealed nesfatin-1 responsive mNTS neurons also express NPY, GAD67, NUCB2, and/or the MC4R, in addition to the putative nesfatin-1 receptor. While the number of co-activated peptide systems we uncovered in this RT-PCR work is already relatively large and complex, the primers we selected for our studies certainly do not represent all the neuropeptides and receptors expressed by these neurons, making it readily apparent how intricate signaling in this neuronal region truly is. Our findings have, however, indeed provided direct cellular evidence of the potential synergy between both nesfatin-1 and melanocortin systems at the level of the NTS. Future studies should also address whether a similar possible overlap between nesfatin-1 and oxytocin or CRH signaling at the single cell level exists in the NTS. Ideally, although technically challenging, experiments should also combine application of ligands for all four of these neuropeptide systems to a single cell to provide a direct evaluation of how each system may modulate another. Moreover, the work completed in Chapter 4 has provided evidence for the dynamically regulated integration of both neuropeptides and the nutrient constituent glucose at the single cell level in the NTS in line with the metabolic state of the slice and, by extension, the animal. Thus it is clear from the work presented in this thesis that there are multiple layers of complexity to the detection of signals related to energy balance by neurons in the NTS, and this level of intricacy likely applies to other brain areas as well. Ultimately, the challenge for

scientists in the field will be to understand how many systems work together centrally in both homeostatic and hedonic centers, all in accordance with energy state. There is evidently much work to be done before a unified model of the central control of energy homeostasis can be thoroughly and accurately delineated.

Reference List

Abbott CR, Monteiro M, Small CJ, Sajedi A, Smith KL, Parkinson JR, Ghatei MA, & Bloom SR (2005). The inhibitory effects of peripheral administration of peptide YY(3-36) and glucagon-like peptide-1 on food intake are attenuated by ablation of the vagal-brainstem-hypothalamic pathway. *Brain Res* **1044**, 127-131.

Abdala AP, Haibara AS, & Colombari E (2003). Cardiovascular responses to substance P in the nucleus tractus solitarius: microinjection study in conscious rats. *Am J Physiol Heart Circ Physiol* **285**, H891-H898.

Abdel-Malek ZA (2001). Melanocortin receptors: their functions and regulation by physiological agonists and antagonists. *Cell Mol Life Sci* **58**, 434-441.

Adachi A, Kobashi M, & Funahashi M (1995). Glucose-responsive neurons in the brainstem. *Obes Res* **3 Suppl 5**, 735S-740S.

Adage T, Scheurink AJ, de Boer SF, de VK, Kongsman JP, Kuipers F, Adan RA, Baskin DG, Schwartz MW, & van DG (2001). Hypothalamic, metabolic, and behavioral responses to pharmacological inhibition of CNS melanocortin signaling in rats. *J Neurosci* **21**, 3639-3645.

ANAND BK & BROBECK JR (1951). Hypothalamic control of food intake in rats and cats. *Yale J Biol Med* **24**, 123-140.

ANAND BK, CHHINA GS, SHARMA KN, DUA S, & SINGH B (1964). ACTIVITY OF SINGLE NEURONS IN THE HYPOTHALAMIC FEEDING CENTERS: EFFECT OF GLUCOSE. *Am J Physiol* **207**, 1146-1154.

Andresen MC & Peters JH (2008). Comparison of baroreceptive to other afferent synaptic transmission to the medial solitary tract nucleus. *Am J Physiol Heart Circ Physiol* **295**, H2032-H2042.

Andresen MC & Yang M (1995). Dynamics of sensory afferent synaptic transmission in aortic baroreceptor regions on nucleus tractus solitarius. *J Neurophysiol* **74**, 1518-1528.

Andresen MC & Yang MY (1990). Non-NMDA receptors mediate sensory afferent synaptic transmission in medial nucleus tractus solitarius. *Am J Physiol* **259**, H1307-H1311.

Angelone T, Filice E, Pasqua T, Amodio N, Galluccio M, Montesanti G, Quintieri AM, & Cerra MC (2012). Nesfatin-1 as a novel cardiac peptide: identification, functional characterization, and protection against ischemia/reperfusion injury. *Cell Mol Life Sci*.

Aponte Y, Atasoy D, & Sternson SM (2011). AGRP neurons are sufficient to orchestrate feeding behavior rapidly and without training. *Nat Neurosci* **14**, 351-355.

Appleyard SM, Bailey TW, Doyle MW, Jin YH, Smart JL, Low MJ, & Andresen MC (2005). Proopiomelanocortin neurons in nucleus tractus solitarius are activated by visceral afferents: regulation by cholecystokinin and opioids. *J Neurosci* **25**, 3578-3585.

Ashford CA & Dixon KC (1935). The effect of potassium on the glucolysis of brain tissue with reference to the Pasteur effect. *Biochem J* **29**, 157-168.

Attwell D & Laughlin SB (2001). An energy budget for signaling in the grey matter of the brain. *J Cereb Blood Flow Metab* **21**, 1133-1145.

Azzara AV, Sokolnicki JP, & Schwartz GJ (2002). Central melanocortin receptor agonist reduces spontaneous and scheduled meal size but does not augment duodenal preload-induced feeding inhibition. *Physiol Behav* **77**, 411-416.

Bado A, Levasseur S, Attoub S, Kermorgant S, Laigneau JP, Bortoluzzi MN, Moizo L, Lehy T, Guerre-Millo M, Le Marchand-Brustel Y, & Lewin MJ (1998). The stomach is a source of leptin. *Nature* **394**, 790-793.

Bagnol D, Lu XY, Kaelin CB, Day HE, Ollmann M, Gantz I, Akil H, Barsh GS, & Watson SJ (1999). Anatomy of an endogenous antagonist: relationship between Agouti-related protein and proopiomelanocortin in brain. *J Neurosci* **19**, RC26.

Bailey TW, Jin YH, Doyle MW, & Andresen MC (2002). Vanilloid-sensitive afferents activate neurons with prominent A-type potassium currents in nucleus tractus solitarius. *J Neurosci* **22**, 8230-8237.

Balfour RH, Hansen AM, & Trapp S (2006). Neuronal responses to transient hypoglycaemia in the dorsal vagal complex of the rat brainstem. *J Physiol* **570**, 469-484.

Balfour RH & Trapp S (2007). Ionic currents underlying the response of rat dorsal vagal neurones to hypoglycaemia and chemical anoxia. *J Physiol* **579**, 691-702.

Balthasar N, Dalgaard LT, Lee CE, Yu J, Funahashi H, Williams T, Ferreira M, Tang V, McGovern RA, Kenny CD, Christiansen LM, Edelman E, Choi B, Boss O, Aschkenasi C, Zhang CY, Mountjoy K, Kishi T, Elmquist JK, & Lowell BB (2005). Divergence of melanocortin pathways in the control of food intake and energy expenditure. *Cell* **123**, 493-505.

Barber WD & Burks TF (1983). Brain stem response to phasic gastric distension. *Am J Physiol* **245**, G242-G248.

Baron-Houy B, Roux J, Tardivel C, Trouslard J, Jean A, & Lebrun B (2009). Brain-derived neurotrophic factor/tropomyosin-related kinase receptor type B signaling is a downstream effector of the brainstem melanocortin system in food intake control. *Endocrinology* **150**, 2646-2653.

Barraco RA, Ergene E, Dunbar JC, & el-Ridi MR (1990). Cardiorespiratory response patterns elicited by microinjections of neuropeptide Y in the nucleus tractus solitarius. *Brain Res Bull* **24**, 465-485.

Baskin DG, Kim F, Gelling RW, Russell BJ, Schwartz MW, Morton GJ, Simhan HN, Moralejo DH, & Blevins JE (2010). A new oxytocin-saporin cytotoxin for lesioning oxytocin-receptive neurons in the rat hindbrain. *Endocrinology* **151**, 4207-4213.

Bednar I, Qian M, Qureshi GA, Kallstrom L, Johnson AE, Carrer H, & Sodersten P (1994). Glutamate inhibits ingestive behaviour. *J Neuroendocrinol* **6**, 403-408.

Berger AJ, Averill DB, & Cameron WE (1984). Morphology of inspiratory neurons located in the ventrolateral nucleus of the tractus solitarius of the cat. *J Comp Neurol* **224**, 60-70.

Berglund ED, Liu T, Kong X, Sohn JW, Vong L, Deng Z, Lee CE, Lee S, Williams KW, Olson DP, Scherer PE, Lowell BB, & Elmquist JK (2014). Melanocortin 4 receptors in autonomic neurons regulate thermogenesis and glycemia. *Nat Neurosci* **17**, 911-913.

Berthoud HR (2008). The vagus nerve, food intake and obesity. *Regul Pept* **149**, 15-25.

Berthoud HR (2011). Metabolic and hedonic drives in the neural control of appetite: who is the boss? *Curr Opin Neurobiol* **21**, 888-896.

Bicknell AB (2008). The tissue-specific processing of pro-opiomelanocortin. *J Neuroendocrinol* **20**, 692-699.

Blanton MG, Lo Turco JJ, & Kriegstein AR (1989). Whole cell recording from neurons in slices of reptilian and mammalian cerebral cortex. *J Neurosci Methods* **30**, 203-210.

Bonnet MS, Djelloul M, Tillement V, Tardivel C, Mounien L, Trouslard J, Troadec JD, & Dallaporta M (2013). Central NUCB2/Nesfatin-1-expressing neurones belong to the hypothalamic-brainstem circuitry activated by hypoglycaemia. *J Neuroendocrinol* **25**, 1-13.

Brailoiu GC, Deliu E, Tica AA, Rabinowitz JE, Tilley DG, Benamar K, Koch WJ, & Brailoiu E (2013). Nesfatin-1 activates cardiac vagal neurons of nucleus ambiguus and elicits bradycardia in conscious rats. *J Neurochem* **126**, 739-748.

Brailoiu GC, Dun SL, Brailoiu E, Inan S, Yang J, Chang JK, & Dun NJ (2007). Nesfatin-1: distribution and interaction with a G protein-coupled receptor in the rat brain. *Endocrinology* **148**, 5088-5094.

Branchereau P, Champagnat J, & Denavit-Saubie M (1993). Cholecystokinin-gated currents in neurons of the rat solitary complex in vitro. *J Neurophysiol* **70**, 2584-2595.

Breit A, Buch TR, Boekhoff I, Solinski HJ, Damm E, & Gudermann T (2011). Alternative G protein coupling and biased agonism: new insights into melanocortin-4 receptor signalling. *Mol Cell Endocrinol* **331**, 232-240.

Broberger C, Johansen J, Johansson C, Schalling M, & Hokfelt T (1998). The neuropeptide Y/agouti gene-related protein (AGRP) brain circuitry in normal, anorectic, and monosodium glutamate-treated mice. *Proc Natl Acad Sci U S A* **95**, 15043-15048.

Bronstein DM, Schafer MK, Watson SJ, & Akil H (1992). Evidence that beta-endorphin is synthesized in cells in the nucleus tractus solitarius: detection of POMC mRNA. *Brain Res* **587**, 269-275.

Browning KN & Travagli RA (2010). Plasticity of vagal brainstem circuits in the control of gastric function. *Neurogastroenterol Motil* **22**, 1154-1163.

Burdakov D, Gerasimenko O, & Verkhatsky A (2005). Physiological changes in glucose differentially modulate the excitability of hypothalamic melanin-concentrating hormone and orexin neurons in situ. *J Neurosci* **25**, 2429-2433.

Burdakov D, Jensen LT, Alexopoulos H, Williams RH, Fearon IM, O'Kelly I, Gerasimenko O, Fugger L, & Verkhatsky A (2006). Tandem-pore K⁺ channels mediate inhibition of orexin neurons by glucose. *Neuron* **50**, 711-722.

Burns GA & Ritter RC (1997). The non-competitive NMDA antagonist MK-801 increases food intake in rats. *Pharmacol Biochem Behav* **56**, 145-149.

Cao X, Liu XM, & Zhou LH (2013). Recent progress in research on the distribution and function of NUCB2/nesfatin-1 in peripheral tissues. *Endocr J* **60**, 1021-1027.

Champagnat J, Jacquin T, & Richter DW (1986). Voltage-dependent currents in neurones of the nuclei of the solitary tract of rat brainstem slices. *Pflugers Arch* **406**, 372-379.

Chebib M & Johnston GA (1999). The 'ABC' of GABA receptors: a brief review. *Clin Exp Pharmacol Physiol* **26**, 937-940.

Chen X, Dong J, & Jiang ZY (2012). Nesfatin-1 influences the excitability of glucosensing neurons in the hypothalamic nuclei and inhibits the food intake. *Regul Pept* **177**, 21-26.

Chiba T & Kato M (1978). Synaptic structures and quantification of catecholaminergic axons in the nucleus tractus solitarius of the rat: possible modulatory roles of catecholamines in baroreceptor reflexes. *Brain Res* **151**, 323-338.

Claps A & Torrealba F (1988). The carotid body connections: a WGA-HRP study in the cat. *Brain Res* **455**, 123-133.

Cone RD (2005). Anatomy and regulation of the central melanocortin system. *Nat Neurosci* **8**, 571-578.

Conner JM, Lauterborn JC, Yan Q, Gall CM, & Varon S (1997). Distribution of brain-derived neurotrophic factor (BDNF) protein and mRNA in the normal adult rat CNS: evidence for anterograde axonal transport. *J Neurosci* **17**, 2295-2313.

Corbett EK, Sinfield JK, McWilliam PN, Deuchars J, & Batten TF (2005). Differential expression of vesicular glutamate transporters by vagal afferent terminals in rat nucleus of the solitary tract: projections from the heart preferentially express vesicular glutamate transporter 1. *Neuroscience* **135**, 133-145.

Cowley MA, Pronchuk N, Fan W, Dinulescu DM, Colmers WF, & Cone RD (1999). Integration of NPY, AGRP, and melanocortin signals in the hypothalamic paraventricular nucleus: evidence of a cellular basis for the adipostat. *Neuron* **24**, 155-163.

Cowley MA, Smart JL, Rubinstein M, Cerdan MG, Diano S, Horvath TL, Cone RD, & Low MJ (2001). Leptin activates anorexigenic POMC neurons through a neural network in the arcuate nucleus. *Nature* **411**, 480-484.

Cowley MA, Smith RG, Diano S, Tschop M, Pronchuk N, Grove KL, Strasburger CJ, Bidlingmaier M, Esterman M, Heiman ML, Garcia-Segura LM, Nillni EA, Mendez P, Low MJ, Sotonyi P, Friedman JM, Liu H, Pinto S, Colmers WF, Cone RD, & Horvath TL (2003). The distribution and mechanism of action of ghrelin in the CNS demonstrates a novel hypothalamic circuit regulating energy homeostasis. *Neuron* **37**, 649-661.

Czachurski J, Lackner KJ, Ockert D, & Seller H (1982). Localization of neurones with baroreceptor input in the medial solitary nucleus by means of intracellular application of horseradish peroxidase in the cat. *Neurosci Lett* **28**, 133-137.

Dai L, Smith PM, Kuksis M, & Ferguson AV (2013). Apelin acts in the subfornical organ to influence neuronal excitability and cardiovascular function. *J Physiol* **591**, 3421-3432.

Dallaporta M, Himmi T, Perrin J, & Orsini JC (1999). Solitary tract nucleus sensitivity to moderate changes in glucose level. *Neuroreport* **10**, 2657-2660.

Dallaporta M, Perrin J, & Orsini JC (2000). Involvement of adenosine triphosphate-sensitive K⁺ channels in glucose-sensing in the rat solitary tract nucleus. *Neurosci Lett* **278**, 77-80.

Dean C & Seagard JL (1995). Expression of c-fos protein in the nucleus tractus solitarius in response to physiological activation of carotid baroreceptors. *Neuroscience* **69**, 249-257.

Dekin MS & Getting PA (1984). Firing pattern of neurons in the nucleus tractus solitarius: modulation by membrane hyperpolarization. *Brain Res* **324**, 180-184.

Deuchars J, Li YW, Kasparov S, & Paton JF (2000). Morphological and electrophysiological properties of neurones in the dorsal vagal complex of the rat activated by arterial baroreceptors. *J Comp Neurol* **417**, 233-249.

Dietrich WD, Lowry OH, & Loewy AD (1982). The distribution of glutamate, GABA and aspartate in the nucleus tractus solitarius of the cat. *Brain Res* **237**, 254-260.

Dingledine R, Dodd J, & Kelly JS (1980). The in vitro brain slice as a useful neurophysiological preparation for intracellular recording. *J Neurosci Methods* **2**, 323-362.

DiRocco RJ & Grill HJ (1979). The forebrain is not essential for sympathoadrenal hyperglycemic response to glucoprivation. *Science* **204**, 1112-1114.

Doba N & Reis DJ (1973). Acute fulminating neurogenic hypertension produced by brainstem lesions in the rat. *Circ Res* **32**, 584-593.

Dong J, Guan HZ, Jiang ZY, & Chen X (2014). Nesfatin-1 influences the excitability of glucosensing neurons in the dorsal vagal complex and inhibits food intake. *PLoS One* **9**, e98967.

Doyle MW & Andresen MC (2001). Reliability of monosynaptic sensory transmission in brain stem neurons in vitro. *J Neurophysiol* **85**, 2213-2223.

Dunbar JC & Lu H (2000). Proopiomelanocortin (POMC) products in the central regulation of sympathetic and cardiovascular dynamics: studies on melanocortin and opioid interactions. *Peptides* **21**, 211-217.

Edwards FA, Konnerth A, Sakmann B, & Takahashi T (1989). A thin slice preparation for patch clamp recordings from neurones of the mammalian central nervous system. *Pflugers Arch* **414**, 600-612.

Emond M, Ladenheim EE, Schwartz GJ, & Moran TH (2001a). Leptin amplifies the feeding inhibition and neural activation arising from a gastric nutrient preload. *Physiol Behav* **72**, 123-128.

Emond M, Schwartz GJ, Ladenheim EE, & Moran TH (1999). Central leptin modulates behavioral and neural responsivity to CCK. *Am J Physiol* **276**, R1545-R1549.

Emond M, Schwartz GJ, & Moran TH (2001b). Meal-related stimuli differentially induce c-Fos activation in the nucleus of the solitary tract. *Am J Physiol Regul Integr Comp Physiol* **280**, R1315-R1321.

Ewart WR & Wingate DL (1984). Central representation of arrival of nutrient in the duodenum. *Am J Physiol* **246**, G750-G756.

Fan W, Boston BA, Kesterson RA, Hruby VJ, & Cone RD (1997). Role of melanocortinergic neurons in feeding and the agouti obesity syndrome. *Nature* **385**, 165-168.

Fan W, Dinulescu DM, Butler AA, Zhou J, Marks DL, & Cone RD (2000). The central melanocortin system can directly regulate serum insulin levels. *Endocrinology* **141**, 3072-3079.

Fan W, Ellacott KL, Halatchev IG, Takahashi K, Yu P, & Cone RD (2004). Cholecystokinin-mediated suppression of feeding involves the brainstem melanocortin system. *Nat Neurosci* **7**, 335-336.

Farooqi IS, Yeo GS, Keogh JM, Aminian S, Jebb SA, Butler G, Cheetham T, & O'Rahilly S (2000). Dominant and recessive inheritance of morbid obesity associated with melanocortin 4 receptor deficiency. *J Clin Invest* **106**, 271-279.

Ferreira M, Jr., Browning KN, Sahibzada N, Verbalis JG, Gillis RA, & Travagli RA (2001). Glucose effects on gastric motility and tone evoked from the rat dorsal vagal complex. *J Physiol* **536**, 141-152.

Flynn FW & Grill HJ (1983). Insulin elicits ingestion in decerebrate rats. *Science* **221**, 188-190.

Foo KS, Brauner H, Ostenson CG, & Broberger C (2010). Nucleobindin-2/nesfatin in the endocrine pancreas: distribution and relationship to glycaemic state. *J Endocrinol* **204**, 255-263.

Foo KS, Brismar H, & Broberger C (2008). Distribution and neuropeptide coexistence of nucleobindin-2 mRNA/nesfatin-like immunoreactivity in the rat CNS. *Neuroscience* **156**, 563-579.

Fort P, Salvert D, Hanriot L, Jego S, Shimizu H, Hashimoto K, Mori M, & Luppi PH (2008). The satiety molecule nesfatin-1 is co-expressed with melanin concentrating hormone in tuberal hypothalamic neurons of the rat. *Neuroscience* **155**, 174-181.

Fry M & Ferguson AV (2009). Ghrelin modulates electrical activity of area postrema neurons. *Am J Physiol Regul Integr Comp Physiol* **296**, R485-R492.

Gantz I, Miwa H, Konda Y, Shimoto Y, Tashiro T, Watson SJ, DelValle J, & Yamada T (1993). Molecular cloning, expression, and gene localization of a fourth melanocortin receptor. *J Biol Chem* **268**, 15174-15179.

Garcia-Galiano D, Navarro VM, Roa J, Ruiz-Pino F, Sanchez-Garrido MA, Pineda R, Castellano JM, Romero M, Aguilar E, Gaytan F, Dieguez C, Pinilla L, & Tena-Sempere M (2010). The anorexigenic neuropeptide, nesfatin-1, is indispensable for normal puberty onset in the female rat. *J Neurosci* **30**, 7783-7792.

Ghamari-Langroudi M, Srisai D, & Cone RD (2011). Multinodal regulation of the arcuate/paraventricular nucleus circuit by leptin. *Proc Natl Acad Sci U S A* **108**, 355-360.

Giraudo SQ, Billington CJ, & Levine AS (1998). Feeding effects of hypothalamic injection of melanocortin 4 receptor ligands. *Brain Res* **809**, 302-306.

Goebel M, Stengel A, Wang L, Lambrecht NW, & Tache Y (2009a). Nesfatin-1 immunoreactivity in rat brain and spinal cord autonomic nuclei. *Neurosci Lett* **452**, 241-246.

Goebel M, Stengel A, Wang L, & Tache Y (2009b). Restraint stress activates nesfatin-1-immunoreactive brain nuclei in rats. *Brain Res* **1300**, 114-124.

Goebel M, Stengel A, Wang L, & Tache Y (2011). Central nesfatin-1 reduces the nocturnal food intake in mice by reducing meal size and increasing inter-meal intervals. *Peptides* **32**, 36-43.

Goke R, Larsen PJ, Mikkelsen JD, & Sheikh SP (1995). Distribution of GLP-1 binding sites in the rat brain: evidence that exendin-4 is a ligand of brain GLP-1 binding sites. *Eur J Neurosci* **7**, 2294-2300.

Gonzalez R, Perry RL, Gao X, Gaidhu MP, Tsushima RG, Ceddia RB, & Unniappan S (2011). Nutrient responsive nesfatin-1 regulates energy balance and induces glucose-stimulated insulin secretion in rats. *Endocrinology* **152**, 3628-3637.

Gonzalez R, Tiwari A, & Unniappan S (2009). Pancreatic beta cells colocalize insulin and nesfatin immunoreactivity in rodents. *Biochem Biophys Res Commun* **381**, 643-648.

Gouveia CF & Chowdhury TA (2013). Managing hyperglycaemic emergencies: an illustrative case and review of recent British guidelines. *Clin Med* **13**, 160-162.

Graham M, Shutter JR, Sarmiento U, Sarosi I, & Stark KL (1997). Overexpression of Agprt leads to obesity in transgenic mice. *Nat Genet* **17**, 273-274.

Grill HJ, Ginsberg AB, Seeley RJ, & Kaplan JM (1998). Brainstem application of melanocortin receptor ligands produces long-lasting effects on feeding and body weight. *J Neurosci* **18**, 10128-10135.

Grill HJ & Hayes MR (2012). Hindbrain neurons as an essential hub in the neuroanatomically distributed control of energy balance. *Cell Metab* **16**, 296-309.

Grill HJ & Kaplan JM (1992). Sham feeding in intact and chronic decerebrate rats. *Am J Physiol* **262**, R1070-R1074.

Grill HJ & Norgren R (1978). Chronically decerebrate rats demonstrate satiation but not bait shyness. *Science* **201**, 267-269.

Grill HJ, Schwartz MW, Kaplan JM, Foxhall JS, Breininger J, & Baskin DG (2002). Evidence that the caudal brainstem is a target for the inhibitory effect of leptin on food intake. *Endocrinology* **143**, 239-246.

Grill HJ & Smith GP (1988). Cholecystokinin decreases sucrose intake in chronic decerebrate rats. *Am J Physiol* **254**, R853-R856.

Gropp E, Shanabrough M, Borok E, Xu AW, Janoschek R, Buch T, Plum L, Balthasar N, Hampel B, Waisman A, Barsh GS, Horvath TL, & Bruning JC (2005). Agouti-related peptide-expressing neurons are mandatory for feeding. *Nat Neurosci* **8**, 1289-1291.

Hagan MM, Rushing PA, Schwartz MW, Yagaloff KA, Burn P, Woods SC, & Seeley RJ (1999). Role of the CNS melanocortin system in the response to overfeeding. *J Neurosci* **19**, 2362-2367.

HARRIS JI & LERNER AB (1957). Amino-acid sequence of the alpha-melanocyte-stimulating hormone. *Nature* **179**, 1346-1347.

Harrold JA, Widdowson PS, & Williams G (1999). Altered energy balance causes selective changes in melanocortin-4(MC4-R), but not melanocortin-3 (MC3-R), receptors in specific hypothalamic regions: further evidence that activation of MC4-R is a physiological inhibitor of feeding. *Diabetes* **48**, 267-271.

Hayes MR, Skibicka KP, Leichner TM, Guarnieri DJ, DiLeone RJ, Bence KK, & Grill HJ (2010). Endogenous leptin signaling in the caudal nucleus tractus solitarius and area postrema is required for energy balance regulation. *Cell Metab* **11**, 77-83.

Heisler LK, Cowley MA, Tecott LH, Fan W, Low MJ, Smart JL, Rubinstein M, Tatro JB, Marcus JN, Holstege H, Lee CE, Cone RD, & Elmquist JK (2002). Activation of central melanocortin pathways by fenfluramine. *Science* **297**, 609-611.

Heisler LK, Jobst EE, Sutton GM, Zhou L, Borok E, Thornton-Jones Z, Liu HY, Zigman JM, Balthasar N, Kishi T, Lee CE, Aschkenasi CJ, Zhang CY, Yu J, Boss O, Mountjoy KG, Clifton PG, Lowell BB, Friedman JM, Horvath T, Butler AA, Elmquist JK, & Cowley MA (2006). Serotonin reciprocally regulates melanocortin neurons to modulate food intake. *Neuron* **51**, 239-249.

Herman MA, Cruz MT, Sahibzada N, Verbalis J, & Gillis RA (2009). GABA signaling in the nucleus tractus solitarius sets the level of activity in dorsal motor nucleus of the vagus cholinergic neurons in the vagovagal circuit. *Am J Physiol Gastrointest Liver Physiol* **296**, G101-G111.

Hill C & Dunbar JC (2002). The effects of acute and chronic alpha melanocyte stimulating hormone (alphaMSH) on cardiovascular dynamics in conscious rats. *Peptides* **23**, 1625-1630.

HILLMAN HH & McILWAIN H (1961). Membrane potentials in mammalian cerebral tissues in vitro: dependence on ionic environment. *J Physiol* **157**, 263-278.

Hisadome K, Reimann F, Gribble FM, & Trapp S (2010). Leptin directly depolarizes proglucagon neurons in the nucleus tractus solitarius: electrical properties of glucagon-like Peptide 1 neurons. *Diabetes* **59**, 1890-1898.

Hoyda TD, Smith PM, & Ferguson AV (2009). Adiponectin acts in the nucleus of the solitary tract to decrease blood pressure by modulating the excitability of neuropeptide Y neurons. *Brain Res* **1256**, 76-84.

Hu Y & Wilson GS (1997). Rapid changes in local extracellular rat brain glucose observed with an in vivo glucose sensor. *J Neurochem* **68**, 1745-1752.

Huo L, Grill HJ, & Bjorbaek C (2006). Divergent regulation of proopiomelanocortin neurons by leptin in the nucleus of the solitary tract and in the arcuate hypothalamic nucleus. *Diabetes* **55**, 567-573.

Huszar D, Lynch CA, Fairchild-Huntress V, Dunmore JH, Fang Q, Berkemeier LR, Gu W, Kesterson RA, Boston BA, Cone RD, Smith FJ, Campfield LA, Burn P, & Lee F (1997). Targeted disruption of the melanocortin-4 receptor results in obesity in mice. *Cell* **88**, 131-141.

Ibrahim N, Bosch MA, Smart JL, Qiu J, Rubinstein M, Ronnekleiv OK, Low MJ, & Kelly MJ (2003). Hypothalamic proopiomelanocortin neurons are glucose responsive and express K(ATP) channels. *Endocrinology* **144**, 1331-1340.

Inhoff T, Stengel A, Peter L, Goebel M, Tache Y, Bannert N, Wiedenmann B, Klapp BF, Monnikes H, & Kobelt P (2010). Novel insight in distribution of nesfatin-1 and phospho-mTOR in the arcuate nucleus of the hypothalamus of rats. *Peptides* **31**, 257-262.

Ishida E, Hashimoto K, Shimizu H, Okada S, Satoh T, Kato I, Yamada M, & Mori M (2012). Nesfatin-1 induces the phosphorylation levels of cAMP response element-binding protein for intracellular signaling in a neural cell line. *PLoS One* **7**, e50918.

Iwasaki Y, Nakabayashi H, Kakei M, Shimizu H, Mori M, & Yada T (2009). Nesfatin-1 evokes Ca²⁺ signaling in isolated vagal afferent neurons via Ca²⁺ influx through N-type channels. *Biochem Biophys Res Commun* **390**, 958-962.

Jacobowitz DM & O'Donohue TL (1978). alpha-Melanocyte stimulating hormone: immunohistochemical identification and mapping in neurons of rat brain. *Proc Natl Acad Sci U S A* **75**, 6300-6304.

Jean A (1991). [The nucleus tractus solitarius: neuroanatomic, neurochemical and functional aspects]. *Arch Int Physiol Biochim Biophys* **99**, A3-52.

Johnson SM & Felder RB (1993). Effects of aging on the intrinsic membrane properties of medial NTS neurons of Fischer-344 rats. *J Neurophysiol* **70**, 1975-1987.

Joseph SA, Pilcher WH, & Bennett-Clarke C (1983). Immunocytochemical localization of ACTH perikarya in nucleus tractus solitarius: evidence for a second opiocortin neuronal system. *Neurosci Lett* **38**, 221-225.

Kadekaro M, Timo-Iaria C, & Vicentini ML (1980). Gastric secretion provoked by functional cytoglucopenia in the nuclei of the solitary tract in the cat. *J Physiol* **299**, 397-407.

Kakei M, Yada T, Nakagawa A, & Nakabayashi H (2002). Glucagon-like peptide-1 evokes action potentials and increases cytosolic Ca²⁺ in rat nodose ganglion neurons. *Auton Neurosci* **102**, 39-44.

Kalia M & Mesulam MM (1980a). Brain stem projections of sensory and motor components of the vagus complex in the cat: I. The cervical vagus and nodose ganglion. *J Comp Neurol* **193**, 435-465.

Kalia M & Mesulam MM (1980b). Brain stem projections of sensory and motor components of the vagus complex in the cat: II. Laryngeal, tracheobronchial, pulmonary, cardiac, and gastrointestinal branches. *J Comp Neurol* **193**, 467-508.

Karnani M & Burdakov D (2011). Multiple hypothalamic circuits sense and regulate glucose levels. *Am J Physiol Regul Integr Comp Physiol* **300**, R47-R55.

Kieffer TJ & Habener JF (1999). The glucagon-like peptides. *Endocr Rev* **20**, 876-913.

Kishi T, Aschkenasi CJ, Lee CE, Mountjoy KG, Saper CB, & Elmquist JK (2003). Expression of melanocortin 4 receptor mRNA in the central nervous system of the rat. *J Comp Neurol* **457**, 213-235.

Konczol K, Pinter O, Ferenczi S, Varga J, Kovacs K, Palkovits M, Zelena D, & Toth ZE (2012). Nesfatin-1 exerts long-term effect on food intake and body temperature. *Int J Obes (Lond)*.

Krude H, Biebermann H, Luck W, Horn R, Brabant G, & Gruters A (1998). Severe early-onset obesity, adrenal insufficiency and red hair pigmentation caused by POMC mutations in humans. *Nat Genet* **19**, 155-157.

Kubo T & Kihara M (1990). Modulation of the aortic baroreceptor reflex by neuropeptide Y, neurotensin and vasopressin microinjected into the nucleus tractus solitarii of the rat. *Naunyn Schmiedebergs Arch Pharmacol* **342**, 182-188.

Kumada M & Nakajima H (1972). Field potentials evoked in rabbit brainstem by stimulation of the aortic nerve. *Am J Physiol* **223**, 575-582.

Kunze DL (1987). Calcium currents of cardiovascular neurons isolated from adult guinea pigs. *Am J Physiol* **252**, H867-H871.

Lakhi S, Snow W, & Fry M (2013). Insulin modulates the electrical activity of subfornical organ neurons. *Neuroreport* **24**, 329-334.

Lamy CM, Sanno H, Labouebe G, Picard A, Magnan C, Chatton JY, & Thorens B (2014). Hypoglycemia-activated GLUT2 neurons of the nucleus tractus solitarius stimulate vagal activity and glucagon secretion. *Cell Metab* **19**, 527-538.

Larsen PJ, Tang-Christensen M, Holst JJ, & Orskov C (1997). Distribution of glucagon-like peptide-1 and other preproglucagon-derived peptides in the rat hypothalamus and brainstem. *Neuroscience* **77**, 257-270.

Lawrence AJ, Castillo-Melendez M, McLean KJ, & Jarrott B (1998). The distribution of nitric oxide synthase-, adenosine deaminase- and neuropeptide Y-immunoreactivity through the entire rat nucleus tractus solitarius: Effect of unilateral nodose ganglionectomy. *J Chem Neuroanat* **15**, 27-40.

Lawrence AJ & Jarrott B (1996). Neurochemical modulation of cardiovascular control in the nucleus tractus solitarius. *Prog Neurobiol* **48**, 21-53.

LEE TH & LERNER AB (1956). Isolation of melanocyte-stimulating hormone from hog pituitary gland. *J Biol Chem* **221**, 943-959.

Levin BE, Magnan C, Dunn-Meynell A, & Le FC (2011). Metabolic sensing and the brain: who, what, where, and how? *Endocrinology* **152**, 2552-2557.

Levin BE, Routh VH, Kang L, Sanders NM, & Dunn-Meynell AA (2004). Neuronal glucosensing: what do we know after 50 years? *Diabetes* **53**, 2521-2528.

Lewis LD & Williams JA (1990). Regulation of cholecystokinin secretion by food, hormones, and neural pathways in the rat. *Am J Physiol* **258**, G512-G518.

Li G, Zhang Y, Rodrigues E, Zheng D, Matheny M, Cheng KY, & Scarpace PJ (2007). Melanocortin activation of nucleus of the solitary tract avoids anorectic tachyphylaxis and induces prolonged weight loss. *Am J Physiol Endocrinol Metab* **293**, E252-E258.

Li SJ, Varga K, Archer P, Hruby VJ, Sharma SD, Kesterson RA, Cone RD, & Kunos G (1996). Melanocortin antagonists define two distinct pathways of cardiovascular control by alpha- and gamma-melanocyte-stimulating hormones. *J Neurosci* **16**, 5182-5188.

Li Z, Gao L, Tang H, Yin Y, Xiang X, Li Y, Zhao J, Mulholland M, & Zhang W (2013a). Peripheral effects of nesfatin-1 on glucose homeostasis. *PLoS One* **8**, e71513.

Li Z, Xu G, Li Y, Zhao J, Mulholland MW, & Zhang W (2012). mTOR-dependent modulation of gastric nesfatin-1/NUCB2. *Cell Physiol Biochem* **29**, 493-500.

Li ZL, Xu L, Sun XR, Guo FF, Gong YL, & Gao SL (2013b). Central nesfatin-1 influences the excitability of ghrelin-responsive gastric distension neurons in the arcuate nucleus and reduces gastric motility in rats. *Eur J Neurosci* **38**, 3636-3643.

Lipton P (1973). Effects of membrane depolarization on nicotinamide nucleotide fluorescence in brain slices. *Biochem J* **136**, 999-1009.

Liu H, Kishi T, Roseberry AG, Cai X, Lee CE, Montez JM, Friedman JM, & Elmquist JK (2003). Transgenic mice expressing green fluorescent protein under the control of the melanocortin-4 receptor promoter. *J Neurosci* **23**, 7143-7154.

Llinas R & Sugimori M (1980). Electrophysiological properties of in vitro Purkinje cell somata in mammalian cerebellar slices. *J Physiol* **305**, 171-195.

Loup F, Tribollet E, Dubois-Dauphin M, Pizzolato G, & Dreifuss JJ (1989). Localization of oxytocin binding sites in the human brainstem and upper spinal cord: an autoradiographic study. *Brain Res* **500**, 223-230.

Ludwig DS, Mountjoy KG, Tatro JB, Gillette JA, Frederick RC, Flier JS, & Maratos-Flier E (1998). Melanin-concentrating hormone: a functional melanocortin antagonist in the hypothalamus. *Am J Physiol* **274**, E627-E633.

Luquet S, Perez FA, Hnasko TS, & Palmiter RD (2005). NPY/AgRP neurons are essential for feeding in adult mice but can be ablated in neonates. *Science* **310**, 683-685.

Maejima Y, Sedbazar U, Suyama S, Kohno D, Onaka T, Takano E, Yoshida N, Koike M, Uchiyama Y, Fujiwara K, Yashiro T, Horvath TL, Dietrich MO, Tanaka S, Dezaki K, Oh I, Hashimoto K, Shimizu H, Nakata M, Mori M, & Yada T (2009). Nesfatin-1-regulated oxytocinergic signaling in the paraventricular nucleus causes anorexia through a leptin-independent melanocortin pathway. *Cell Metab* **10**, 355-365.

Mahaut S, Dumont Y, Fournier A, Quirion R, & Moyses E (2010). Neuropeptide Y receptor subtypes in the dorsal vagal complex under acute feeding adaptation in the adult rat. *Neuropeptides* **44**, 77-86.

Medeiros N, Dai L, & Ferguson AV (2012). Glucose-responsive neurons in the subfornical organ of the rat--a novel site for direct CNS monitoring of circulating glucose. *Neuroscience* **201**, 157-165.

Melnick IV, Price CJ, & Colmers WF (2011). Glucosensing in parvocellular neurons of the rat hypothalamic paraventricular nucleus. *Eur J Neurosci* **34**, 272-282.

Mendelowitz D, Yang M, Andresen MC, & Kunze DL (1992). Localization and retention in vitro of fluorescently labeled aortic baroreceptor terminals on neurons from the nucleus tractus solitarius. *Brain Res* **581**, 339-343.

Mercer RE, Michaelson SD, Chee MJ, Atallah TA, Wevrick R, & Colmers WF (2013). Magel2 is required for leptin-mediated depolarization of POMC neurons in the hypothalamic arcuate nucleus in mice. *PLoS Genet* **9**, e1003207.

Meye FJ & Adan RA (2014). Feelings about food: the ventral tegmental area in food reward and emotional eating. *Trends Pharmacol Sci* **35**, 31-40.

Mimee A & Ferguson AV (2013). Cellular Actions Of Nesfatin-1 On Hypothalamic And Medullary Neurons. *Curr Pharm Des*.

Mimee A, Kuksis M, & Ferguson AV (2014). alpha-MSH exerts direct postsynaptic excitatory effects on NTS neurons and enhances GABAergic signaling in the NTS. *Neuroscience* **262**, 70-82.

Mimee A, Smith PM, & Ferguson AV (2012). Nesfatin-1 influences the excitability of neurons in the nucleus of the solitary tract and regulates cardiovascular function. *Am J Physiol Regul Integr Comp Physiol* **302**, R1297-R1304.

Mizuno TM, Kleopoulos SP, Bergen HT, Roberts JL, Priest CA, & Mobbs CV (1998). Hypothalamic pro-opiomelanocortin mRNA is reduced by fasting and [corrected] in ob/ob and db/db mice, but is stimulated by leptin. *Diabetes* **47**, 294-297.

Mizuno TM & Mobbs CV (1999). Hypothalamic agouti-related protein messenger ribonucleic acid is inhibited by leptin and stimulated by fasting. *Endocrinology* **140**, 814-817.

Mizuno Y & Oomura Y (1984). Glucose responding neurons in the nucleus tractus solitarius of the rat: in vitro study. *Brain Res* **307**, 109-116.

Moak JP & Kunze DL (1993). Potassium currents of neurons isolated from medical nucleus tractus solitarius. *Am J Physiol* **265**, H1596-H1602.

Muroya S, Yada T, Shioda S, & Takigawa M (1999). Glucose-sensitive neurons in the rat arcuate nucleus contain neuropeptide Y. *Neurosci Lett* **264**, 113-116.

Nakanishi S, Inoue A, Kita T, Nakamura M, Chang AC, Cohen SN, & Numa S (1979). Nucleotide sequence of cloned cDNA for bovine corticotropin-beta-lipotropin precursor. *Nature* **278**, 423-427.

Ng M, Fleming T, Robinson M, Thomson B, Graetz N, Margono C, Mullany EC, Biryukov S, Abbafati C, Abera SF, Abraham JP, Abu-Rmeileh NM, Achoki T, AlBuhairan FS, Alemu ZA, Alfonso R, Ali MK, Ali R, Guzman NA, Ammar W, Anwari P, Banerjee A, Barquera S, Basu S, Bennett DA, Bhutta Z, Blore J, Cabral N, Nonato IC, Chang JC, Chowdhury R, Courville KJ, Criqui MH, Cundiff DK, Dabhadkar KC, Dandona L, Davis A, Dayama A, Dharmaratne SD, Ding EL, Durrani AM, Esteghamati A, Farzadfar F, Fay DF, Feigin VL, Flaxman A, Forouzanfar MH, Goto A, Green MA, Gupta R, Hafezi-Nejad N, Hankey GJ, Harewood HC, Havmoeller R, Hay S, Hernandez L, Husseini A, Idrisov BT, Ikeda N, Islami F, Jahangir E, Jassal SK, Jee SH, Jeffreys M, Jonas JB, Kabagambe EK, Khalifa SE, Kengne AP, Khader YS, Khang YH, Kim D, Kimokoti RW, Kinge JM, Kokubo Y, Kosen S, Kwan G, Lai T, Leinsalu M, Li Y, Liang X, Liu S, Logroscino G, Lotufo PA, Lu Y, Ma J, Mainoo NK, Mensah GA, Merriman TR, Mokdad AH, Moschandreas J, Naghavi M, Naheed A, Nand D, Narayan KM, Nelson EL, Neuhouser ML, Nisar MI, Ohkubo T, Oti SO, Pedroza A, Prabhakaran D, Roy N, Sampson U, Seo H, Sepanlou SG, Shibuya K, Shiri R, Shiue I, Singh GM, Singh JA, Skirbekk V, Stapelberg NJ, Sturua L, Sykes BL, Tobias M, Tran BX, Trasande L, Toyoshima H, van d, V, Vasankari TJ, Veerman JL, Velasquez-Melendez G, Vlassov VV, Vollset SE, Vos T, Wang C, Wang SX, Weiderpass E, Werdecker A, Wright JL, Yang YC, Yatsuya H, Yoon J, Yoon SJ, Zhao Y, Zhou M, Zhu S, Lopez AD, Murray CJ, & Gakidou E (2014). Global, regional, and national prevalence of overweight and obesity in children and adults during 1980-2013: a systematic analysis for the Global Burden of Disease Study 2013. *Lancet*.

Obici S, Feng Z, Tan J, Liu L, Karkani G, & Rossetti L (2001). Central melanocortin receptors regulate insulin action. *J Clin Invest* **108**, 1079-1085.

Oh-I S, Shimizu H, Satoh T, Okada S, Adachi S, Inoue K, Eguchi H, Yamamoto M, Imaki T, Hashimoto K, Tsuchiya T, Monden T, Horiguchi K, Yamada M, & Mori M (2006). Identification of nesfatin-1 as a satiety molecule in the hypothalamus. *Nature* **443**, 709-712.

Ollmann MM, Wilson BD, Yang YK, Kerns JA, Chen Y, Gantz I, & Barsh GS (1997). Antagonism of central melanocortin receptors in vitro and in vivo by agouti-related protein. *Science* **278**, 135-138.

Ono T, Steffens AB, & Sasaki K (1983). Influence of peripheral and intracerebroventricular glucose and insulin infusions on peripheral and cerebrospinal fluid glucose and insulin levels. *Physiol Behav* **30**, 301-306.

Oomura Y, KIMURA K, OYAMA H, MAENO T, IKI M, & KUNIYOSHI M (1964). RECIPROCAL ACTIVITIES OF THE VENTROMEDIAL AND LATERAL HYPOTHALAMIC AREAS OF CATS. *Science* **143**, 484-485.

Osaki A, Shimizu H, Ishizuka N, Suzuki Y, Mori M, & Inoue S (2012). Enhanced expression of nesfatin/nucleobindin-2 in white adipose tissue of ventromedial hypothalamus-lesioned rats. *Neurosci Lett* **521**, 46-51.

Palkovits M, Mezey E, & Eskay RL (1987). Pro-opiomelanocortin-derived peptides (ACTH/beta-endorphin/alpha-MSH) in brainstem baroreceptor areas of the rat. *Brain Res* **436**, 323-338.

Pan W, Hsueh H, & Kastin AJ (2007). Nesfatin-1 crosses the blood-brain barrier without saturation. *Peptides* **28**, 2223-2228.

Parker JA, McCullough KA, Field BC, Minnion JS, Martin NM, Ghatei MA, & Bloom SR (2013). Glucagon and GLP-1 inhibit food intake and increase c-fos expression in similar appetite regulating centres in the brainstem and amygdala. *Int J Obes (Lond)*.

Pavia JM, Schioth HB, & Morris MJ (2003). Role of MC4 receptors in the depressor and bradycardic effects of alpha-MSH in the nucleus tractus solitarius of the rat. *Neuroreport* **14**, 703-707.

Perello M, Stuart RC, & Nillni EA (2007). Differential effects of fasting and leptin on proopiomelanocortin peptides in the arcuate nucleus and in the nucleus of the solitary tract. *Am J Physiol Endocrinol Metab* **292**, E1348-E1357.

Peters JH, McDougall SJ, Kellett DO, Jordan D, Llewellyn-Smith IJ, & Andresen MC (2008). Oxytocin enhances cranial visceral afferent synaptic transmission to the solitary tract nucleus. *J Neurosci* **28**, 11731-11740.

Peters JH, McKay BM, Simasko SM, & Ritter RC (2005). Leptin-induced satiation mediated by abdominal vagal afferents. *Am J Physiol Regul Integr Comp Physiol* **288**, R879-R884.

Pilcher WH & Joseph SA (1986). Differential sensitivity of hypothalamic and medullary opiocortin and tyrosine hydroxylase neurons to the neurotoxic effects of monosodium glutamate (MSG). *Peptides* **7**, 783-789.

Pinto S, Roseberry AG, Liu H, Diano S, Shanabrough M, Cai X, Friedman JM, & Horvath TL (2004). Rapid rewiring of arcuate nucleus feeding circuits by leptin. *Science* **304**, 110-115.

Price CJ, Hoyda TD, Samson WK, & Ferguson AV (2008a). Nesfatin-1 influences the excitability of paraventricular nucleus neurones. *J Neuroendocrinol* **20**, 245-250.

Price CJ, Samson WK, & Ferguson AV (2008b). Nesfatin-1 inhibits NPY neurons in the arcuate nucleus. *Brain Res* **1230**, 99-106.

Price CJ, Samson WK, & Ferguson AV (2009). Neuropeptide W has cell phenotype-specific effects on the excitability of different subpopulations of paraventricular nucleus neurones. *J Neuroendocrinol* **21**, 850-857.

Price TO, Samson WK, Niehoff ML, & Banks WA (2007). Permeability of the blood-brain barrier to a novel satiety molecule nesfatin-1. *Peptides* **28**, 2372-2381.

Raffin-Sanson ML, de KY, & Bertagna X (2003). Proopiomelanocortin, a polypeptide precursor with multiple functions: from physiology to pathological conditions. *Eur J Endocrinol* **149**, 79-90.

Ramanjaneya M, Chen J, Brown JE, Tripathi G, Hallschmid M, Patel S, Kern W, Hillhouse EW, Lehnert H, Tan BK, & Randeve HS (2010). Identification of Nesfatin-1 in Human and Murine Adipose Tissue: A Novel Depot-Specific Adipokine with Increased Levels in Obesity. *Endocrinology*.

Reis DJ, Granata AR, Perrone MH, & Talman WT (1981). Evidence that glutamic acid is the neurotransmitter of baroreceptor afferent terminating in the nucleus tractus solitarius (NTS). *Auton Nerv Syst* **3**, 321-334.

Ricardo JA & Koh ET (1978). Anatomical evidence of direct projections from the nucleus of the solitary tract to the hypothalamus, amygdala, and other forebrain structures in the rat. *Brain Res* **153**, 1-26.

Richardson J, Cruz MT, Majumdar U, Lewin A, Kingsbury KA, Dezfuli G, Vicini S, Verbalis JG, Dretchen KL, Gillis RA, & Sahibzada N (2013). Melanocortin signaling in the brainstem influences vagal outflow to the stomach. *J Neurosci* **33**, 13286-13299.

Riediger T, Schmid HA, Lutz TA, & Simon E (2002). Amylin and glucose co-activate area postrema neurons of the rat. *Neurosci Lett* **328**, 121-124.

Ritter RC, Slusser PG, & Stone S (1981). Glucoreceptors controlling feeding and blood glucose: location in the hindbrain. *Science* **213**, 451-452.

Ritter S, Dinh TT, & Zhang Y (2000). Localization of hindbrain glucoreceptive sites controlling food intake and blood glucose. *Brain Res* **856**, 37-47.

Ritter S, Llewellyn-Smith I, & Dinh TT (1998). Subgroups of hindbrain catecholamine neurons are selectively activated by 2-deoxy-D-glucose induced metabolic challenge. *Brain Res* **805**, 41-54.

Rogers RC & McCann MJ (1993). Intramedullary connections of the gastric region in the solitary nucleus: a biocytin histochemical tracing study in the rat. *J Auton Nerv Syst* **42**, 119-130.

Roseberry AG, Liu H, Jackson AC, Cai X, & Friedman JM (2004). Neuropeptide Y-mediated inhibition of proopiomelanocortin neurons in the arcuate nucleus shows enhanced desensitization in ob/ob mice. *Neuron* **41**, 711-722.

Rossi J, Balthasar N, Olson D, Scott M, Berglund E, Lee CE, Choi MJ, Lauzon D, Lowell BB, & Elmquist JK (2011). Melanocortin-4 receptors expressed by cholinergic neurons regulate energy balance and glucose homeostasis. *Cell Metab* **13**, 195-204.

Rossi M, Kim MS, Morgan DG, Small CJ, Edwards CM, Sunter D, Abusnana S, Goldstone AP, Russell SH, Stanley SA, Smith DM, Yagaloff K, Ghatei MA, & Bloom SR (1998). A C-terminal fragment of Agouti-related protein increases feeding and antagonizes the effect of alpha-melanocyte stimulating hormone in vivo. *Endocrinology* **139**, 4428-4431.

Routh VH (2002). Glucose-sensing neurons: are they physiologically relevant? *Physiol Behav* **76**, 403-413.

Sakmann B, Edwards F, Konnerth A, & Takahashi T (1989). Patch clamp techniques used for studying synaptic transmission in slices of mammalian brain. *Q J Exp Physiol* **74**, 1107-1118.

Sato K, Kiyama H, & Tohyama M (1993). The differential expression patterns of messenger RNAs encoding non-N-methyl-D-aspartate glutamate receptor subunits (GluR1-4) in the rat brain. *Neuroscience* **52**, 515-539.

Schreihof AM & Guyenet PG (2002). The baroreflex and beyond: control of sympathetic vasomotor tone by GABAergic neurons in the ventrolateral medulla. *Clin Exp Pharmacol Physiol* **29**, 514-521.

Schwartz GJ (2006). Integrative capacity of the caudal brainstem in the control of food intake. *Philos Trans R Soc Lond B Biol Sci* **361**, 1275-1280.

Schwartz GJ & Moran TH (2002). Leptin and neuropeptide y have opposing modulatory effects on nucleus of the solitary tract neurophysiological responses to gastric loads: implications for the control of food intake. *Endocrinology* **143**, 3779-3784.

Schwartz MW, Woods SC, Porte D, Jr., Seeley RJ, & Baskin DG (2000). Central nervous system control of food intake. *Nature* **404**, 661-671.

Scott NA, Webb V, Boublik JH, Rivier J, & Brown MR (1989). The cardiovascular actions of centrally administered neuropeptide Y. *Regul Pept* **25**, 247-258.

Sedbazar U, Maejima Y, Nakata M, Mori M, & Yada T (2013). Paraventricular NUCB2/nesfatin-1 rises in synchrony with feeding suppression during early light phase in rats. *Biochem Biophys Res Commun* **434**, 434-438.

Seeley RJ, Yagaloff KA, Fisher SL, Burn P, Thiele TE, van DG, Baskin DG, & Schwartz MW (1997). Melanocortin receptors in leptin effects. *Nature* **390**, 349.

Shimizu H, Oh I, Hashimoto K, Nakata M, Yamamoto S, Yoshida N, Eguchi H, Kato I, Inoue K, Satoh T, Okada S, Yamada M, Yada T, & Mori M (2009). Peripheral administration of nesfatin-1 reduces food intake in mice: the leptin-independent mechanism. *Endocrinology* **150**, 662-671.

Silver IA & Erecinska M (1994). Extracellular glucose concentration in mammalian brain: continuous monitoring of changes during increased neuronal activity and upon limitation in oxygen supply in normo-, hypo-, and hyperglycemic animals. *J Neurosci* **14**, 5068-5076.

Singru PS, Wittmann G, Farkas E, Zseli G, Fekete C, & Lechan RM (2012). Refeeding-activated glutamatergic neurons in the hypothalamic paraventricular nucleus (PVN) mediate effects of melanocortin signaling in the nucleus tractus solitarius (NTS). *Endocrinology* **153**, 3804-3814.

- Skibicka KP & Grill HJ (2008). Energetic responses are triggered by caudal brainstem melanocortin receptor stimulation and mediated by local sympathetic effector circuits. *Endocrinology* **149**, 3605-3616.
- Skibicka KP & Grill HJ (2009). Hypothalamic and hindbrain melanocortin receptors contribute to the feeding, thermogenic, and cardiovascular action of melanocortins. *Endocrinology* **150**, 5351-5361.
- Skrede KK & Westgaard RH (1971). The transverse hippocampal slice: a well-defined cortical structure maintained in vitro. *Brain Res* **35**, 589-593.
- Smith PM & Ferguson AV (2008). Neurophysiology of hunger and satiety. *Dev Disabil Res Rev* **14**, 96-104.
- Sohn JW, Harris LE, Berglund ED, Liu T, Vong L, Lowell BB, Balthasar N, Williams KW, & Elmquist JK (2013). Melanocortin 4 receptors reciprocally regulate sympathetic and parasympathetic preganglionic neurons. *Cell* **152**, 612-619.
- Song Z, Levin BE, McArdle JJ, Bakhos N, & Routh VH (2001). Convergence of pre- and postsynaptic influences on glucosensing neurons in the ventromedial hypothalamic nucleus. *Diabetes* **50**, 2673-2681.
- Spanswick D, Smith MA, Groppi VE, Logan SD, & Ashford ML (1997). Leptin inhibits hypothalamic neurons by activation of ATP-sensitive potassium channels. *Nature* **390**, 521-525.
- Ste ML, Miura GI, Marsh DJ, Yagaloff K, & Palmiter RD (2000). A metabolic defect promotes obesity in mice lacking melanocortin-4 receptors. *Proc Natl Acad Sci U S A* **97**, 12339-12344.
- Stengel A, Goebel M, Wang L, Rivier J, Kobelt P, Monnikes H, Lambrecht NW, & Tache Y (2009a). Central nesfatin-1 reduces dark-phase food intake and gastric emptying in rats: differential role of corticotropin-releasing factor2 receptor. *Endocrinology* **150**, 4911-4919.
- Stengel A, Goebel M, Yakubov I, Wang L, Witcher D, Coskun T, Tache Y, Sachs G, & Lambrecht NW (2009b). Identification and characterization of nesfatin-1 immunoreactivity in endocrine cell types of the rat gastric oxyntic mucosa. *Endocrinology* **150**, 232-238.
- Stengel A, Goebel-Stengel M, Wang L, Kato I, Mori M, & Tache Y (2012). Nesfatin-1(30-59) but not the N- and C-terminal fragments, nesfatin-1(1-29) and nesfatin-1(60-82) injected

intracerebroventricularly decreases dark phase food intake by increasing inter-meal intervals in mice. *Peptides* **35**, 143-148.

Su Y, Zhang J, Tang Y, Bi F, & Liu JN (2010). The novel function of nesfatin-1: anti-hyperglycemia. *Biochem Biophys Res Commun* **391**, 1039-1042.

Sundaram K, Johnson SM, & Felder RB (1997). Altered expression of delayed excitation in medial NTS neurons of spontaneously hypertensive rats. *Neurosci Lett* **225**, 205-209.

Sutton GM, Duos B, Patterson LM, & Berthoud HR (2005). Melanocortinergic modulation of cholecystokinin-induced suppression of feeding through extracellular signal-regulated kinase signaling in rat solitary nucleus. *Endocrinology* **146**, 3739-3747.

Tai MH, Weng WT, Lo WC, Chan JY, Lin CJ, Lam HC, & Tseng CJ (2007). Role of nitric oxide in alpha-melanocyte-stimulating hormone-induced hypotension in the nucleus tractus solitarii of the spontaneously hypertensive rats. *J Pharmacol Exp Ther* **321**, 455-461.

Takahashi KA & Cone RD (2005). Fasting induces a large, leptin-dependent increase in the intrinsic action potential frequency of orexigenic arcuate nucleus neuropeptide Y/Agouti-related protein neurons. *Endocrinology* **146**, 1043-1047.

Tan BK, Hallschmid M, Kern W, Lehnert H, & Randeve HS (2011). Decreased cerebrospinal fluid/plasma ratio of the novel satiety molecule, nesfatin-1/NUCB-2, in obese humans: evidence of nesfatin-1/NUCB-2 resistance and implications for obesity treatment. *J Clin Endocrinol Metab* **96**, E669-E673.

Tell F & Bradley RM (1994). Whole-cell analysis of ionic currents underlying the firing pattern of neurons in the gustatory zone of the nucleus tractus solitarii. *J Neurophysiol* **71**, 479-492.

Thiele TE, van DG, Yagaloff KA, Fisher SL, Schwartz M, Burn P, & Seeley RJ (1998). Central infusion of melanocortin agonist MTII in rats: assessment of c-Fos expression and taste aversion. *Am J Physiol* **274**, R248-R254.

Torrealba F & Claps A (1988). The carotid sinus connections: a WGA-HRP study in the cat. *Brain Res* **455**, 134-143.

TORVIK A (1956). Afferent connections to the sensory trigeminal nuclei, the nucleus of the solitary tract and adjacent structures; an experimental study in the rat. *J Comp Neurol* **106**, 51-141.

- Travagli RA, Hermann GE, Browning KN, & Rogers RC (2006). Brainstem circuits regulating gastric function. *Annu Rev Physiol* **68**, 279-305.
- Tseng CJ, Mosqueda-Garcia R, Appalsamy M, & Robertson D (1989). Cardiovascular effects of neuropeptide Y in rat brainstem nuclei. *Circ Res* **64**, 55-61.
- Tsujii S & Bray GA (1989). Acetylation alters the feeding response to MSH and beta-endorphin. *Brain Res Bull* **23**, 165-169.
- Vaisse C, Clement K, Durand E, Hercberg S, Guy-Grand B, & Froguel P (2000). Melanocortin-4 receptor mutations are a frequent and heterogeneous cause of morbid obesity. *J Clin Invest* **106**, 253-262.
- van de Wall EH, Duffy P, & Ritter RC (2005). CCK enhances response to gastric distension by acting on capsaicin-insensitive vagal afferents. *Am J Physiol Regul Integr Comp Physiol* **289**, R695-R703.
- van DG, Bottone AE, Strubbe JH, & Steffens AB (1994). Hormonal and metabolic effects of paraventricular hypothalamic administration of neuropeptide Y during rest and feeding. *Brain Res* **660**, 96-103.
- Vincent A & Tell F (1997). Postnatal changes in electrophysiological properties of rat nucleus tractus solitarius neurons. *Eur J Neurosci* **9**, 1612-1624.
- Voss-Andreae A, Murphy JG, Ellacott KL, Stuart RC, Nillni EA, Cone RD, & Fan W (2007). Role of the central melanocortin circuitry in adaptive thermogenesis of brown adipose tissue. *Endocrinology* **148**, 1550-1560.
- Wan S & Browning KN (2008a). D-glucose modulates synaptic transmission from the central terminals of vagal afferent fibers. *Am J Physiol Gastrointest Liver Physiol* **294**, G757-G763.
- Wan S & Browning KN (2008b). Glucose increases synaptic transmission from vagal afferent central nerve terminals via modulation of 5-HT₃ receptors. *Am J Physiol Gastrointest Liver Physiol* **295**, G1050-G1057.
- Wan S, Browning KN, Coleman FH, Sutton G, Zheng H, Butler A, Berthoud HR, & Travagli RA (2008). Presynaptic melanocortin-4 receptors on vagal afferent fibers modulate the excitability of rat nucleus tractus solitarius neurons. *J Neurosci* **28**, 4957-4966.

Wang L, Martinez V, Barrachina MD, & Tache Y (1998). Fos expression in the brain induced by peripheral injection of CCK or leptin plus CCK in fasted lean mice. *Brain Res* **791**, 157-166.

Wang R, Liu X, Hentges ST, Dunn-Meynell AA, Levin BE, Wang W, & Routh VH (2004). The regulation of glucose-excited neurons in the hypothalamic arcuate nucleus by glucose and feeding-relevant peptides. *Diabetes* **53**, 1959-1965.

Wang YH, Tache Y, Sheibel AB, Go VL, & Wei JY (1997). Two types of leptin-responsive gastric vagal afferent terminals: an in vitro single-unit study in rats. *Am J Physiol* **273**, R833-R837.

Wang YT & Bieger D (1991). Role of solitary GABAergic mechanisms in control of swallowing. *Am J Physiol* **261**, R639-R646.

Watanabe M, Mishina M, & Inoue Y (1994). Distinct distributions of five NMDA receptor channel subunit mRNAs in the brainstem. *J Comp Neurol* **343**, 520-531.

Wernecke K, Lamprecht I, Jöhren O, Lehnert H, & Schulz C (2014). Nesfatin-1 increases energy expenditure and reduces food intake in rats. *Obesity (Silver Spring)* **22**, 1662-1668.

Williams DL, Bowers RR, Bartness TJ, Kaplan JM, & Grill HJ (2003). Brainstem melanocortin 3/4 receptor stimulation increases uncoupling protein gene expression in brown fat. *Endocrinology* **144**, 4692-4697.

Williams DL, Kaplan JM, & Grill HJ (2000). The role of the dorsal vagal complex and the vagus nerve in feeding effects of melanocortin-3/4 receptor stimulation. *Endocrinology* **141**, 1332-1337.

Williams RH, Alexopoulos H, Jensen LT, Fugger L, & Burdakov D (2008). Adaptive sugar sensors in hypothalamic feeding circuits. *Proc Natl Acad Sci U S A* **105**, 11975-11980.

Wirth MM, Olszewski PK, Yu C, Levine AS, & Giraudo SQ (2001). Paraventricular hypothalamic alpha-melanocyte-stimulating hormone and MTHII reduce feeding without causing aversive effects. *Peptides* **22**, 129-134.

Woods SC & D'Alessio DA (2008). Central control of body weight and appetite. *J Clin Endocrinol Metab* **93**, S37-S50.

Wright J, Campos C, Herzog T, Covasa M, Czaja K, & Ritter RC (2011). Reduction of food intake by cholecystokinin requires activation of hindbrain NMDA-type glutamate receptors. *Am J Physiol Regul Integr Comp Physiol* **301**, R448-R455.

Wu D, Yang M, Chen Y, Jia Y, Ma ZA, Boden G, Li L, & Yang G (2014). Hypothalamic nesfatin-1/NUCB2 knockdown augments hepatic gluconeogenesis that is correlated with inhibition of mTOR-STAT3 signaling pathway in rats. *Diabetes* **63**, 1234-1247.

Xia ZF, Fritze DM, Li JY, Chai B, Zhang C, Zhang W, & Mulholland MW (2012). Nesfatin-1 inhibits gastric acid secretion via a central vagal mechanism in rats. *Am J Physiol Gastrointest Liver Physiol* **303**, G570-G577.

Yang M, Zhang Z, Wang C, Li K, Li S, Boden G, Li L, & Yang G (2012). Nesfatin-1 action in the brain increases insulin sensitivity through Akt/AMPK/TORC2 pathway in diet-induced insulin resistance. *Diabetes* **61**, 1959-1968.

Yaswen L, Diehl N, Brennan MB, & Hochgeschwender U (1999). Obesity in the mouse model of pro-opiomelanocortin deficiency responds to peripheral melanocortin. *Nat Med* **5**, 1066-1070.

Yettefti K, Orsini JC, & Perrin J (1997). Characteristics of glycemia-sensitive neurons in the nucleus tractus solitarii: possible involvement in nutritional regulation. *Physiol Behav* **61**, 93-100.

Yosten GL, Redlinger L, & Samson WK (2012). Evidence for a role of endogenous nesfatin-1 in the control of water drinking. *J Neuroendocrinol* **24**, 1078-1084.

Yosten GL & Samson WK (2009). Nesfatin-1 exerts cardiovascular actions in brain: possible interaction with the central melanocortin system. *Am J Physiol Regul Integr Comp Physiol* **297**, R330-R336.

Yosten GL & Samson WK (2010). The anorexigenic and hypertensive effects of nesfatin-1 are reversed by pretreatment with an oxytocin receptor antagonist. *Am J Physiol Regul Integr Comp Physiol*.

Yosten GL & Samson WK (2014). Neural circuitry underlying the central hypertensive action of nesfatin-1: melanocortins, corticotropin-releasing hormone, and oxytocin. *Am J Physiol Regul Integr Comp Physiol* **306**, R722-R727.

Yox DP, Stokesberry H, & Ritter RC (1991). Vagotomy attenuates suppression of sham feeding induced by intestinal nutrients. *Am J Physiol* **260**, R503-R508.

Yuan CS, Liu D, & Attele AS (1998). GABAergic effects on nucleus tractus solitarius neurons receiving gastric vagal inputs. *J Pharmacol Exp Ther* **286**, 736-741.

Zeltser LM, Seeley RJ, & Tschop MH (2012). Synaptic plasticity in neuronal circuits regulating energy balance. *Nat Neurosci* **15**, 1336-1342.

Zhan C, Zhou J, Feng Q, Zhang JE, Lin S, Bao J, Wu P, & Luo M (2013). Acute and long-term suppression of feeding behavior by POMC neurons in the brainstem and hypothalamus, respectively. *J Neurosci* **33**, 3624-3632.

Zhang AQ, Li XL, Jiang CY, Lin L, Shi RH, Chen JD, & Oomura Y (2010). Expression of nesfatin-1/NUCB2 in rodent digestive system. *World J Gastroenterol* **16**, 1735-1741.

Zhang W, Zhang C, Fritze D, Chai B, Li J, & Mulholland MW (2013). Modulation of food intake by mTOR signalling in the dorsal motor nucleus of the vagus in male rats: focus on ghrelin and nesfatin-1. *Exp Physiol* **98**, 1696-1704.

Zheng H, Kelly L, Patterson LM, & Berthoud HR (1999). Effect of brain stem NMDA-receptor blockade by MK-801 on behavioral and fos responses to vagal satiety signals. *Am J Physiol* **277**, R1104-R1111.

Zheng H, Patterson LM, Phifer CB, & Berthoud HR (2005). Brain stem melanocortinergic modulation of meal size and identification of hypothalamic POMC projections. *Am J Physiol Regul Integr Comp Physiol* **289**, R247-R258.

Zheng H, Patterson LM, Rhodes CJ, Louis GW, Skibicka KP, Grill HJ, Myers MG, Jr., & Berthoud HR (2010). A potential role for hypothalamomedullary POMC projections in leptin-induced suppression of food intake. *Am J Physiol Regul Integr Comp Physiol* **298**, R720-R728.